TRANSIENT THERMAL CHARACTERISTICS OF AUTOMOTIVE COIL SPRING IN WALKING BEAM TYPE HEATING FURNACE

CHAVALIT JAROENRAT

A THESIS SUBMITTED IN PARTIAL FULFILLMENT

OF THE REQUIREMENT FOR THE DEGREE OF

MASTER OF ENGINEERING IN AUTOMOTIVE ENGINEERING

(INTERNATIONAL PROGRAM)

INTERNATIONAL COLLEGE

KING MONGKUT'S INSTITUTE OF TECHNOLOGY LADKRABANG

2011

KMITL-2011-IC-M-004-006

Thesis Title	**Transient thermal characteristics of automotive coil spring in walking beam type heating furnace.**
Student	**Mr. Chavalit Jaroenrat**
Student ID	**50061904**
Degree	**Master of Engineering**
Program	**Automotive Engineering (International Program)**
Year	**2011**
Thesis Advisor	**Assoc. Prof. Dr. Pongjet Promvonge**
Thesis Co-Advisor	**Prof. Dr. Katsunori Hanamura**

ABSTRACT

The thesis presents the experimental and numerical investigation of transient temperature distributions inside a round bar needed to heat up to at least 940°C in a forming process of an automotive coil spring. The heat absorbed by the bar is via radiation emitted by hot gases and hot furnace walls at the effective temperature inside a heating furnace. From the analysis of experiments, a mathematical conduction heat transfer model has been developed for prediction of transient temperature characteristics in the round bar. Of the furnace caused by the burner flames and the continuous heat absorption through the transient heat conducting ability of round bar are recorded by various conditions in the experiments. Radiative heat flux calculated from the radiative heat exchange within the furnace modeled by considering the effect of effective temperature inside the furnace, round bar and combustion gases is introduced as the boundary condition of the transient conduction equation of the round bar. Heat transfer and temperature behaviors of the round bar are investigated by changing such parameters as emissivity of the hot gas. Comparison with the experimental data shows that the present heat transfer model performs well in prediction of thermal behaviors of the round bar in the heating furnace.

ACKNOWLEDGEMENT

This thesis could not be completed without the assistance of many persons to whom I would like to express my sincere appreciation.

First, I would like to sincerely thank my advisor, Assoc.Prof. Dr. Pongjet Promvonge, who has given me many helpful suggestions.

I would like to sincerely thank my co-advisor, Prof. Dr. Katsunori Hanamura for the many suggestions of heat transfer analysis.

Moreover, I would like to show gratitude to Bangkok Spring Industrial Co., Ltd (BSK), especially Mr. Yongkiat Kitaphanich, Mrs. Sayamol Kitaphanich and Mr. Somsak Sitthinuncharoen for providing the high performance equipment as well as supporting the time to study in the academic courses.

I am grateful to National Science and Technology Development Agency (NSTDA), which provided the full scholarship for studying in the master program.

Finally, I am very grateful to my family for all love, caring, understanding and motivation throughout my life.

Chavalit Jaroenrat

CONTENTS

CONTENTS (CONT.)

CONTENTS (CONT.)

CONTENTS (CONT.)

LIST OF TABLES

LIST OF FIGURES

LIST OF FIGURES (CONT.)

LIST OF FIGURES (CONT.)

LIST OF APPENDIX

LIST OF APPENDIX (CONT.)

CHAPTER 1

INTRODUCTION

1.1 Background

Somboon Group (SBG) is a Thai conglomerate, which plays a major role in the automotive-part industry in Thailand. SBG was founded in 1941 as an automotive-understructure-part agent by Mr. Somboon Kitaphanich who wanted to manufacture his own automotive parts. As a result, he established the first Thaiowned leaf spring factory near Bangna intersection, Bangkok in 1961. The company has steadily grown through the past 50 years and has been known as a leading automotive-part manufacturer in Thailand.

Bangkok Spring Industrial Co., Ltd. (BSK), one of the three companies in SBG, was found in 1976 as an original equipment manufacturer (OEM). The company has more than 30 years of experience with Japanese high-tech manufacturing processes. For years, BSK has been well known as a full-line spring manufacturer, which currently produces leaf springs, hot and cold coil springs, stabilizer bars, torsion bars, valves and push rods for domestic and oversea OEM customers and after-market. Some of the main customers include Toyota Motors (Thailand) Co., Ltd., Mitsubishi Motors (Thailand) Co., Ltd., Nissan Motors (Thailand) Co., Ltd. and Honda Automobile (Thailand) Co., Ltd.

Coil spring is one of the major products of BSK with a production capacity of about 620 tons (200,000 pieces) per month. According to the annual report of the company in 2010, the expense of energy and fuel consumed in the coil-spring manufacturing process is estimated to be 15 million bahts, representing about 10% of the annual production cost. Due to economic competitions and the rising of energy prices at present, the production engineers at BSK have been questioned on how to effectively utilize energy resources to maximize profits (or minimize the production cost).

In spring manufacturing process, a heating furnace is required to reheat a piece of steel stock so that it is plastic enough to be pressed or rolled, and also to meet specific requirements and objectives in terms of stock heating rates for metallurgicaland productivity reasons. At the BSK factory, a “walking-beam” type furnace has been installed in its coil spring production line to reheat pieces of steel bars prior to winding into coils. From the production point of view, it is required that the energy consumption and operating time during the heating operation of the walking-beam furnace to be optimized; therefore contributing to reduced production cost and increased productivity. In this research, the heating operation of the walking-beam furnace will be investigated with a focus on

achieving optimized operating conditions with respect to energy consumption, operating time and heating efficiency. Thermal analysis of the furnace will be performed based on experimental measurements and theoretical calculations of heat transfer within the furnace to achieve the optimization of the heating operation. Finally, correlations will also be made between the experimental and theoretical data to suggest optimized operating conditions for the production of various sizes of coil spring.

1.2 Objectives of the Research

1.2.1 To investigate the operation of a walking-beam furnace used for reheating round bars in a coil spring manufacturing process

1.2.2 To be capable of specifying optimized operating conditions of the walking-beam furnace's heating operation for the production of different sizes of coil springs.

1.3 Scopes of the Research

1.3.1 The coil-spring manufacturing process is based on the process used by BSK.

1.3.2 The stocks are round bars, made of SUP 12 steel. The material specifications are given in Appendix C.

1.3.3 The round bars are available in three diameter sizes of 10.5 mm, 13.5 mm and 17.4 mm.

CHAPTER 2

THEORY AND LITERATURE REVIEW

2.1 Manufacturing of Coil Spring

2.1.1 Coil Spring

Coil spring, also known as helical spring, is a mechanical device, which is used to store energy and subsequently release it, to absorb shock, or to maintain a force between contacting surfaces. Coil springs are used in numerous practical applications; however, the term "coil spring" is generally used to describe a spring commonly used in automobiles to absorb load and defection variations from the vehicle suspension. In an automobile, coil springs are mounted between the frame and the axle housing (see Figure .2.1). Rubber insulators are used between a spring and its contact point preventing metal-to-metal contact.

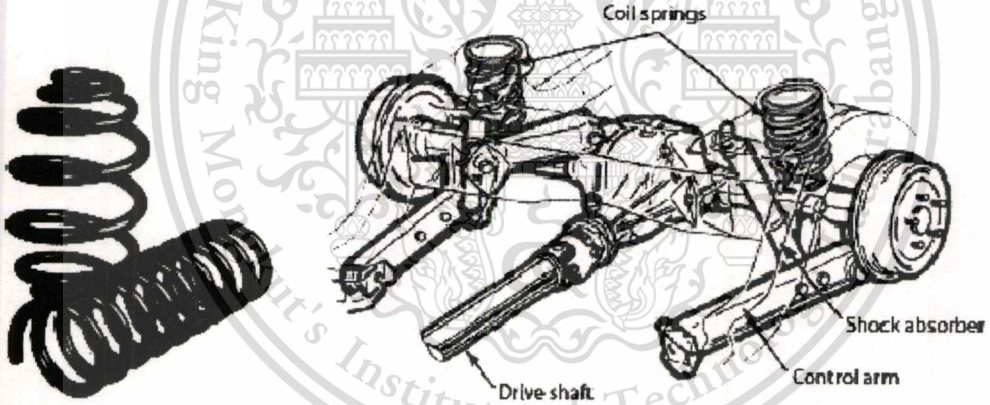

Figure 2.1 Coil springs and their arrangement in automobile

2.1.2 Coil Spring Manufacturing Process

Coil springs are made of an elastic material (such as carbon or alloy steel) formed into the shape of a helix, which returns to its natural length when unloaded. They are made in various diameters, heights and load carrying capacities to meet the specifications required by automotive companies. In general, coil springs are made from a spring round bar heated and shaped into a coil. The bar is first heated in a furnace, wound around a cylindrical shaped former in an annealed

condition, tempered to achieve its strength as a spring and then powder coated to protect against corrosion and rust. A typical flowchart of a complete manufacturing process of coil spring is demonstrated in Figure 2.2. In brief, the process can be viewed as a 3-stage process: (1) heating, (2) coiling and quenching, and (3) tempering.

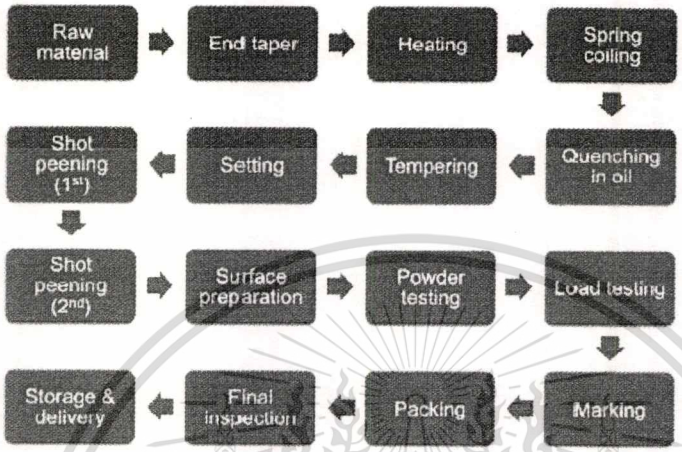

Figure 2.2 Flowchart of manufacturing process of coil spring

Heating. Heat treatment of round bars in a furnace is used to obtain the austenite structure in steel and a plastic condition of the bars prior to winding into a coil. This procedure requires a large amount of energy to heat the bars to a predetermined (austenization) temperature, one of which is known that the martensitic structure is formed in the finished product. The formation of martensitic structure is important because it enhances the strength and hardness in the coil springs.

Coiling and *Quenching.* Coiling a round bar can be accomplished by any number of means using an coiling machine, automatic or hand-operated, or equally automatic winding machine, but mostly depends upon the bar size (diameter or thickness). The larger the bar size, the more heat that is needed to bend (plasticize) and coil the bar. Steel bars with a diameter less than 0.75 inch could be wrapped into a coil without the application of heat by wrapping the bars around a mandrel inserted into a power drill. The bars with a large diameter are heated and wrapped by an automatic machine around a mandrel and then cooled in oil. The cooled bars are then tempered to give them extra hardness.

Tempering. The coil springs are tempered to give the springs a hardness that will keep their form. Tempering the springs is performed in a furnace. After heating, the springs are allowed to gradually cool and harden.

2.2 Heat Treatment of Carbon Steel

2.2.1 Carbon Steel

Carbon steels are widely used for applications where mechanical strength is of importance. Carbon steel, also called *plain-carbon steel*, is steel where the main alloying constituent is carbon. According to the definition given by The American Iron and Steel Institute (AISI), steel is considered to be carbon steel when [1]:

- No minimum content is specified or required for chromium, cobalt, niobium, molybdenum, nickel, titanium, tungsten, vanadium or zirconium, or any other element to be added to obtain a desired alloying effect
- The specified minimum for copper does not exceed 0.40 percent, and
- The maximum content specified for any of the following elements does not exceed the percentages noted: manganese 1.65, silicon 0.60, copper 0.60. Regardless of heat treatment, carbon steel becomes lower in the melting point as the carbon content rises. It has the ability to become harder and stronger through heat treatment, which also makes it less ductile.

Carbon steels can be classified based on carbon content, into four classes [2]: *mild and low*, and *higher* (*medium*, *high* and *ultra-high*).

Mild and Low Carbon Steels. Mild and Low carbon steels approximately contain 0.05 – 0.15% carbon and 0.16 – 0.29% carbon, respectively; therefore they are neither brittle nor ductile. Their prices are relatively low while providing properties acceptable for many applications. Mild steel is the most common form of steel. It has a relatively low tensile strength with a density of 7.85 g/cm3 and Young's modulus of 210 GPa, approximately. It is often used when large quantities of steel are needed, for example as structural steel.

Higher Carbon Steels. Higher carbon steels are broken down into three classes, including medium carbon steel, high carbon steel and ultra-high carbon steel. Medium carbon steel contains approximately 0.30 – 0.59% carbon content. It has balance ductility and strength, and good wear resistance. Typically, it is used for large parts, forging and automotive components. High carbon steel contains approximately 0.60 – 0.99% carbon content. It is very strong and suitable for spring and highstrength wire applications. Ultra-high carbon steel contains approximately 1.0 – 2.0% carbon content. It can be tempered to great hardness for use in special applications, such as knives, axles or punches. Note that carbon steel with a carbon content above 2% is considered *cast iron*

2.2.2 Phase Diagram of Iron-Carbon System

The nature of carbon steel can be considered using the iron-carbon metstable phase diagram, shown in Figure 2.3 [3]. The phase diagram is based on the transformation that occurs as a result of slowly heating carbon steel.

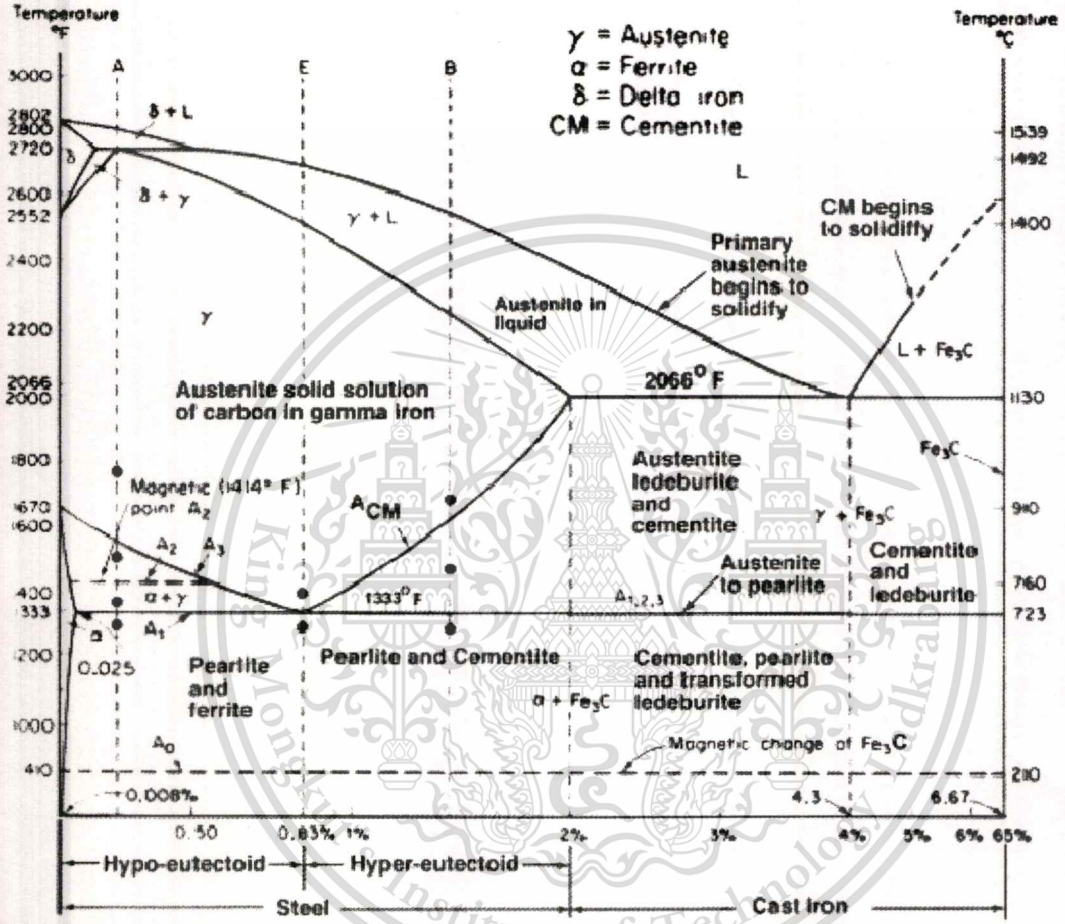

Figure 2.3 Iron-Carbon metastable phase diagram [3]

Figure 2.3 shows the equilibrium diagram for combinations of carbon in a solid solution of iron. Three significant regions can be made relative to the steel portion of the diagram. They are the *eutectoid* E, the hypoeutectoid A, and the hyperutectoid B. The right side of the pure iron line is carbon in combination with various forms of iron called alpha (α) iron (ferrite), gamma (γ) iron (austenite), and delta (δ) iron.

Eutectoid. The iron-carbon system is considered a *eutectic system*. A eutectic system is a mixture of chemical compounds or elements that has a single chemical composition that solidifies at a

lower temperature than any other composition. This composition is known as the *eutectic composition* and the temperature is known as the *eutectic temperature*. On a phase diagram, the intersection of the eutectic temperature and the eutectic composition gives the *eutectoid point*. In the iron-carbon system (see Figure 2.3), the eutectoid point occurs at 723 °C and about 0.83% carbon content.

Austenite. The austenite phase exists in carbon steel at high temperature. It has a Face-Centered Cubic (F.C.C) atomic structure, which can contain up to 2% carbon in solution.

Ferrite. The ferrite phase has a Body-Centered Cubic (B.C.C) atomic structure, which can hold very little carbon (typically 0.0001%) at room temperature. It can exist as either *alpha* or *delta* ferrite.

Cementite. Cementite is a very hard intermetallic compound consisting of 6.7% carbon content. Its chemical symbol is Fe3C. Cementite is very hard, but its hardness is reduced considerably when mixed with soft ferrite layers. Slow cooling of cementite gives coarse pearlite, which is soft and easy to machine but poor in toughness. Faster cooling gives very fine layers of ferrite and cementite, which are harder and tougher.

Pearlite. Pearlite is a mixture of alternate strips of ferrite and cementite in a single grain. The distance between the plates (strips) and their thickness depends upon the cooling rate of the material. The name "pearlite" is derived from its mother of pearl appearance under a microscope. A fully pearlitic structure occurs at 0.8% carbon content.

Martensite. Martensite is formed by rapid cooling, or quenching, of austenite. This causes the F.C.C. structure in the austenite rapidly changes to B.C.C. structure, leaving insufficient time for carbon atoms to diffuse out of the crystal structure. As a result, a distorted structure that has the appearance of fine needles is formed. Martensite has a Body-Centered Tetragonal (B.C.T.) structure. It has a lower density than austenite, so that the martensitic transformation results in a relative change of volume. As martensite is formed by fast cooling rates, it is not shown in the ironcarbon metastable phase diagram because it is not an equilibrium phase. The hardness of martensite is solely dependent on carbon content. Its hardness is usually very high, unless the carbon content is particularly low.

2.2.3 Phase Transformations in Carbon Steels [4]

The mechanical properties of steel are controlled by controlling its microstructure and the nature of the phases within the microstructure. This can be done by choosing appropriate chemical compositions and heat treatments. The heat treatments can change the microstructure of steel by processes such as recovery, recrystallization, grain growth and phase transformations.

Austenitization. Austenitization is the process that converts steel into F.C.C. solid solution called "austenite" by heating the steel into the austenitic phase field and holding there for a long period. The nature of the austenite obtained is important because it has a direct effect on the microstructure produced during subsequent treatments in which the austenite is transformed into other phases and the steel is returned to ambient temperature.

From the iron-carbon metastable phase diagram in Figure 2.3, the range of temperatures from which one could be selected for the austenitization process lies in the austenite phase field. When the temperature is chosen, the time has then to be selected. The selection of optimum temperature and time depends on the objectives of the heat treatment process and upon the microstructure of the steel before austenitization. If the austenitization heat-up time is long, the microstructure could change somewhat before austenitization begins. The heating rate is therefore an important factor in the overall practical process.

Since the purpose of an austenitization treatment is to produce austenite so that it is then transformed into something else to have the desirable mechanical properties in the final product, it is usually necessary that the austenite be fine-grained. A large austenitic grain size is undesirable because it leads to a coarse microstructure when the austenite is transformed back into the microstructure in which it will be used. The formation of the austenite occurs by a nucleation and growth process in which its grain size depends upon the nucleation rate, which in turn depends upon the availability of nucleation sites and also upon the temperature at which the nuclei form. In most practices, it is desirable that the austenite be transformed as soon as possible. The microstructure of the steel obtained by heat treatments depend on the manner in which austenite transforms when it is cooled to ambient temperatures. Transformation of austenite during a quenching process of steel is expected for applications where high mechanical strength is of importance. The austenite deformation prior to quenching can lead to an increase in strength without adverse effects on ductility or toughness. For example, it has been demonstrated that the grain size and grain substructure of a medium carbon chromium vanadium steel can be controlled by deforming the austenite in such a way to produce high strength martens tic steels with excellent ductility, toughness and endurance limit [5].

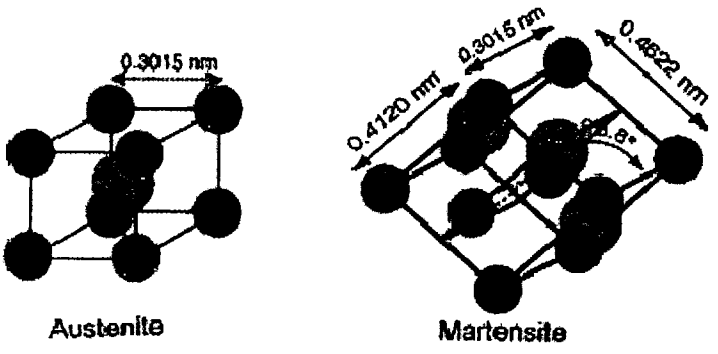

Figure 2.4 Atomic structures of austenite (F.C.C.) and martensite (B.C.T.)

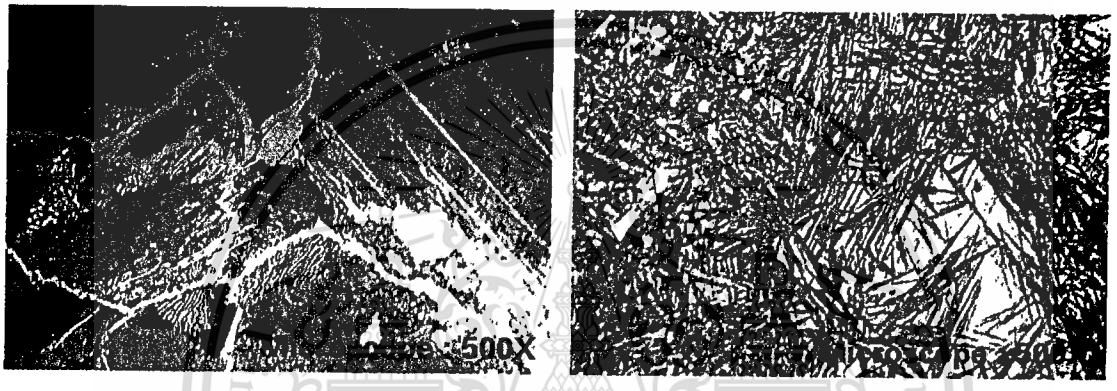

(A) (B)

Figure 2.5 Micrographs of austenite (A) and martensite (B) [3] (microscope: 500 xs)

Martensitic Transformation. The martensitic transformation can be defined as a mechanism for changing crystallographic structure that does not require atomic diffusion. It is a result of transformation of austenite during a quenching process. Figure 2.4 and Figure 2.5 show the atomic structures and micrographs for austenite and martensite, respectively. When austenite is quenched to below a particular temperature (about 220°C), it is no longer possible to retain all of the original austenite and fine crystals of a BCT phase appear. The amount of the new phase that is formed depends on the temperature to which the austenite is cooled rather than the time it is held at that temperature. The temperature at which the martensitic transformation starts is called the martensitic temperature, *Ms*. When rapid quenching suppresses, a free energy is reduced by transforming the F.C.C. structure in the austenite to B.C.C. structure, which is consequently distorted to B.C.T. structure by the supersaturation of carbon that remains in solid solution. The phase that is produced in the steel as it is quenched below the *Ms* point is called "*martensite*".

Martensite is a supersaturated solid solution in which the interstitial solutes interact strongly with dislocations. It is also composed of very fine crystals with many intercrystalline boundaries. It can be highly dislocated or twinned. For these reasons, it is the strongest form of carbon steel [4]. The hardness of freshly formed martensite is directly dependent upon its hardness content. The freshly formed martensite, however, lacks toughness and is not tolerant of small flaws, which can initiate brittle fracture. For this reason, freshly quenched martensite is not usually used in practical applications. It is further treated with heat in order to impart to it with some toughness. The additional heat treatments are called "tempering" treatments and are disregarded in the scope of this study.

2.2.4 Influence of Heat Treatment on Spring Steel Material

Carbon steels of spring steel grades are designed for quenching and tempering to a condition called "tempered martensite", which is suitable for hot-coiled springs. This condition has a high ultimate and yield strength, combined with good fracture toughness all of great value for the load, fatigue and relaxation performance [6]. The heating conditions have an effect on the decarburization and the grain boundary oxidation and also on the steel structure after quenching and tempering. These factors have an influence on the material performance.

In industrial practice of coil spring production where steel wires or round bars of thicker diameters are used as stock, the steel bars are first austenitized and then coiled prior to quenching to receive the high strength needed. The steel bars need to be heated to austenitic temperature, where, at this temperature, the steel bars are soft and plastic, and can easily be formed to specified shape. Therefore, according to the iron-carbon metastable phase diagram in Figure 2.3, the austenitization temperature must be well above 900°C (this temperature is known as the "A3-temperature") to avoid any other phase transformation before the martensite transformation occurs. At the same time, to receive a good martensitic structure, the alloying elements, or carbides, in the carbon steel must give their effect on the harden ability of the steel when quenching. This means that the carbides must have dissolved into the austenitic structure and a homogeneous solid solution of the austenite must be achieved to obtain maximum hardness or strength in the as-quenched martensite before the quenching [7]. During heating to and at the austenitization temperature, it takes some time for the carbides to dissolve into austenite. The formation of fine austenite grains by recrystallization is expected, as it is beneficial for ductility and toughness. The grains re-crystallize to the smallest possible grain size controlled by the chemical composition of the steel. After the grains have re-crystallized, they start to grow in size. The speed of the growth increases with increased temperature; hence the time at the austenitization temperature controls the grain size together with the chemical composition.

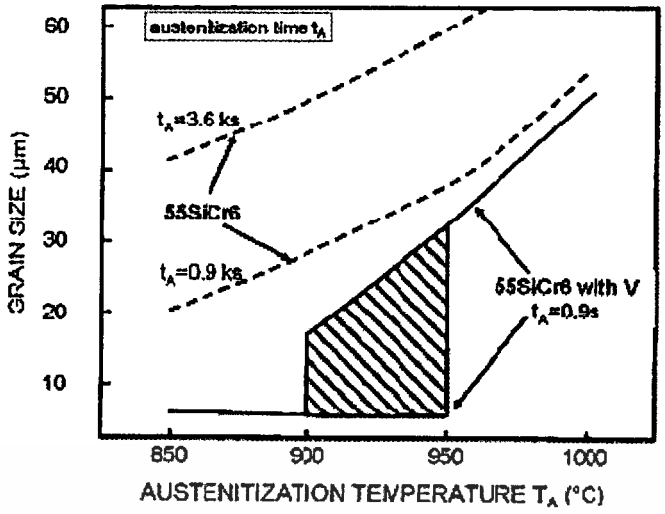

Figure 2.6 Austenite grain diameter for different austenitization conditions [8]

The steel with small grain size has higher fracture toughness compared to those with larger grains; hence higher fatigue resistance. The austenite grain size and the hardness for different austenitization conditions have been investigated for base alloys with and without vanadium [8]. The result is shown in Figure 2.6. Based on the result, the austenitization holding time and temperature are defined respectively to be 300s holding time at 900°C, considering on both the necessary time (decrease of temperature) for coiling the wire and the optimum grain size and time for achieving

solid solution to obtain maximum hardness. It is also reported that the maximum in strength and ductility of martensite can be achieved when prior to quenching the austenite is deformed around 900°C with a strain slightly below the peak strain [7].

2.3 Furnace

Furnaces are specialized equipment for heating. They are used for many different purposes such as heating up homes, commercial buildings, making pottery and ceramic objects, and melting raw metals for the creation of different objects, among others. Industrial furnaces are furnaces especially used for industrial plants and factories, usually bigger than household furnaces, capable of producing more heat and stronger flames. Furnaces play crucial role in the operation of a number of industries, especially in the production of goods and manufacturing of products.

2.3.1 Classification of Different Furnaces [9]

Based on Heat Generating Method. Furnaces are broadly classified into two types, *Combustion type* (using fuels) and *Electric type.* In case of combustion type furnace, depending upon the kind of combustion, it can be broadly classified as *Oil fired*, *Coal fired* or *Gas fired. Based on Mode of Charging of Material.* Furnaces can be classified as *Intermittent* (or *Batch type* furnace or *Periodical* furnace) and *Continuous* furnace. *Based on Mode of Waste Heat Recovery.* Furnaces are classified as *Recuperative* and *Regenerative* furnaces. Another type of furnace classification is made based on mode of heat transfer, mode of charging and mode of heat recovery.

2.3.2 Continuous Steel Reheating Furnaces

Reheating is a continuous process where a stock is charged at a furnace entrance, heated, and discharged. Energy is transferred to the stock during their traverse through the furnace by means of convection and radiation from the hot burner gases and the furnace walls.

The main function of a reheating furnace is to raise the temperature of a piece of steel, typically to between 900°C and 1250°C, until it is plastic enough to be pressed or rolled to the desired section, size or shape. The furnace must also meet specific requirements and objectives in terms of stock heating rates for metallurgical and productivity reasons. In continuous reheating, the steel stock forms a continuous flow of material and is heated to the desired temperature as it travels through the furnace. All furnaces possess the features shown in Figure 2.7.

The refractory chamber of the steel-reheating furnace is constructed of insulating materials for retaining heat at the high operating temperatures. A hearth is used to support or carry the steel. This can consist of refractory materials or an arrangement of metallic supports that may be water-cooled. The burners use liquid or gaseous fuels to raise and maintain the temperature in the chamber. Coal or electricity can be used for reheating. Other facilities include a method of removing the combustion exhaust gases from the chamber and a method of introducing and removing the steel from the chamber. These facilities depend on the size and type of furnace as well as the shape and size of the steel being processed. Common steelreheating furnace systems also include roller tables, conveyors, charging machines and furnace pushers.

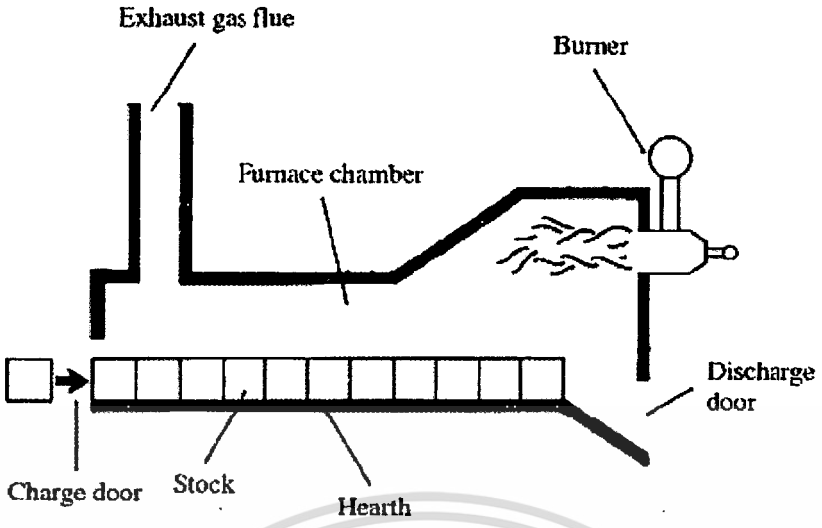

Figure 2.7 Continuous furnace feature

Continuous steel reheating furnaces can be categorized by the method by which stock is transported through the furnace. In general, there are two basic methods [9]:

- Stock is butted together to form a stream of material that is pushed through the furnace. Such furnaces are called *pusher type* furnaces.
- Stock is placed on a moving hearth or supporting structure which transports the steel through the furnace. Such types include walking beam, walking hearth, rotary hearth and continuous recirculating bogie furnaces.

Pusher Type Furnace. The pusher type furnace relatively low installation and maintenance costs compared to moving hearth furnaces. The furnace may have a solid hearth, but it is also possible to push the stock along skids with water-cooled supports that allow both the top and bottom faces of the stock to he heated. However, pusher type furnaces do have some disadvantages, including:

- Frequent damage of refractory hearth and skid marks on material
- Water cooling energy losses from the skids and stock supporting structure in top and bottom fired furnaces have a detrimental effect on energy use.
- Discharge must be accompanied by charge.
- Stock sizes and weights and furnace length are limited by friction and the possibility of stock pile-ups.
- All round heating of the stock is not possible.

Walking-Hearth Furnace. The walking hearth furnace allows the stock to be transported through the furnace in discrete steps. Such furnaces have several attractive features, including simplicity of design, ease of construction, ability to cater for different stock sizes, negligible water cooling energy losses and minimal physical marking of the stock. The main disadvantage of walking hearth furnaces is the bottom face of the stock cannot be heated. Consequently, the stock residence time may be long, possibly several hours. This may have an adverse effect on furnace flexibility and the yield may be affected by scaling.

Rotary Hearth Furnace. The rotary hearth furnace has tended to supersede the recirculating bogie type. The heating and cooling effects introduced by the bogies are eliminated, so heat storage losses are less. However, the rotary hearth has a more complex design with an annular shape and revolving hearth.

Continuous Recirculating Bogie type Furnace. In this furnace, the stock is placed on a bogie with a refractory hearth, which travels through the furnace with others in the form of a train. The entire furnace length is occupied by bogies. The furnace tends to be long and narrow, thus some disadvantages are that it often suffers from problems arising from inadequate sealing of the gap between the bogies and furnace shell, difficulties in removing scale, and difficulties in firing across a narrow hearth width.

Walking Beam Furnaces. The walking beam furnace overcomes many of the problems of pusher furnaces and permits heating of the bottom face of the stock. This allows shorter stock heating times and furnace lengths and thus better control of heating rates, uniform stock discharge temperatures and operational flexibility. The design of a typical walking-beam furnace is shown schematically in Figure 2.8.

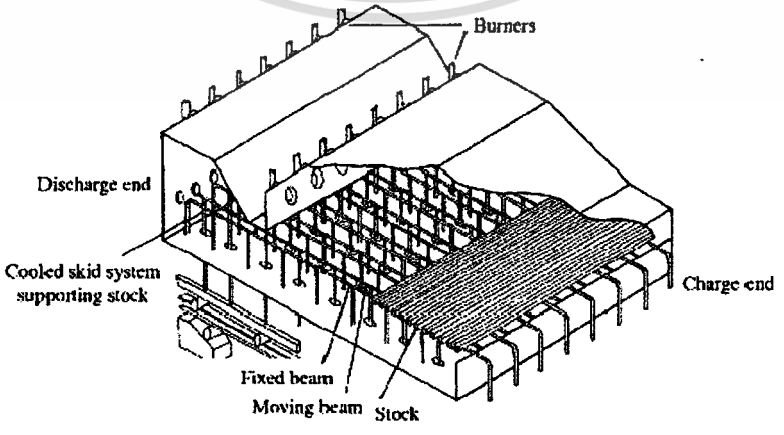

Figure 2.8 Walking-beam type furnace

2.3.3 Walking-Beam Furnace

Walking-beam furnaces are popular in steel industries. They are designed to heat steel stocks from all sides, resulting in a rapid and uniform heating of the stocks. They also occupy a relatively small surface area and can easily be accommodated in the production line.

The operation of a typical walking-beam furnace is shown in Figure 2.9, which can be described as follows [10]. The billets are transported through the furnace by the action of a transfer rail (or walking beam). A complete walking-beam step consists of the following segments:

(i) Raising the transfer rail with all the billets from the fixed rail (Figure 2.9a and Figure 2.9b)

(ii) Shifting the transfer rail with the billets over a length of one step (Figure.2.9c)

(iii) Lowering the transfer rail to put the billets on the fixed rail (Figure 2.9d)

(iv) Shifting the transfer rail back to the start position (Figure 2.9a)

(v) Discharging the billet at the last position from the furnace and charging a new billet to the first position in the furnace.

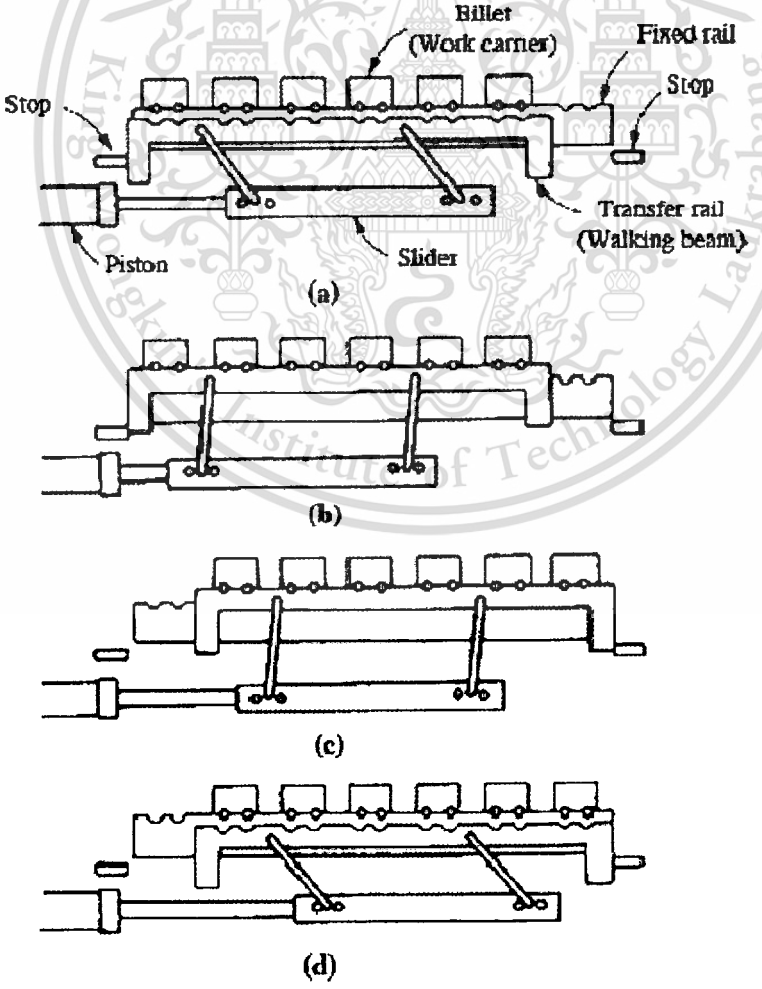

Figure 2.9 Walking-beam transfer system in a typical walking-beam type furnace

Note that the time required for a complete walking-beam step (the sum of the times used in segments (i) through segments (iv)) is called "cycle time of walking beam", a typical parameter used to control the heating operation of a walking-beam furnace. Another operating parameter is the "set-point" temperature at which the furnace will maintain the heating in the heating zone. In practice, reduction in the cycle time at an appropriate set-point temperature could lead to increased productivity, while maintaining the desired quality in the heated product. Too-high set-point temperature may result in excess heating of stock, directly leading to increased energy losses and lower energy efficiency.

Most industrial walking-beam furnaces are equipped with a burner automatic control system, which implements real-time control of the heat production. The common purpose of the control system is to optimize the fuel use for maximum energy efficiency while fulfilling the quality requirements for the heated stock. The burner control system is illustrated in a principle diagram of Figure 2.10.

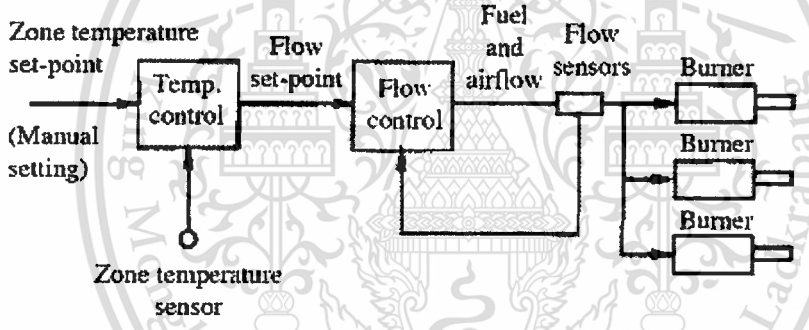

Figure 2.10 Principle diagram showing a burner control system used in a walking beam reheating furnace (Redrawn from [11])

The walking-beam furnace finds its major application in the manufacturing processes of leaf spring and coil spring. It can be used as either a reheating furnace or a tempering furnace. BSK has installed a walking-beam furnace in its coil spring production line for reheating steel-rod stock prior to winding into coils. Figure 2.11 and Figure 2.12 show photographs and interior drawings of the walking-beam furnace. The detailed design of the furnace also can be found in Appendix A. The furnace is installed with three natural gas-fueled burners. The steel-bar stock is brought to the furnace by a conveyor auto-feeding system. The operating conditions including temperature and cycle time are set corresponding to size of the steel bars. The operating temperature can be attained by means of automatically adjusting the amounts of natural gas and oxygen supplied for burning. The three burners are installed within the furnace at the locations shown in Figure 2.13. According to the burner

locations, three different heating zones are indicated as specified by Zone 1, Zone 2 and Zone 3 in the Figure.. It should be noted that steel-rod stock is subject to heat exposure in Zone 2 greater than those in Zone 1 and Zone 3.

Figure 2.11 BSK's Walking-beam furnace
(Courtesy of Bangkok Spring Industrial Co., Ltd.)

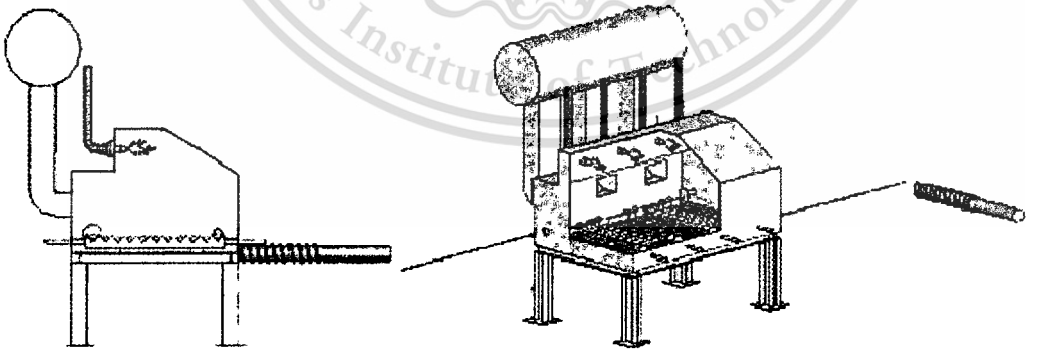

Figure 2.12 Interior of walking-beam furnace
(Courtesy of Bangkok Spring Industrial Co., Ltd.)

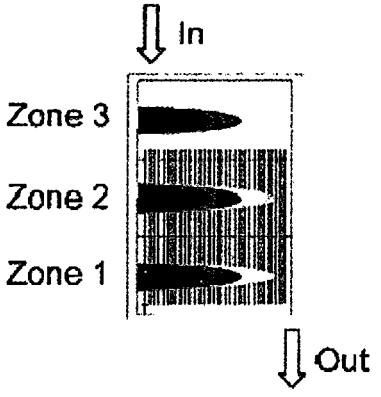

Figure 2.13 Locations of burners and heating zones

2.3.4 Characteristics of Efficient Furnace

Furnace should be designed so that in a given time, as much of material as possible can be heated to an uniform temperature as possible with the least possible fuel and labor. To achieve this end, the following parameters can be considered [9]:

- Determination of the quantity of heat to be imparted to the material or charge.
- Liberation of sufficient heat within the furnace to heat the stock and overcome all heat losses.
- Transfer of available part of that heat from the furnace gases to the surface of the heating stock.
- Equalization of the temperature within the stock.
- Reduction of heat losses from the furnace to the minimum possible extent.

2.3.5 Possibilities for Furnace Performance Improvement

The heating operation of a furnace may be improved in terms of energy efficiency and productivity by considering the following issues:

Measurement problems. Measurements serve to provide information from the process both for monitoring and for control. For an efficient operation of a furnace, knowledge of values for a number of variables is essential, e.g. furnace gas and wall temperatures, stock temperatures, fuel and combustion air flows, oxygen content of exhaust gas and position of each stock item in the furnace. The temperature of each stock item and the temperature distribution within the items should be available.

However, the furnace environment poses problems:

- Sensors placed directly on the stock are not feasible
- Indirect measurements by radiation pyrometers are disturbed by side radiation.

To overcome these problems, a model describing the heating operation can be used on-line to estimate the surface and inner temperatures of the items [11]. Furnace and gas temperatures, fuel flow rates, stock data, and stationary data for the furnace serve as input to the model.

Control authority. The purpose of furnace control is to govern the heat production to give the stock the correct temperature. The control variables available are burner fuel and airflows, or more indirectly zone temperature set-points for burner regulators. Also, maximum burner capacity and constraints on heat flow per unit of stock surface are factors, which must be considered.

Reduction of Fuel Use by Optimization of Combustion Efficiency [11]. Precise control of the combustion process is essential both for fuel economy and for reduction of pollutant emissions to the atmosphere. Accurate combustion control includes the ability to keep the value of oxygen in the flue gas close to optimum, which enables a lower and more stable excess air factor.

Reduction of Fuel Use by Optimization of Furnace Heating Profile [11]. Each type of steel should be heated according to a specific heating rate in order to arrive at the required temperature. The heating should take place as far away as possible from the furnace charging side. This tends to lower the exhaust gas temperature and hence increase the energy efficiency. By means of furnace energy balance, it is possible to analyze the effect on the fuel consumption when the exhaust gas temperature is lowered, see Figure 2.14.

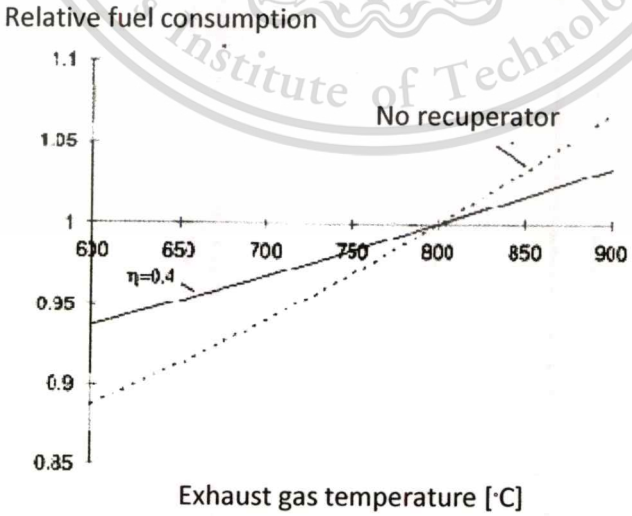

Figure 2.14 Fuel consumption as a function of variation in exhaust gas temperature for a steel reheating furnace [11]

Reduction of Fuel Use by Improvement of Temperature Accuracy [11]. Using unnecessarily high furnace temperatures to avoid insufficient heating of the stock may result in excess stock temperature, directly leading to lower energy efficiency. By computer control, it is possible to achieve a more accurate temperature of the reheated stock items. This can result in reduction of the stock excess heat and hence reduction of fuel use.

Reduction of Fuel Use by Adaptation of Heating to Production Rate [11]. During a delay or at reduced throughput rates, the furnace temperature rises which leads to increased energy losses and excess heating of the stock. By automatic control, it is possible to calculate and apply lower temperature set-points during the delay and period of reduced throughput rates. This would lead to less fuel use and eliminate the risk of overheating.

2.4 Fuel

Fuels are chemical substances, which may be burned in oxygen to generate heat. They mainly consist of carbon and hydrogen and sometimes a small amount of sulfurs or minerals, and may be solid, liquid or gaseous. Coal and coke are examples of solid fuels. Petroleum oils are usually a mixture of several liquid fuels. Gaseous fuels may be a mixture of gases such as methane, ethane and so on. For industrial applications, various types of fuel are available for firing in boilers, furnaces and other combustion equipment. The selection of right type of fuel depends on various factors such as availability, storage, handling, pollution and landed cost of fuel. The knowledge of fuel properties is helpful in selecting the right fuel for the right purpose and efficient use of the fuel.

2.4.1 Classification of Fuel

Fuels can be classified, according to their physical state, into three classes: solid fuels, liquid fuels and gaseous fuels [12]. Solid fuels. Solid fuel is a term given to various types of solid materials that provide energy. This energy is usually released by combustion. Solid fuels include wood and other matter containing cellulose, peat, lignite or brown coal, bituminous coal, anthracite, charcoal and coke. Most of solid fuels left some ash or residues after combustion.

Liquid fuels. Most liquid fuels are derived from fossil fuels. They can be classified according to their volatility. The most volatile fuels are gasoline and kerosene. Less volatile fuels are used in diesel engines and residual fuels, of varying viscosities, are often used in boilers. Liquid fuels are also known as "hydrocarbon oils" because they are distilled from petroleum, which contains hydrogen and

carbon. The main substances into which natural petroleum is thus separated are: light naphtha, gasoline, heavy naphtha, paraffin oil, lubricating oil, vaseline and paraffin wax. The residue is a black, pitch-like substance known as petroleum pitch used in the making of roads.

Gaseous fuels. Gas is a preferred fuel, the combustion of which offers more environmental friendliness over the other fossil fuels. It burns more readily and completely than other fuels. Gaseous fuels are the most convenient, requiring the least amount of handling and are the most maintenance free. Gas is odorless and colorless. Because gaseous fuels are in a molecular form, they are easily mixed with the air as required for combustion, and are oxidized in less time than is required to burn other types of fuel. There are different kinds of gaseous fuels, including natural gas, producer gas, coal gas, blast furnace gas, acetylene, etc.

In the manufacturing process of coil springs at Bangkok Spring Industrial Co., Ltd. (BSK), compressed natural gas (CNG) is used as fuel for providing heat to steel bars in a walking-beam furnace. Thus, a brief introduction to this type of fuel is also given here.

2.4.2 Natural Gas

Natural gas is obtained along with liquid petroleum in large amounts from oil producing wells. It is also called "marsh gas". Its main constituents are methane, ethane and other hydrocarbons. If lower hydrocarbons like methane and ethane are present, the natural gas is called dry or lean. If higher hydrocarbons are present along with methane, the natural gas is called rich or wet. Characteristics of Natural Gas. Natural gas is a mixture of hydrocarbon gases along with some impurities such as water and heavier hydrocarbons. The hydrocarbon gases normally found in natural gas are methane, ethane, propane, butanes, pentanes and small amounts of hexanes, heptanes, octanes and the heavier gases. The natural gas for sale is mostly mixture of methane and ethane with some small percentage of propane. Methane is usually the largest percentage. The average composition of natural gas is given is Table 2.1. The calorific value varies from 8,000 – 14,000 kcal/m3 [13].

Table 2.1 Composition of natural gas

Compound	Weight composition (%)
Methane	88.5
Ethane	5.5
Propane	3.7
Butane	1.8
Pentane	0.5

Natural gas is normally thought of as being a mixture of straight-chain or paraffin hydrocarbon gases. However, cyclic and aromatic hydrocarbon gases are occasionally found in the mixture. Physical Properties of Natural Gas. Natural gas is colorless, odorless, nontoxic and non-poisonous. It is lighter than air (a specific gravity between 0.5 and 0.8 times of air) and is combustible in air at a concentration of 5 – 15% with an autoignition temperature of 537 – 540°C. The overall physical properties of a natural gas are indicators of the behavior of the gas under various processing conditions, and it is therefore important to be able to establish these physical properties. In most practices, the analysis or composition of gas must be determined first, then the various physical properties can be determined by using the physical properties of each pure component in the mixture. Physical properties that are most useful in natural gas processing are molecular weight, freezing point, boiling point, density, critical temperature, critical pressure, heat of vaporization and specific heat.

The Main Uses of Natural Gas. Due to the variety of natural gas constituents, it finds wide application either as an energy source or as feedstock to the chemical/petro-chemical industries [14]:

- As an energy source, natural gas competes with petroleum products, notably fuel oils, diesel and liquefied petroleum gas (LPG). It is less expensive, burns cleaner and is more abundant than all these other fuels.
- As a feedstock to chemical/petrochemical industries, natural gas and natural gas liquid are used to manufacture a gamut of intermediate chemicals and finished products such as ammonia, oxoalcohols, chloromethanes, methanol, fertilizers, etc.
- As a residential fuel in temperate countries, because of the climatic conditions, a sizeable gas market exists in the distribution of natural gas for domestic heating and cooking, and for refrigeration and air conditioning.

2.4.3 Compressed Natural Gas

Compressed natural gas (CNG) is a popular form of high-pressured natural gas, widely used as fuel for vehicles. CNG is considered as an ideal environmentalfriendly fuel, causing minimum pollution and greenhouse effect compared to other conventional fuels. It is produced by pressing natural gas up to 3,600 psi in tanks (less than 1% of the volume it occupies at standard atmospheric pressure. It is stored and distributed in hard containers at a pressure of 2,900 – 3,600 psi, usually in cylindrical or spherical shapes. CNG is now widely used as a substitute for gasoline, diesel and liquefied petroleum gases (LPG). It may also be mixed with biogas, produced from landfills or

wastewater, which does not increase the concentration of carbon in the atmosphere. CNG's volumetric energy density is estimated to be 42% of liquefied natural gas's (LNG) and 25% of diesel.

Advantages of CNG. CNG mixes easily and evenly in air being a gaseous fuel. It is less likely to auto-ignite on hot surfaces, since it has a high auto-ignition temperature (~ 540°C) and a narrow range (5 – 15%) of flammability. CNG emits significantly pollutants such as carbon dioxide (CO_2), hydrocarbons, carbon monoxide (CO), nitrogen oxides (NO_x), sulfur oxides (SO_x) and particulate matters, compared to gasoline. Due to lower CO_2 and NO_x emissions, switching to CNG can help mitigate greenhouse gas emissions. The ability of CNG to reduce greenhouse gas emissions over the entire fuel lifecycle will depend on the source of the natural gas and the fuel it is replacing. The lifecycle greenhouse gas emissions for CNG is given an average value of 67.70 grams of CO_2-equivalent per megajoule (gCO_2e/MJ). CNG produced from landfill biogas has been reported to have the lowest greenhouse gas emissions of any fuel with a value of 11.26 gCO_2e/MJ (over 88% lower than conventional gasoline) in the low-carbon fuel standard [15].

Disadvantages of CNG. Since it is a compressed gas, rather than a liquid like gasoline, CNG take up more space for each gasoline gallon equivalent. Therefore, the tanks used to store the CNG usually take up additional space (especially in a car or a pick up run on CNG).

2.4.4 Heating Value

Heating value (HV), or calorific value (CV), or energy value of a fuel is the amount of heat released during the combustion of a specified amount of it. The heating value is a characteristic for a fuel. It is measured in units of energy per unit mass of the fuel, such as kJ/kg and kcal/kg. The heating value for fuels is expressed as the higher heating value (HHV), lower heating value (LHV), gross heating value (GHV), or net heating value (NHV), Higher Heating Value (HHV). The higher heating value is determined by bringing all the products of combustion back to the original pre-combustion temperature, which is often a temperature of 25 °C. It takes into account the latent heat of vaporization of water in the combustion products. In other words, its value is the same as the thermodynamic heat of combustion.

Lower Heating Value (LHV). The lower heating value is determined by subtracting the heat of vaporization of water from the higher heating value. The LHV assumes that the latent heat of vaporization of water in the fuel and the combustion products is not recovered.

The difference between the values of HHV and LHV depends on the chemical composition of the fuel, and is due to the heat of vaporization of water. Thus,

$$HHV = LHV + \frac{(m_{water} \times h_{fg})}{m_{fuel}} \quad (2.1)$$

Where

m_{water} = Mass of liquid water in the combustion products

m_{fuel} = Mass of fuel

h_{fg} = Latent heat of vaporization of water

Gross Heating Value (GHV). The gross gas heating values are reported either as dry or saturated values. The dry result assumes that the gas contained no water prior to combustion. The saturated result assumes that the gas is saturated with moisture at standard temperature and pressure prior to combustion. The saturated result accounts for the difference in heat released during a complete and ideal combustion of the gas that includes the heating value (enthalpy of condensation) of water. All water formed by the reaction condenses to a liquid.

Net Heating Value (NHV). The net heating value represents the heat released from the total, ideal combustion of the gas at standard temperature and pressure where all the water formed by the reaction remains in the vapor stage. The condensation of excess water vapor does not contribute to the heating value.

2.4.5 Heating Value of Natural Gas

The heating value of natural gas is usually reported as gross or net value. The gross heating value of natural gas is calculated from analysis of the natural gas by:

$$\text{GHV} = \sum_{i=1}^{n} (w_i \times GHV_i) \quad (2.2)$$

where w_i = Mass fraction of pure component i in the natural gas

GHV_i = Gross heating value of pure component i (KJ/Kg)

n = Number of pure components

2.5 Combustion

The burning of a substance is called combustion. It is a sequence of exothermic chemical reactions, i.e. reactions, which give out heat to the surroundings, between a fuel and an oxidant. It is followed by the release of heat and light, in the form of either glowing or a flame, at a rapid rate, thus

the temperature rises. In combustion of fuel, atoms of carbon, hydrogen and other elements combine with atoms of the oxidant with the simultaneous liberation of heat at a rapid rate. This energy is liberated due to the formation of new compounds having less energy in them, thus the energy (heat) released during combustion process is the difference in energy of reactants and that of products generated. Thus, combustion may be represented symbolically by:

$$Fuel + Oxidant \longrightarrow Production + Heat \qquad (2.3)$$

(more heat) (less heat)

In combustion processes, the oxidant is usually air, but could be pure oxygen an oxygen mixture or a substance involving some other oxidizing element such as fluorine. Here, the attention is limited to combustion of a fuel with air or pure oxygen.

Complete combustion of a fuel is possible only in the presence of an adequate supply of oxygen. Oxygen (O_2) is one of the most common elements on earth making up 20.9% of air. Rapid fuel oxidation results in large amount of heat. Solid or liquid fuels must be changed to a gas before they will burn. Usually, heat is required to change liquids or solids into gases. Gaseous fuels will burn in their normal state if enough air is present. Most of the 79% of air (that is not oxygen) is nitrogen, with traces of other elements. Nitrogen (N_2) is considered to be a temperature reducing diluter that must be present to obtain the oxygen required for combustion. Nitrogen reduces combustion efficiency by absorbing heat from the combustion of fuels and diluting the fuel gases. This reduces the heat available for transfer through the heat exchange surfaces. Nitrogen also increases the volume of combustion byproducts. It can combine with oxygen, particularly at high flame temperatures, to produce oxides of nitrogen (NO_x), which are toxic pollutants.

Complete and Incomplete Combustions [16]. Complete combustion is almost impossible to achieve. In reality, as actual combustion reactions come to equilibrium, a wide variety of major and minor species will be present, such as carbon monoxide (CO) and pure carbon (soot and ash). Additionally, any combustion in atmospheric air will also create several forms of nitrogen oxides.

In a complete combustion reaction, a fuel reacts with oxygen and the products are compounds of each element in the fuel with oxygen. Carbon (C), hydrogen (H) and sulfur (S) in the fuel combines with oxygen to form carbon dioxide (CO_2), water vapor (H_2O) and sulfur dioxide (SO_2), releasing 8,084 kcals, 28,922 kcals and 2,224 kcals of heat, respectively:

$$C + O_2 \longrightarrow CO_2 + 8{,}084 \text{ kcals/kg of carbon} \quad (2.4)$$
$$2H_2 + O_2 \longrightarrow 2H_2O + 28{,}922 \text{ kcals/kg of hydrogen}$$
$$S + O_2 \longrightarrow SO_2 + 2{,}224 \text{ kcals/kg of sulfur}$$

Incomplete combustion will only occur when there is not enough oxygen to allow the fuel to react completely to produce carbon dioxide and water. Under certain condi-tions, carbon may also combine with oxygen to form carbon monoxide, which results in the release of a smaller quantity of heat (2,430 kcals/kg of carbon):

$$2C + O_2 \longrightarrow 2CO + 2{,}430 \text{ kcals/kg of carbon} \quad (2.5)$$

Carbon burned to CO2 will produce more heat per unit of fuel than when CO, or smoke, is produced. Each kilogram of CO formed means a loss of 5,654 kcals of heat (8,084 – 2,430).

Three T's of Combustion [16]. The objective of good combustion is to release all of the heat in the fuel. This is accomplished by controlling the "three T's" of combustion, which are:

(1) Temperature high enough to ignite and maintain ignition of the fuel

(2) Turbulence or intimate mixing of the fuel and oxygen

(3) Time, sufficient for complete combustion

Natural gas generally consists of carbon and hydrogen. Water vapor is a byproduct of burning hydrogen. This removes heat from the flue gases, which would otherwise be available for more heat transfer. Natural gas contains more hydrogen and less carbon per kg than fuel oils and as such produces more water vapor. Consequently, more heat will be carried away by exhaust while firing natural gas.

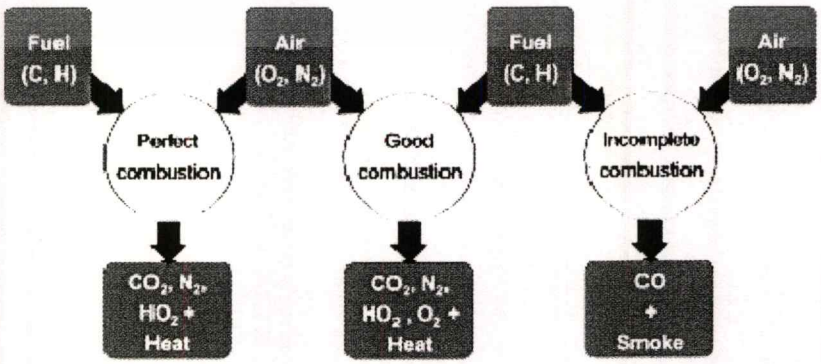

Figure 2.15 Possible modes of fuel combustion in air (Redrawn from [16])

When a fuel is burned in air, the combustion process could possibly take place as perfect combustion, good combustion and incomplete combustion, as shown in Figure 2.15. Too much, or too little fuel with the available combustion air may potentially result in unburned fuel and carbon monoxide generation. A very specific amount of oxygen is needed for perfect combustion and some additional (excess) air is required for complete combustion. However, too much excess air will result in heat and efficiency losses. Not all of the fuel is converted to heat. Usually, all of the hydrogen in the fuel is burned and most fuels, allowable with today's air pollution standards, contain little or no sulfur, so the main challenge in combustion efficiency is directed toward unburned carbon (in the form of ash or incompletely burned gases), which forms carbon monoxide instead of carbon dioxide.

2.5.1 Combustion of Hydrocarbon [17]

Generally, the chemical equation for stoichiometric combustion of hydrocarbon (C_xH_y) in oxygen is:

$$C_xH_y + (x + \frac{y}{4})O_2 \longrightarrow xCO_2 + \frac{y}{2}H_2O \quad (2.6)$$

For example, the combustion of methane (CH4) in oxygen is:

$$CH_4 + 2O_2 \longrightarrow CO_2 + 2H_2O \quad (2.7)$$

For incomplete combustion of hydrocarbon in oxygen, the stoichiometric chemical equation is as follows:

$$zC_xH_y + z(\frac{x}{2} + \frac{y}{4})O_2 \longrightarrow \frac{zx}{3}CO_2 + \frac{zy}{2}H_2O + \frac{zx}{3}C + \frac{zx}{3}CO \quad (2.8)$$

For example, the incomplete combustion of methane in oxygen is:

$$6CH_4 + 9O_2 \longrightarrow 2CO_2 + 12H_2O + 2C + 2CO \quad (2.9)$$

If the combustion takes place in air, the nitrogen can be added to the equation to show the composition of the flue gas:

$$C_xH_y + (x + \frac{y}{4})O_2 + 3.76(x + \frac{y}{4})N_2 \longrightarrow xCO_2 + \frac{y}{2}H_2O + 3.76(x + \frac{y}{4})N_2 \quad (2.10)$$

For example, the combustion of methane in air is:

$$CH_4 + 2O_2 + 7.52\,N_2 \longrightarrow CO_2 + 2H_2O + 7.52\,N_2 \quad (2.11)$$

2.5.2 Combustion of Methane [17]

Combustion of Methane in Oxygen. Consider the complete combustion of methane (CH_4) in pure oxygen (O_2),

$$CH_4 + 2O_2 \longrightarrow CO_2 + 2H_2O \quad (2.12)$$

The equation states that:

- A methane molecule reacts with four atoms of oxygen to yield carbon dioxide (CO_2) and water (H_2O).
- One mole of methane reacts with two moles of oxygen to form one mole of carbon dioxide and two moles of water.
- 44 kgs of carbon dioxide are produced for every 16 kgs of methane that are consumed.

Other observations may be made with respect to the above equation. There are 2 moles of water in the 3 moles of combustion products; therefore, the mole fractions (x) of water and carbon dioxide in the combustion products are respectively:

$$x_{water} = \frac{2}{3} = 0.67 \quad (2.13)$$

$$x_{carbon\ dioxide} = \frac{1}{3} = 0.33$$

There are 36 mass units of water and 44 mass units of carbon dioxide in the 80 mass units of the combustion products. The mass fractions (w) of water and carbon dioxide are respectively:

$$w_{water} = \frac{36}{80} = 0.45 \quad (2.14)$$

$$w_{carbon\ dioxide} = \frac{44}{80} = 0.55$$

Combustion of Methane in Air. Consider the complete combustion of methane in air,

$$CH_4 + 2O_2 + 7.52\,N_2 \longrightarrow CO_2 + 2H_2O + 7.52\,N_2 \quad (2.15)$$

One mole of methane is involved in this equation as well as in the combustion of methane in pure oxygen. Since the same amount of fuel is present in both cases, both reactions release the same amount of energy. However, the presence of nitrogen acts to dilute the reaction, both chemically and thermally. With air as oxidizer, there are 2 moles of water vapor per 10.52 moles of combustion

products, compared with 2 moles of water per 3 moles of products for combustion in oxygen. Similarly, with air, there are a mass fraction of CO_2 of 0.1514 and a carbon mass fraction of 0.0413 in the combustion products, compared with 0.55 and 0.15, respectively, for combustion in oxygen.

When combustion is in air, the diluting energetic effect of nitrogen may be reasoned as follows. Since the same amount of fuel is completely consumed in both reactions, the same amount of energy is therefore released. However, the non-reacting nitrogen molecules in the air have heat capacity. This added heat capacity of nitrogen molecules absorbs much of the energy released, resulting in a lower internal energy per unit mass of products; and hence a lower temperature of the products. Thus the energy released by the reaction is shared by a greater mass of combustion products when the combustion is in air.

2.5.3 Air – Fuel Ratio

The quantity of oxygen or air supplied must be known for complete combustion of a given quantity of fuel. This information is required in sizing fans and ducts that supply oxygen or air to combustion chambers.

The mass air - fuel ratio, A/F, or oxygen - fuel ratio, *O/F*, for complete combustion may be determined by calculating the masses of oxygen and fuel from the reaction equation of methane combustion in air:

$$CH_4 + 2O_2 + 7.52\,N_2 \quad CO_2 + 2H_2O + 7.52\,N_2 \tag{2.16}$$

The *A/F* for methane is

$$\left(\frac{A}{F}\right)_{\text{methane}} = \frac{(2)(32)+(7.52)(28)}{12+4} = 17.16 \tag{2.17}$$

and the *O/F* is

$$\frac{O}{F} = \frac{(2)(32)}{12+4} = 4 \tag{2.18}$$

Thus, 4 kg of O_2 or 17.16 kg of air must be supplied for each kilogram of methane completely consumed. The calculated values are known respectively as "theoretical" *O/F* and *A/F* ratios for methane. These ratios indicate that, if less than the stoichiometric amount of air is supplied, unburned fuel will be contained in the combustion products. Regardless of the magnitude of *A/F*, the combustion is said to be incomplete (when unburned fuel remains in the products, including carbon, carbon monoxide, or hydrogen). Because air is free and fuel is expensive, it is important to burn all of the fuel by using more air than the theoretical air - fuel ratio indicates is needed. Thus burners should operate with "excess air".

Excess Air. Excess air is defined as the difference between the actual and the theoretical air supplied. The percentage of excess air is defined as:

$$\%\ excess\ air = \frac{\left(\frac{A}{F}\right)_{actual} - \left(\frac{A}{F}\right)_{theoretical}}{\left(\frac{A}{F}\right)_{theoretical}} \times 100 \tag{2.19}$$

where $(A/F)_{actual}$ is the actual air - fuel ratio used in a burner, which is stated as a percentage of the theoretical air - fuel ratio:

$$\left(\frac{A}{F}\right)_{actual} = \frac{\%\ theoretical\ air \times \left(\frac{A}{F}\right)_{theoretical}}{100} \tag{2.20}$$

For methane, 120% theoretical air is usually applied, implying an actual mass air – fuel ratio of:

$$\left(\frac{A}{F}\right)_{actual} = \frac{120 \times 17.16}{100} = 20.59 \tag{2.21}$$

and the percentage of excess air is calculated as

$$\%\ excess\ air = \frac{20.59 - 17.16}{17.16} \times 100 = 20\ \% \tag{2.22}$$

Note also that the following general result is yielded

$$\%\ excess\ air = \%\ theoretical\ air - 100\ \% \tag{2.23}$$

Equivalent ratio. Equivalent ratio (Φ) is a measure of how much fuel is actually supplied for a given amount of air. It is defined based on fuel – air ratios (F/A), the inverse of the air – fuel ratio (A/F) as

$$\phi = \frac{\left(\frac{F}{A}\right)_{actual}}{\left(\frac{F}{A}\right)_{theoretical}} = \frac{\left(\frac{A}{F}\right)_{theoretical}}{\left(\frac{A}{F}\right)_{actual}} \tag{2.24}$$

$$\phi = \frac{100}{\%\ theoretical\ air}$$

Thus, for methane, 20% excess air, or 120% theoretical air, corresponds to anequivalent ratio of:

$$\phi = \frac{100}{120} = 0.833 \tag{2.25}$$

Note that the mixture of air and fuel is called "lean" when $\Phi < 1$ and "rich" when $\Phi > 1$.

2.5.4 Combustion Efficiency [17]

The performance of a burner is typically measured by combustion efficiency, η, which is a measure of combustion completeness. It describes the efficiency of conversion of the chemical energy of fuel into sensible enthalpy in the products. In general, the combustion efficiency is defined based on heat release as:

$$\eta = \frac{Actual\ heat\ release}{Theoretical\ heat\ release} \times 100\ \% \tag{2.26}$$

The theoretical heat release is calculated from heating values (or calorific values) of fuel. The actual heat release is somewhat difficult to measure. Instead, composition of exhaust gas is measured, which gives information on products of incomplete combustion. The quantity of constituents in the exhaust gas is then used for indication of the actual heat release:

$$Actual\ heat\ release = Theoretical\ heat\ release - Exhaust\ heat\ loss$$

Thus, the combustion efficiency can be rewritten as:

$$\eta = (1 - \frac{Exhaust\ heat\ loss}{Theoretical\ heat\ release}) \times 100\ \% \tag{2.27}$$

$$\eta = 100\ \% - (\frac{Exhaust\ heat\ loss}{Theoretical\ heat\ release} \times 100\ \%)$$

Exhaust heat loss is calculated using gas concentration and temperature measurements from combustion analysis, and using the fuel's specifications for chemical composition and heat content. The exhaust heat loss is primarily from the heated dry exhaust gases (CO_2, CO, N_2, O_2 and S) and from water vapor formed from the reaction of hydrogen in the fuel with O_2 in the air. Others can be included, such as heat loss from moisture in the air and fuel and losses from the formation of CO rather than CO_2. The exhaust heat loss is determined according to the following equation:

$$Exhaust\ heat\ loss = L_g + L_H + L_m + L_{CO} \tag{2.28}$$

where

L_g = Heat loss due to dry gas (CO_2, CO, N_2, O_2, S)

L_h = Heat loss from burning hydrogen

L_m = Heat loss due to moisture in fuel

L_{CO} = Heat loss from the formation of CO

Heat joss due to dry gas (L_g). The following equation is used:

$$L_g = W_g \times C_p \times (T_{exhaust} - T_{supply}) \quad (2.29)$$

where W_g is weight of the exhaust gas per unit mass of fuel, C_p is specific heat of the exhaust gas, Texhaust and Tsupply are exhaust gas temperature and supply air temperature, respectively.

The weight of the exhaust gas per unit mass of fuel, W_g, can be calculated from:

$$W_g = \left(\frac{44CO_2 \times 32O_2 \times 28N_2 \times 28CO}{12\,(CO_2 + CO)} \right) \times \left(C_b + \frac{12 \times 5}{32} \right) \quad (2.30)$$

where CO_2, CO, N_2, O_2, and S are gas concentrations of CO_2, CO, N_2, O2 and S in percentage. The coefficients 44, 32, 28 are the molecular weights of constituents. C_b is the carbon content, specific to fuel. The specific heat of the exhaust gas, C_p, varies with temperature and its ultimate value is seemingly independent on type of fuel. The value of C_p (in kcal/kg- °C) may be estimated from the following simple equation:

$$C_p = 0.24 + 0.000038\,(T_{exhaust} - 200) \quad (2.31)$$

Heat loss from burning hydrogen (due to H_2O from combustion of hydrogen, L_h). The following equation is used:

$$L_h = 8.936 \times H \times (h_l - h_{rw}) \quad (2.32)$$

where 8.936 = Weight of water formed for each hydrogen atom

H = Fractional hydrogen content of the fuel

h_l = Enthalpy of water at the exhaust temperature and pressure

h_{rw} = Enthalpy of water as a saturated liquid at fuel supply temperature

Heat loss due to moisture in fuel (L_m). The following equation is used:

$$L_m = F_m \times (h_l - h_{rw}) \quad (2.33)$$

where F_m = Fractional fuel moisture or weight ratio of moisture in the fuel, usually obtained from the fuel supplier.

h_l = Enthalpy of water at the exhaust temperature and pressure

h_{rw} = Enthalpy of water as a saturated liquid at fuel supply temperature

Heat loss from the formation of carbon monoxide (L_{co}). The following equation is used:

$$L_{co} = \frac{CO}{CO + CO_2} \times C_b \times 10.720 \quad (2.34)$$

where CO_2 and CO are gas concentrations (in percentage) of CO_2 and CO in the exhaust gas. C_b is carbon content, specific to fuel.

Siegert Formula [18]. The Siegert formula is widely used in Europe to determine combustion efficiency:

$$\eta = 100\,\% - \left(\frac{A}{21 + O_2}\right) \times (T_{exhaust} - T_{supply}) \times 100\,\% \quad (2.35)$$

where O_2 is volumetric concentration of O_2 (in percentage) in the exhaust gas. A and B are Siegert constants, depending on type of fuel. Typically, for natural gas, $A = 0.66$ and $B = 0.009$. $T_{exhaust}$ and T_{supply} are exhaust gas temperature and supply air temperature, respectively.

2.5.5 Furnace Efficiency

The purpose of a heating process is to introduce a certain amount of thermal energy into a material, raising it to a temperature to prepare it for additional processing or change its properties. To carry out this, the material is heated in a furnace. This results in energy losses in different areas and forms. For most furnaces, a large amount of the heat supplied is wasted in the form of exhaust gases. Other losses include [18]:

- Heat storage in the furnace structure
- Losses from the furnace outside walls or structure
- Heat transported out of the furnace by the load conveyors, fixtures, trays, etc.
- Radiation losses from openings, hot exposed parts, etc.
- Heat carried by the cold air infiltration into the furnace
- Heat carried by the excess air used in the burners.

Stored Heat Loss. The structure and insulation of the furnace must be heated so their interior surfaces are about at the same temperature as the material they contain. This stored heat is held in the structure until the furnace shuts down, then it leaks out into the surrounding area. The more frequently

the furnace is cycled from cold to hot and back to cold again, the more frequently this stored heat must be replaced. Fuel is consumed with no useful output.

Wall Losses. Wall or transmission losses are caused by the conduction of heat through the walls, roof, and floor of the furnace. Once that heat reaches the outer skin of the furnace and radiates to the surrounding area or is carried away by air currents, it must be replaced by an equal amount taken from the combustion gases. This process continues as long as the furnace is at an elevated temperature.

Material Handling Losses. The equipment used to convey the material into and out of the furnace chamber can lead to heat losses. Conveyor belts or product hangers that enter the heating chamber cold and leave it at higher temperatures drain energy from the combustion gases.

Cooling Media Losses. Water or air cooling protects rolls, bearings, and doors in hot furnace environments. These components and their cooling media, such as water and air, become the conduit for additional heat losses from the furnace.

Radiation (Opening) Losses. Furnaces operating at temperatures above 540°C might have significant radiation losses. Hot surfaces radiate energy to colder surfaces, and the rate of heat transfer increases with the fourth power of the surface's absolute temperature. At any opening in the furnace enclosure, heat is lost by radiation at a rapid rate.

Waste Gas Losses. Waste-gas loss, also known as *flue gas* or *stack loss*, is made up of the heat that cannot be removed from the combustion gases inside the furnace. The reason is that heat flows from the higher temperature source to the lower temperature heat receiver.

In this research, the Japanese Industrial Standard (JIS) GO702, known as *"Method of heat balance for continuous furnaces for steel"*, is used for the purpose of establishing heat losses and furnace efficiency [9]. According to JIS, the efficiency of a furnace is the ratio of useful output to heat input. The furnace efficiency can be determined by two methods, *direct* and *indirect*.

Direct Method Testing. The efficiency of the furnace, η, can be computed by measuring the amount of fuel consumed per unit mass of material produced from the furnace (stock):

$$\eta = \frac{H_{stock}}{H_{fuel}} \times 100\ \% \tag{2.36}$$

where H_{stock} = Amount of heat in the stock, or heat to be imparted to the stock

H_{fuel} = Amount of heat in the fuel consumed

The amounts of heat in the stock and heat in the fuel can be calculated respectively from the formulas:

$$H_{stock} = m \times C_p \times (T_f - T_i) \quad (2.37)$$

$$H_{fuel} = m \times GHV_{fuel}$$

where m = Mass flow rate of the stock

C_p = Specific heat of the stock

T_f = Final temperature of the stock

T_i = Initial temperature of the stock

GHV_{fuel} = Gross heating value of the fuel

Indirect Method Testing. Similar to the method of evaluating combustion efficiency, furnace efficiency can also be calculated by subtracting sensible heat loss in flue gas, loss due to moisture in flue gas, loss due to evaporation of water formed due to hydrogen in fuel, heat loss due to openings of furnace, heat loss through furnace skin and other unaccounted losses from the input to the furnace. In most industrial furnaces, the loss due to openings of furnace, the loss through furnace skin and the unaccounted loss are very small and can be assumed negligible in the heat balance considerations. Thus, the furnace efficiency is determined by subtracting the sensible heat loss, the loss due to moisture in the fuel and the loss due to hydrogen in the fuel from 100% :

$$\eta = 100\ \% - L_{flue} - L_m - L_h \quad (2.38)$$

where L_{fuel} = Sensible heat loss in the flue gas

L_m = Loss due to moisture in the fuel

L_h = Loss due to hydrogen in the fuel

The *sensible heat loss in the flue gas* is determined from:

$$L_{flue} = \frac{m \times C_p \times (T_{flue} - T_{supply}) \times 100\ \%}{GHV_{fuel}} \quad (2.39)$$

where m = Mass of the flue gas

C_p = Specific heat of the flue gas

T_{flue} = Temperature of the flue gas

T_{supply} = Supply air temperature

GHV_{fuel} = Gross heating value of the fuel

The mass of the flue gas can be calculated from:

$$m = 1 + \{ Theoretical\ air \times (1 \frac{O_2}{21 + O_2}) \} \quad (2.40)$$

where the theoretical air is the amount of air required theoretically to burn a unit mass (1 kg) of the fuel, and O_2 is concentration of oxygen in the flue gas. The specific heat of the flue gas can be assumed to be 0.24 kcal/kg-°C , or may be estimated from:

where C_p = Specific heat of the flue gas (kcal/kg-°C)

T_{flue} = Temperature of the flue gas (°C)

The loss due to moisture in the fuel is determined from:

where M = Amount (in kg) of moisture in 1 kg of the fuel

T_{flue} = Temperature of the flue gas

T_{supply} = Supply air temperature

GHV_{fuel} = Gross heating value of the fuel

The loss due to hydrogen in the fuel is determined from:

$$L_h = \frac{9 \times H_2 \times \{ 584 + 0.45 \times (T_{flue} - T_{supply}) \times 100\ \%}{GHV_{fuel}} \quad (2.41)$$

Where H_2 = Amount (in kg) of hydrogen in 1 kg of the fuel

T_{flue} = Temperature of the flue gas

T_{supply} = Supply air temperature

GHV_{fuel} = Gross heating value of the fuel

2.6 Heat Transfer

Heat transfer concerns the exchange of thermal energy from one system to another. It only occurs because of a temperature-difference driving force and heatflows from the high to the low temperature region. The fundamental modes of heat transfer include [19]:

- Thermal conduction or diffusion, the heat transfer between objects that are in physical contact
- Thermal convection, the heat transfer between an object and its environment due to circular fluid motion
- Thermal radiation, the heat transfer to or from a body by means of emission or absorption of electromagnetic radiation

2.6.1 Thermal Conduction

Heat conduction, or diffusion, represents the process of distribution of thermal energy at direct contact of individual particles of a body or the separate bodies that have different temperatures. On a microscopic scale, heat conduction is caused by movement of particles of a substance. In gases, energy transfer (or heat transfer) is carried out by diffusion of molecules and atoms. In liquids and solid non-conductor bodies, the energy transfer is carried out by elastic waves. In metals, the energy transfer basically is carried out by diffusion of free electrons. Heat conduction is the most significant means of heat transfer within a solid or between solid objects in thermal contact. Liquids and especially gases are less conductive.

Fourier's Law [19]. Fourier's law is known as the law of heat conduction, which states that the time rate of heat transfer through a material is proportional to the negative gradient in the temperature and to the area, at right angles to that gradient, through which the heat is flowing. The Fourier's law is written as:

$$\vec{q} = -k \times \nabla T \tag{2.42}$$

Where $\vec{q}$ = Heat flux (W/m^2)

k = Material's conductivity ($W/m \cdot K$)

∇T = Temperature gradient (K/m)

The thermal conductivity, k, varies with temperature, but, for some common materials, it is often treated as a constant since the variation with temperature is very small over a significant range of temperatures. For many simple applications, the Fourier's law is used in one-dimensional (x-direction) form:

$$q_x = -k \times \frac{dT}{dx} \tag{2.43}$$

2.6.2 Thermal Convection

Heat convection is the transfer of heat from one place to another by the movement of fluids. Convection actually describes the combined effects of conduction and fluid flow, and is usually the dominant form of heat transfer in liquids and gases. There are two types of heat convection, free or natural convection and forced convection.

Free or Natural Convection. In free convection, heat transfer is caused by fluid motion due to buoyancy forces that result from the density variations or variations of temperature in the fluid.

Forced convection. In forced convection, heat is transferred by motion of fluid, which is forced to flow over a surface by external sources such as fans, stirrers and pumps).

Newton's Law of Cooling [20]. The amount of heat transfer by convection can be determined by Newton's law of cooling, which requires a constant heat transfer coefficient. The Newton's law of cooling states that the rate of heat loss of a body is proportional to the difference in temperatures between the body and its surroundings. It is expressed by the following equation:

$$q = h \times (T - T_{env}) \tag{2.44}$$

where

q = Heat flux (W/m^2)

h = Heat transfer coefficient ($W/m^2 \cdot K$)

T = Temperature of the body surface (K)

T_{env} = Temperature of the environment (K)

2.6.3 Thermal Radiation

All bodies constantly emit energy by a process of electromagnetic radiation. The intensity of such energy flux depends upon the temperature of the body and the nature of its surface. The energy emission varies as the forth power of absolute temperature. Very often, the energy emission, or thermal radiation, from cooler bodies can be neglected in comparison with thermal conduction and convection. But, at high temperature, heat transfer processes usually involve a significant fraction of radiation. To calculate heat transfer by thermal radiation, the Stefan-Boltzmann law is applied.

Stefan-Boltzmann Law [20]. When electromagnetic radiation is exchanged between two bodies that are not black, the Stefan-Boltzmann law is applied to calculate the heat flux between the bodies:

$$q = \varepsilon \times \sigma \times (T_1^4 - T_2^4) \quad (2.45)$$

where q = Heat flux ($W/^{m2}$)

ε = Emissivity ($0 \varepsilon < \leq 1$)

σ = Stefan-Boltzmann constant

= 5.6704×10^{-8} $W/m^2 \cdot K^4$

T_1 = Absolute temperature of body 1 (K)

T_2 = Absolute temperature of body 2 (K)

Heat Transfer in Furnaces. In a heating furnace, most of the heat is transferred to the stock, especially steel, by:

- Thermal radiation from the flame, hot combustion products and the furnace walls and roof.
- Thermal convection due to the movement of hot gases over the stock surface

At high temperatures, the dominant mode of heat transfer is wall radiation. Heat transfer by gas radiation is dependent on the gas composition, mainly the carbon dioxide and water vapor concentrations, the temperature and the furnace geometry.

2.7 Material and Energy Balance

In industrial processing operations, the quantities of material and energy can be described by material and energy balances. Such balances are statements on the conservations of mass and energy. If there is no accumulation, what goes into a process must come out. This is true for both batch operation and continuous operation over any chosen time interval. If a unit operation is represented diagrammatically as a box, the mass and energy going into the box must balance with the mass and energy coming out, as shown in Figure 2.16

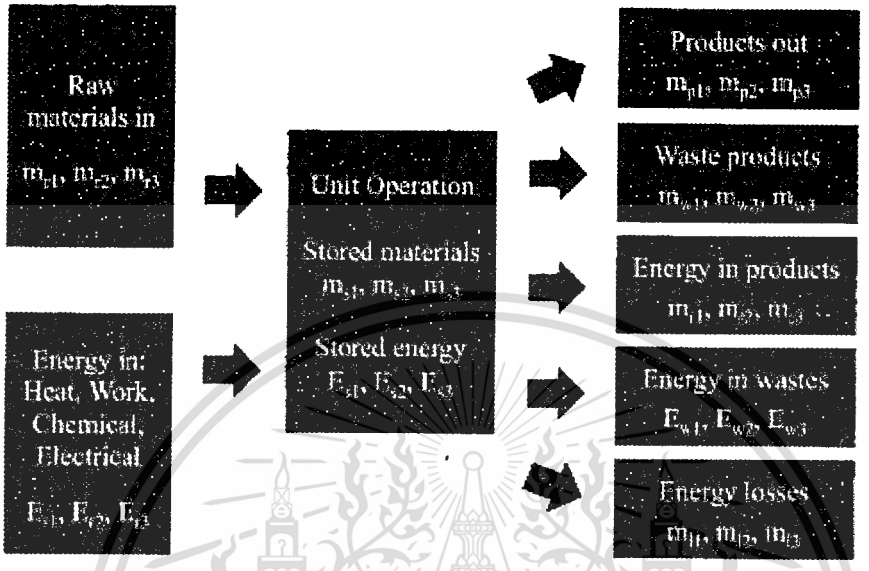

Figure 2.16 Mass and energy balance for a unit operation

By the conservation of mass, a material balance can be written as:

$$Mass\ in = Mass\ out + Mass\ stored \tag{2.46}$$

Appling to Figure 2.16 yields:

$$Raw\ material = Production + Wastes + Stored\ Materials$$

or

$$\sum m_r = \sum m_p + \sum m_w + \sum m_s \tag{2.47}$$

where

$$\sum m_r = m_{r1} + m_{r2} + m_{r3} + \ldots = Total\ raw\ materials$$

$$\sum m_p = m_{p1} + m_{p2} + m_{p3} + \ldots = Total\ raw\ materials$$

$$\sum m_w = m_{w1} + m_{w2} + m_{w3} + \ldots = Total\ raw\ materials$$

$$\sum m_s = m_{s1} + m_{s2} + m_{s3} + \ldots = Total\ raw\ materials$$

where Σ (sigma) denotes the sum of all terms. Similarly, by the conservation of energy, the energy coming into a unit operation can be balanced with the energy coming out and the energy stored. Thus, an energy balance written for the unit operation in Figure 2.16 is:

$$Energy\ in = Energy\ out + Enegy\ stored \tag{2.48}$$

or

$$\Sigma E_r = \Sigma E_p + \Sigma E_w + \Sigma E_l + \Sigma E_s \tag{2.49}$$

where

$$\sum E_r = E_{r1} + E_{r2} + E_{r3} + \ldots = Total\ energy\ entering$$

$$\sum E_p = E_{p1} + E_{p2} + E_{p3} + \cdots = Total\ energy\ leaving\ with\ products$$

$$\sum E_w = E_{w1} + E_{w2} + E_{w3} + \cdots = Total\ energy\ leaving\ with\ wastes$$

$$\sum E_l = E_{l1} + E_{l2} + E_{l3} + \ldots = Total\ energy\ lost\ to\ surroundings$$

$$\sum E_s = E_{s1} + E_{s2} + E_{s3} + \ldots = Total\ energy\ stored$$

Energy balances are often complicated because forms of energy can be interconverted, for example mechanical energy to heat energy, but overall the quantities must balance.

The Sankey Diagram [11]. The Sankey diagram is very useful tool to represent an entire input and output energy flow in any energy equipment or system such as boiler generation, fired heaters, furnaces after carrying out energy balance calculation. It represents visually various outputs and losses so that energy managers can focus on finding improvements in a prioritized manner. For a reheating furnace such as the walking-beam furnace used in the manufacturing processes at BSK, a Sankey diagram may be represented by the diagram shown in Figure 2.17. It is clear that exhaust flue gas losses are a key area for priority attention. Since the furnace operates at high temperatures, the exhaust gas leaves at high temperatures resulting in poor efficiency. Hence a heat recovery device such as air preheater has to be necessarily part of the system. The lower the exhaust temperature, higher is the furnace efficiency [22].

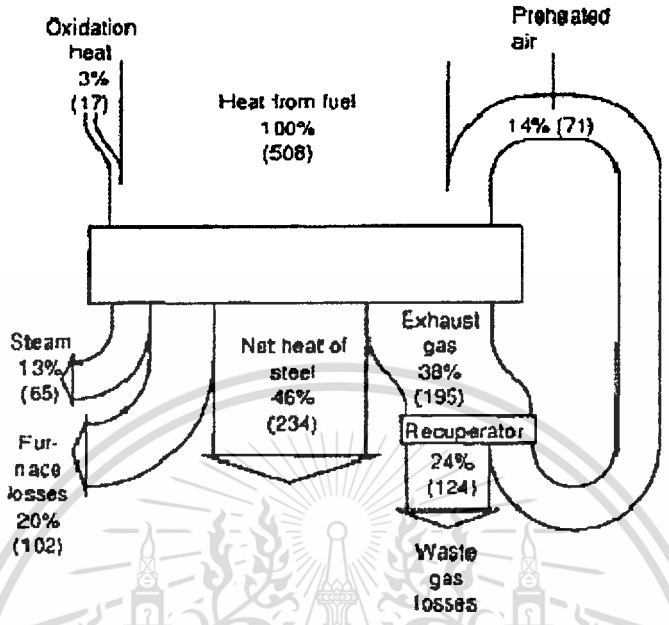

Figure 2.17 Sankey diagram for a typical reheating furnace [11]

2.8 Simulations

2.8.1 Computational Fluid Dynamics (CFD)

Computational fluid dynamics (CFD) is a computer-based tool to simulate the behavior of systems involving fluid flow, heat transfer, mass transfer, and other related physical and chemical processes. The bases of most CFD problems are the Navier-Stokes equations, which can be simplified and linearized to yield equations that can be solved numerically. The most common solution method used in CFD codes is the finite volume technique. After identifying the region of interest of a given problem, this region is divided into small sub-regions. These are called "control volumes" or, more instructively, "grid cells". The flow equations are then solved iteratively for each control volume to gain an approximation of the value of each variable in each grid cell and thus a full picture of the flow in the simulation domain [23].

2.8.2 CFD Codes

CFD codes are structured around the numerical algorithms that can be tackle fluid problems. All CFD codes contain three main elements: (1) Pre-processing, (2) Solver, and (3) Post-processing.

Pre-Processing. This is the first step in building and analyzing a flow model. A pre-processor consists of input of a flow problem by means of an operator. The procedures at the pre-processing stage involve [24]:

- Definition of the geometry of the region, the computational domain
- Grid generation, the subdivision of the domain into a number of smaller, non-overlapping sub domains (or control volumes or elements or cells)
- Selection of physical or chemical phenomena that need to be modeled
- Definition of fluid properties
- Specification of appropriate boundary conditions at cells, which coincide with or touch the boundary. The solution of a flow problem is defined at nodes inside each cell. The accuracy of CFD solutions is governed by number of cells in the grid. In general, the larger numbers of cells better the solution accuracy.

Solver. The CFD solver does the flow calculations and produces the results. FLUENT®, FloWizard®, FIDAP®, CFX® and POLYFLOW® are some of the types of solvers. FLUENT® is used in most industries. To solve Navier–Stokes equations in CFD codes, partial derivatives in the equations are approximated by algebraic expressions, which can be obtained by means of the finite-difference (or finite element) method or the finite volume method. The result is a set of algebraic equations through which mass, momentum, and energy transport are predicted at discrete points in the domain. Because the governing equations are non-linear and coupled, several iterations must be performed before a converged solution is obtained. Each of the iteration is carried out as follows [25]:

(1) Fluid properties are updated in relation to the current solution.

(2) Momentum equations are solved consecutively using the current value for pressure so as to update the velocity field.

(3) Since the velocities obtained in the previous step may not satisfy the continuity equation, one more equation for the pressure correction is derived from the continuity equation and the linearized momentum equations. Once it is solved, it gives the correct pressure so that continuity is satisfied.

(4) Other equations for scalar quantities such as turbulence, chemical species and radiation are solved using the previously updated value of the other variables.

(5) Finally, the convergence of the equations set is checked and all the procedure is repeated until convergence criteria are met.

Post-Processing. This is the final step in CFD analysis, and it involves the organization and interpretation of the predicted flow data and the production of CFD images and animations. The leading CFD software, such as FLUENT® and CFX®, are equipped with versatile data visualization tools, including domain geometry and grid display, vector plots, line and shaded contour plots, 2D and 3D surface plots and particle tracking.

2.8.3 Advantages of CFD

- It costs less than laboratory or field experiments.
- It has a faster than experiments.
- It guides the engineer to the root of problems. It is therefore suitable for troubleshooting.
- It provides comprehensive information about a flow field, especially where measurements are either difficult or impossible to obtain.

2.8.4 Modeling Equations

In simulations of this study, the CFD code ANSYS® FLUENT® is used, which simulates flow based on the Euler equations, simplified versions of the Navier-Stokes equations. For the conservation of mass:

$$\frac{\partial p}{\partial t} + \nabla.(p\vec{v}) = S_m \tag{2.50}$$

For the conservation of momentum:

$$\frac{\partial(p\vec{v})}{\partial t} + \nabla.(p\vec{v}\vec{v}) = -\nabla p + \nabla.\pi + p\vec{g} + \vec{F} \tag{2.51}$$

where S_m is a source term, π is the stress tensor, $\vec{g}$ is the gravitational, and $\vec{F}$ is the external body force, $p, \vec{v}$, and p stand for density, velocity, and pressure, respectively. These equations are valid for laminar flow. ANSYS® FLUENT® also solves the equation of energy conservation:

$$\frac{\partial(pE)}{\partial t} + \nabla.(v(pE+p)) = \nabla.[K_{eff}\nabla T - \sum_i hi\vec{J}t + (\pi_{eff}.v)] + S_h \tag{2.52}$$

where K_{eff} is the effective conductivity, and $\vec{J}$ is the diffusion flux of specie i. The terms on the right represent energy transfer due to conduction, species diffusion, and viscous dissipation, respectively.

S_h includes the heat of chemical reaction and other possible volumetric heat sources that have been defined.

2.8.5 ANSYS® FLUENT® Software : A Brief Introduction

ANSYS® FLUENT® is a general-purpose computational fluid dynamics (CFD) software, which is suitable for incompressible and mildly compressible flows. It utilizes a pressure-based segregated finite-volume method solver and contains physical models for a wide range of applications. ANSYS® FLUENT® can handle any kind of fluid flow and heat transfer problems, including turbulent flows, reacting flows, chemical mixing, combustion, and multiphase flows. The need for modeling and for solving more industrial flow problems with the help of a CFD code determined a strong development of ANSYS® FLUENT® software for various applications, ranging from air flow over an aircraft wing to combustion in a furnace, from bubble columns to oil platforms, from blood flow to semiconductor manufacturing, and from clean room design to wastewater treatment plants [24]. Some of its features include the following:

- Dynamic and Moving Mesh. The user simply sets up the initial mesh and prescribes the motion, while ANSYS® FLUENT® software automatically changes the mesh to follow the motion prescribed. This is useful for modeling flow conditions in and around moving objects.
- Heat Transfer, Phase Change, and Radiation. ANSYS® FLUENT® software contains many options for modeling convection, conduction and radiation.
- Multiphase. It is possible to model several different fluids in a single domain with ANSYS® FLUENT®.
- Turbulence. A large number of turbulence models are used to approximate the effects of turbulence in a wide array of flow regimes.
- Acoustics. The acoustics model allows users perform "on-the-fly" sound calculations.
- Reacting Flows. ANSYS® FLUENT® technology has the ability to model combustion as well as finite rate chemistry and accurate modeling of surface chemistry.
- Post-processing. Users can post-process their data in ANSYS® FLUENT® software, creating among other things (contours, path lines, and vectors) to display the data.

2.9 Literature reviews

Jinwu Kang et.al. (2005) [27] presented hybrid method based on numerical simulation and analytical equations to calculate the radiation, convection and conduction heat transfers in heat treatment processes. In the radiation model view factor between the furnace and work pieces, among work pieces were calculated by the exposed surface area over the total surface area. In the conduction model work pieces were classified into lumped capacitance and massive objects. And work pieces were further classified into three basic shapes: sphere, cylinder and sheet for the application of Fourier differential equation. Natural and forced convections were solved by analytical algorithms for aligned and staggered load patterns. The comparison showed that the calculated results were in good agreement with the experimental results. And the effects of load pattern and work piece quantity were evaluated.

Sang Heon Han et.al (2006) [28] developed numerical program to investigate the heating characteristics of the slab in a bench scale reheating furnace. Its numerical results were validated by comparison with the experimental data obtained in the test facility installed in POSCO company It was found that over 90% of the total heat transfer from the gas to the slab occurred by radiation. Therefore, a very accurate method would be necessary in solving the radiative transfer equation. Numerical method for radiation has to be able to treat gas emission as well as wall emission with appropriate accuracy. In this respects, the finite volume method for radiation was turned out to be very suitable for the simulation of a reheating furnace through the comparison of prediction with experimental results.

Man Young Kim (2007) [29] developed mathematical model for the prediction of heat flux on the slab surface and temperature distribution in the slab by considering the thermal radiation in the furnace chamber and transient heat conduction governing equations in the slab, respectively. The furnace was modeled as radiating medium with spatially varying temperature and constant absorption coefficient. The steel slabs were moved on the next fixed beam by the walking beam after being heated up through the non-firing, charging, preheating, heating, and soaking zones in the furnace. Radiative heat flux calculated from the radiative heat exchange within the furnace modeled using the

FVM by considering the effect of furnace wall, slab, and combustion gases was introduced as the boundary condition of the transient conduction equation of the slab. Heat transfer characteristics and temperature behavior of the slab was investigated by changing such parameters as absorption coefficient and emissivity of the slab. Comparison with the experimental work show that the present heat transfer model works well for the prediction of thermal behavior of the slab in the reheating furnace.

Sang Heon Han et.al. (2008) [30] presented transient radiative heating characteristics of slabs in a walking beam type reheating furnace is predicted by the finite-volume method (FVM) for radiation. The FVM can calculate the radiative intensity absorbed and emitted by hot gas as well as emitted by the wall with curvilinear geometry. The non-gray weighted sum of gray gas model (WSGGM) which is more realistic than the gray gas model was used for better accurate prediction of gas radiation. The block-off procedure was applied to the treatment of the slabs inside which intensity has no meaning. Entire domain was divided into eight sub-zones to specify temperature distribution, and each sub-zone has different temperatures and the same species composition. Temperature field of a slab is acquired by solving the transient 3D heat conduction equation. Incident radiation flux into a slab was used for the boundary condition of the heat conduction equation governing the slab temperature. The movement of the slabs was taken into account and calculation was performed during the residence time of a slab in the furnace. The slab heating characteristics was also investigated for the various slab residence times. Main interest of this study was the transient variation of the average temperature and temperature non-uniformity of the slabs.

Sang Heon Han et.al. (2010) [31] presented numerical analysis of slab heating characteristics in a reheating furnace and User-Define-Function program was developed to process of the movement of slabs. When the mean temperature of a slab emitted to the rolling mill does not change, calculation was considered to have converged and is stopped. This convergence criterion was appropriate for achieving an analytical solution. With the boundary and initial conditions given, over 55 new slabs were inserted to get a converged solution. Skid posts and beams were included in the calculation because they disturb radiation heat transfer from hot combustion gas to the slabs. This article examines what the slabs experience in the furnace before they were emitted to the rolling mill and whether a slab emitted to the rolling mill satisfies the required slab conditions, such as target temperature and skid severity.

CHAPTER 3

INVESTIGATION PROCEDURES

3. Experimental

3.1 Experimental Apparatus

A walking-beam type furnace has been installed in the coil-spring production line of Bangkok Spring Industrial Co., Ltd. (BSK), and is used in the present investigation. The detailed description of the furnace is given in Appendix A. The furnace was equipped with a temperature-measurement system and a gas-sampling bag at the exhaust duct. A schematic diagram of the furnace with the temperature measurement and gas-analysis systems is shown in Figure ure3.1.

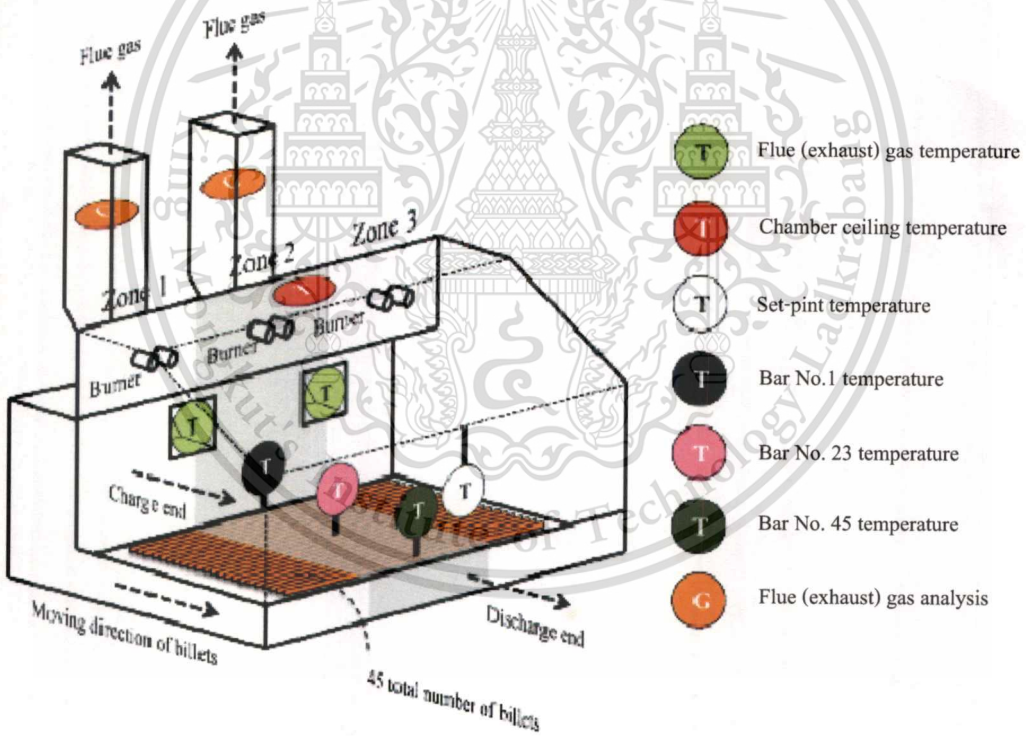

Figure 3.1 Schematic diagram of the experimental system

The heating operation of round bars in the furnace was continuous and was controlled by two parameters: (1) cycle time of the walking beam and (2) set point temperature. To obtain the information on temperature distribution within the furnace chamber, a monitoring system (Datapaq®'s

Furnace Tracker System, Datapaq Ltd.) was employed for online-measurement of temperature with six thermocouples installed at different locations, as shown in the Figure .3.1 The description for each thermocouple is also given in Figure ure3.1. The monitoring system was installed with a data logger (Tpaq21® model, Datapaq Ltd.) having a memory capacity up to 130,000 data points and equipped with type-K thermocouples, which is capable of monitoring a heating process up to 3.5 hours long with an average temperature up to 1,250°C [26The heating area within the furnace chamber can be divided, according to the burner location, into 3 zones: Zone 1, Zone 2 and Zone 3, as shown in Figure ure3.1. Due to the space between both ends of the steel bars and the chamber walls, the zone division does not correspond to an equal-length partition of the bars, i.e. Zone 2 occupies the most part of the bars, while Zone 1 and Zone 3 occupy the rest part equally. This results in a more uniform heating of the billets in the portion occupied by Zone 2. To avoid the effect of non-heating space around the bar ends on the heating behavior of the entire bars, it is more reasonable to define the heating space of observation as scoped to the partition occupied by Zone 2.

3.2 Experimental Procedure

The experimental work in this study can be divided into six main areas:

(1) Investigation of temperature distribution within the heating chamber of furnace operating under no-load condition and load condition

(2) Investigation of temperature profile across the cross-sectional area of heated steel round bar

(3) Simulation implement and indirect measurement of core temperature of heated round bar

(4) Prediction of temperature distribution of heated round bar in the direction of furnace length

(5) Determination of optimum furnace operating parameters for the heating of steel round bars of various sizes

3.2.1. Investigation of Thermal Distribution within the Heating Chamber of Furnace Operating Under No-Load Condition and Load Condition

Without supplying steel bars (Under No-Load Condition), the furnace was given a test run to examine the thermal distribution within its heating chamber and to ensure that it was working

properly. The furnace was operated at a fixed cycle time of 9 seconds for 95 minutes. During the period, several adjustments were made to the set-point temperature settings in the range between 940°C and 980°C. Temperatures at different locations within the furnace chamber were measured on-line by the furnace tracker monitoring system, with respect to the thermocouple positions mentioned in Figure ure3.1. Table 3.1 summarizes the experimental parameters used in the investigation. Table 3.1 Experimental parameters used in the study of section 3.2.1

Table 3.1 Experimental parameters of No-load condition used in the study of section 3.2.1

Walking-beam cycle time (s)	9
Set-point temperature (°C)	940 - 980
Total residence time (s)	95 min (0 - 95 min)

Supplying steel bars (Under Load Condition), the furnace was given a test run to examine the thermal distribution within its heating chamber and to ensure that it was working properly. The furnace was operated at a fixed cycle time of 9 seconds for 35 minutes. During the period, the 17.4 mm. steel rod are fed in to the furnace under 980°C. Temperatures at different locations within the furnace chamber were measured on-line by the furnace tracker monitoring system, with respect to the thermocouple positions mentioned in Figure ure3.1. Table 3.2 summarizes the experimental parameters used in the investigation. Table 3.1 Experimental parameters used in the study of section 3.2.2

Table 3.2 Experimental parameters of load condition used in the study of section 3.2.2

Bar diameter (mm)	ø 17.4 mm.
Walking-beam cycle time (s)	9
Set-point temperature (°C)	980
Total residence time (s)	35 min (95 – 120 min)

3.2.2. Investigation of Temperature Profile across the Cross-sectional Area of Heated Round bar

At any instant of time during the heating of round bar, the round bar score tends to be heated slower than its surface due to radial heat conduction from the surface and skin effects. This results in the presence of temperature distribution across the cross section of the round bar in which a surface-to-core temperature uniformity is often assumed. As a result, the coldest temperature is always located at the core of the round bar and the maximum temperature is always located at its surface. It can be assumed that insufficient heating does not occur if core temperature measured by a thermocouple exceeds the minimum permissible level. Since the austenization temperature of steel must be reached at anywhere within the round bar before quenching the bar in a spray of oil, it is therefore required that the core temperature of the round bar must exceed a predetermined minimum temperature and must be monitored during practices of the heating operation. For SUP 12 steel (with 0.55% carbon content) used in this study, an austenization temperature of 800°C - 820°C is read from the iron-carbon met stable phase diagram in Figure ure2.3. A preliminary investigation suggested that, due to heat loss to the ambient air, a temperature drop of 100°C - 120°C is usually experienced in the heated round bar while being transferred from the furnace outlet to the quenching area. Hence, a core temperature of 940°C in the heated bar leaving the furnace should indicate a sufficient heating to ensure the desired quality in the coil spring product.

A series of experiments were carried out to investigate the behavior of core temperature of round bars while heating in the walking-beam furnace. The heating of round bars having diameters of 10.5 mm, 13.5 mm and 17.4 mm was operated at a fixed cycle time of 9 minutes and set-point temperature of 980°C. Table 3.3 summarizes the experimental parameters used in this investigation. In each experiment, the round bar was equipped with a set of three thermocouples to measure temperatures at its core and its surface and at a position 5 mm away from the surface. The arrangement of these thermocouples over a cross section of the round bar is shown in Figure ure3.2 and Figure ure3.3. It is also assumed that the temperature at any distance (radius) away from the center of the cross section is constant along the entire length of the bar.

Table 3.3 Experimental parameters used in the study of sections 3.2.3

Bar diameter (mm)	10.5 , 13.5 , 17.4
Walking-beam cycle time (s)	9
Set-point temperature (°C)	980
Total residence time (s)	423

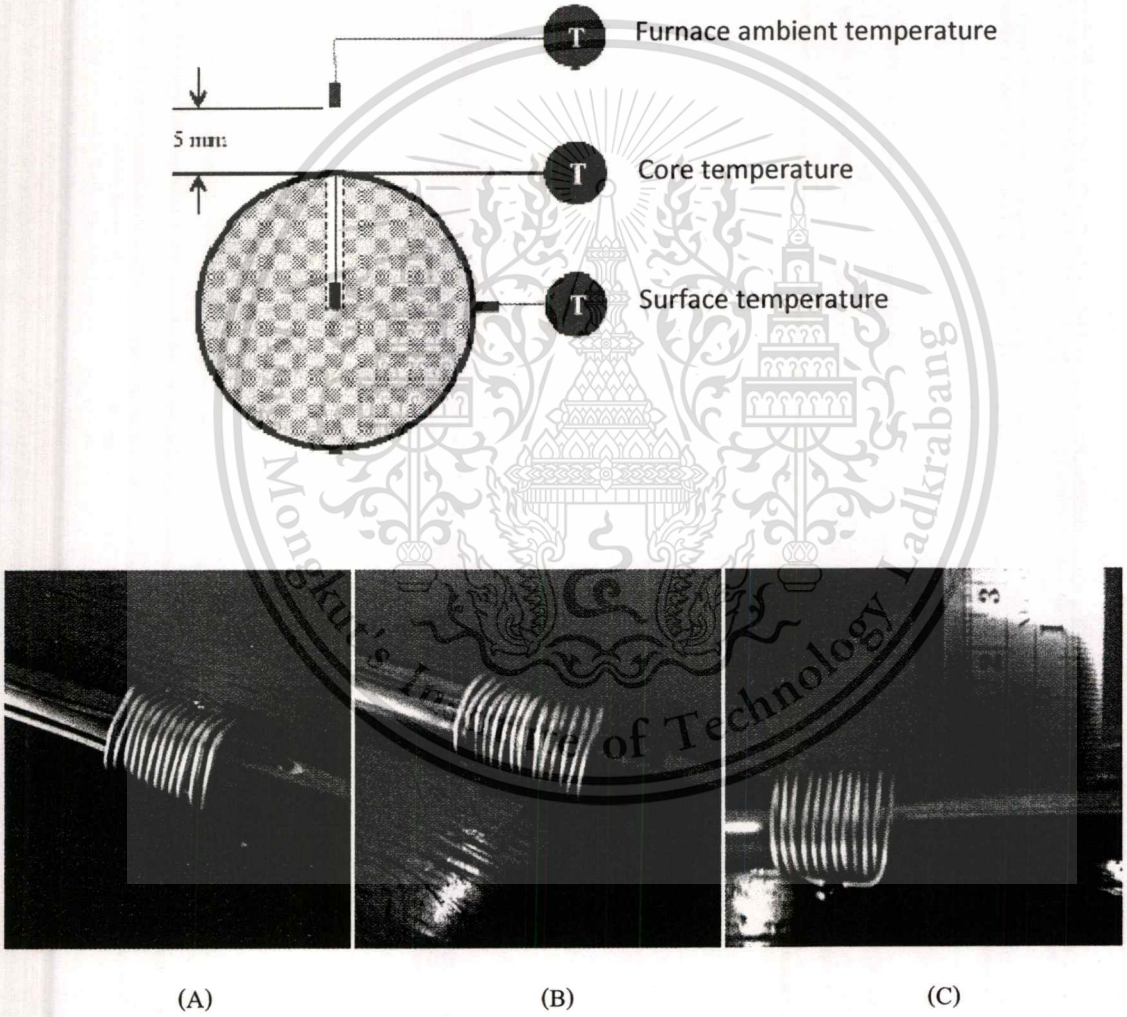

(A) (B) (C)

Figure 3.2 Arrangement of thermocouples for measuring core temperature (A), surface temperature (B) and ambient temperature (C) (Scale 1:1)

3.2.3. Simulation Implement and Indirect Measurement of Core Temperature of Heated Round bar

As mentioned earlier, it is important that the core temperature of each round bar must be known and monitored all the way along the heating operation. However, the measurements of core temperature during the operation of the walking-beam furnace encounter difficulties since it is not feasible to place thermocouples directly on the round bars and indirect measurements by radiation pyrometers are often disturbed by side radiation. To overcome these problems, the measurements of core temperature were performed indirectly through prediction and simulation by using the temperature data of the furnace ambient at the vicinity of the round bars. The experimental results obtained in section 3.1.2.2 were employed to develop model predictions of the core temperatures for different bar diameters using ANSYS® FLUENT® software. The results of numerical simulations were compared with the experimental data to validate the developed models for applying to the measurements of core temperature in this study.

3.2.4. Prediction of Temperature Distribution of Heated Steel Round Bar in the Direction of Furnace Length

The quantity of heat absorbed by a round bar in the heating operation of the walking-beam furnace can be estimated from the Stefan-Boltzmann law, which requires knowledge of temperatures of the bar (heat absorber) and effective temperature around the bar (heat transferer). Under steady-state operation, the wall temperature can be considered constant, whereas the bar temperature rises as it moves through the furnace chamber. The data on these temperatures can be obtained by the monitoring system with the thermocouples indicated in Figure ure3.1.

For each condition of the heating experiment, the chamber's wall temperature and the local ambient temperatures of the bar were read from the thermocouples located at the chamber ceiling and at the vicinity of the bar no.1, the bar no.23 and the bar no.45. The data on the local ambient temperatures were applied using the models obtained in section 3.2.3 to the core temperature of the bar at the corresponding locations. The predicted temperatures were then plotted versus time (or distance from the furnace inlet) and the relationships between these temperatures and time were examined. All experimental parameters used in the study are summarized in Table 3.3.

Table 3.4 Experimental parameters used in the study of sections 3.2.4 and 3.2.5

Bar diameter (mm)	10.5 , 13.5 , 17.4
Walking-beam cycle time (s)	9, 10, 11
Set-point temperature (°C)	940, 960, 980
Total resistance time (s)	423

3.2.5. Determination of Optimum Furnace Operating Parameters for the Heating of Round bars of Various Sizes

From the results obtained in section 3.2.4, it is possible to determine the core temperature of the bar leaving the furnace for each condition of the heating experiments. This temperature must be checked if it satisfies the temperature required in the bar to meet the metallurgical requirements. As mentioned earlier, a measurement of the core temperature of about 940°C can be used to indicate a successful heating operation; hence, the heating parameters leading to this level of the core temperature were chosen as the optimum operating conditions.

CHAPTER 4

RESULTS AND DISCUSSIONS

4. Experimental Results and Discussions

4.1 Temperature Distribution within the Heating Chamber of Furnace Operating Under No-Load Condition and load condition

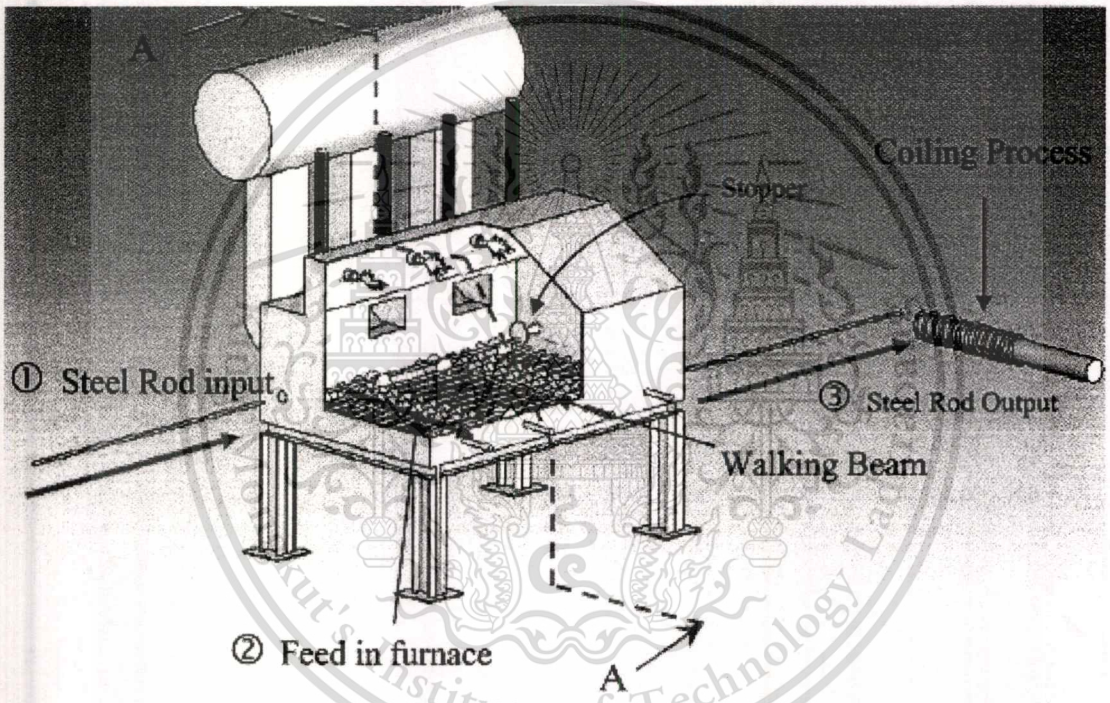

Figure 4.1 (A) Round bar heating process.

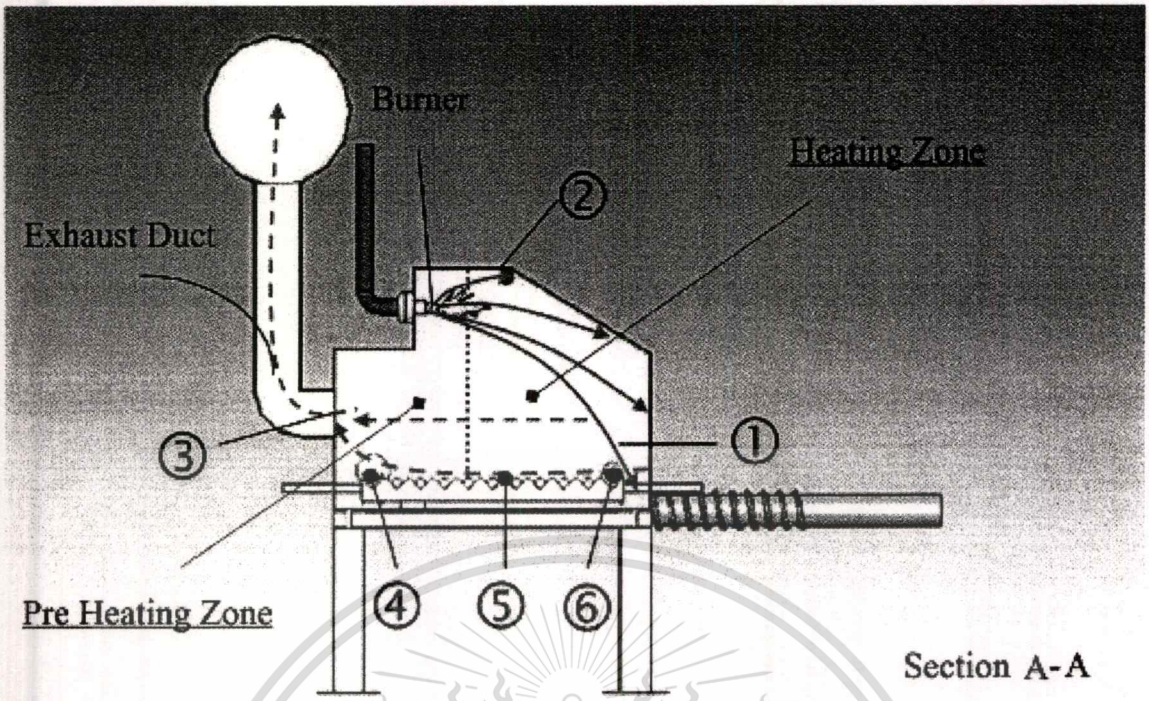

Figure 4.1 (B) Cross section of Figure 4.1 (A)

In this experiment, its purpose is to investigate the furnace's temperature distribution. The heating operation is separated for two periods which are no load (without round bars feeding) and load condition. The temperature distribution of the furnace is measured for different locations as shown in Figure 4.1 (B) which are set-point, chamber ceil (roof), exhaust gas, inlet, middle and outlet. Note that the inlet, middle and outlet temperature is measured above steel rod about 5 mm.

In furnace principle, the temperature of furnace is controlled by three burners so that the desired set-point temperature is achieved. The burner regulates the amount of fuel flow to be burned and continuously causes the high temperature gas flowing and transfer of the heat between the roof, set-point location, outlet, middle, outlet before exiting at exhaust duct as illustrated in 4.1(B)

Under no load condition staring time 0.00 -1.35 hours shown in Figure 4.2, the furnace temperature distribution is firstly regulated from room temperature to the 940°C desired set-point. The result shows that the temperature of the roof, set-point, middle and outlet location are relatively close; however, there are some 20 °C temperature higher than the set-point temperature because of the uncovered thermocouples of each location but differently tube-covered one for set-point location.

Moreover, these temperature locations are different from inlet and exhaust. It implies that the heat, which is carried by high temperature gas, is much absorbed in the regions of roof, set-point, middle and outlet than the inlet and exhaust. So as to these temperature distributions, the location around inlet and exhaust are called as pre-heating zone (low temperature) while the middle and outlet are really heating zone (high temperature). Additionally, the temperature of furnace system produces some overshoot before achieving the steady state by controller. After step-up and step-down furnace configure ration of 960, 980, 960, 940 and 980 °C desired set-point temperature sequences, the result shows that furnace can efficiently operates and approximately maintain at the desired set-point temperature levels under no load condition as illustrated in Figure 4.2.

Under load condition starting time 1.35-2.00 hours also shown in Figure 4.2, the 17.4 mm steel rod are fed into the furnace under 980 °C desired set-point temperature and 9 second feeding time. The result shows that temperature of inlet, middle and exhaust decreases to the new steady state while the temperature of roof, set-point, outlet location remain the approximate as no load condition. This behavior implies that the heat, which is carried by high temperatures has, is more absorbed to the round bars while the furnace efficiently supplies the more fuel rate to gain the desired set-point temperature under load condition.

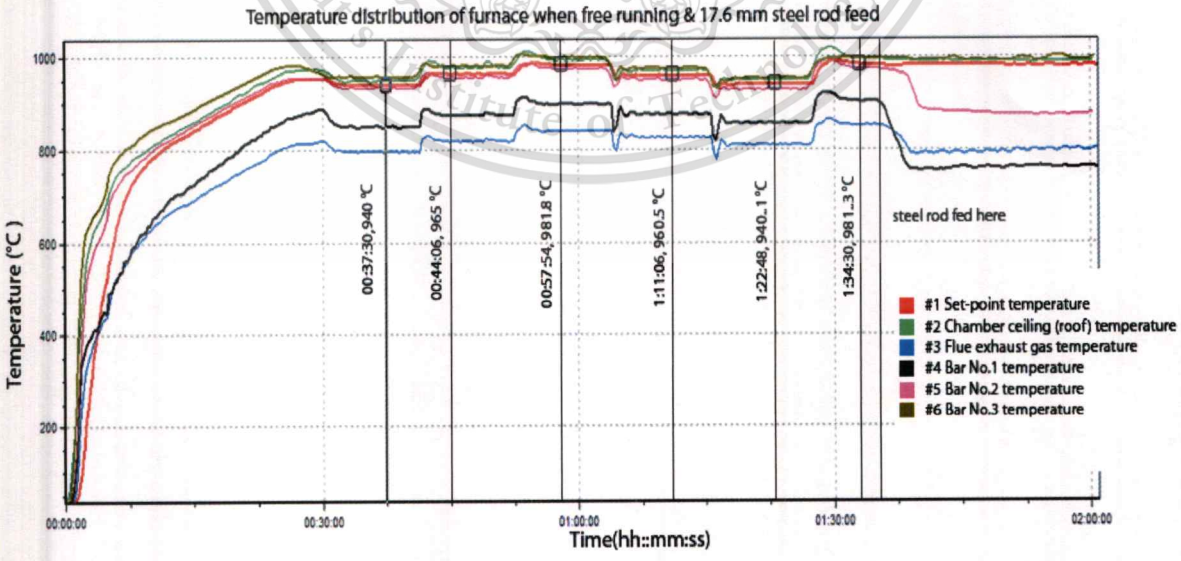

Figure 4.2 Temperature distributions under no load and load conditions

4.2 Investigation of Temperature Profile across the Cross-Sectional Area of Heated Round bar

In this experiment, its objective is to investigate the temperature distribution across the cross-section of three different round bars when they travel along the furnace. The round bars, whose diameters are 10.5, 13.5 and 17.4 millimeter, are fed into the furnace at the same desired set-point temperatures as 980°C. The feeding time is fixed at 9 second for all sizes so each bar stays in furnace for total 423 second. The temperatures of round bar are measured at the surface, core and ambient vicinity of them, which is above the bar around 5 millimeters as shown in Figure 4.3. And also, it is to investigate the operation of heating process that affects to the steel quality for those three sizes of round bar under 980 °C set-point temperature and 9 second feeding time. Note that the heating process properly works when the core temperature is reached around 940 °C which guarantees the standard of steel quality to be further processed in procedure of coil spring manufacturing.

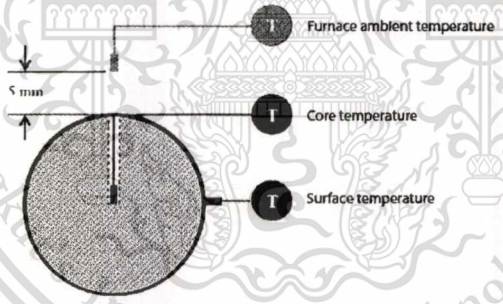

Figure 4.3 Temperature measurement of round bar

In case of 10.5 mm. round bar, 980 °C set-point and 9 second feeding time per each of round bar, the experimental results shows that temperatures of ambient vicinity, surface and core of round bar initiate from the room temperature while the set-point and exhaust temperatures have been steady. Firstly, the ambient vicinity, surface and core temperature are simultaneously increased with some difference when entering the furnace. The ambient vicinity temperature is the highest, the second and third are surface and core temperature respectively. It implies that the amount of heat is much transferred from ambient vicinity around round bar through the surface and conducted to the core in earlier stage. For steel quality of the 10.5 mm round bar, core temperature finally exceeds 940 °C as

shown in Figure 4.4 when it exits from the furnace. It implies that the round bars stay much longer in furnace and heat is transferred to them so much that theirs core temperature are over the desired level of heating process. To solve the problem, the feeding time should be reduced to achieve the temperature level, and also give the improvement of productivity due to reduced feeding time.

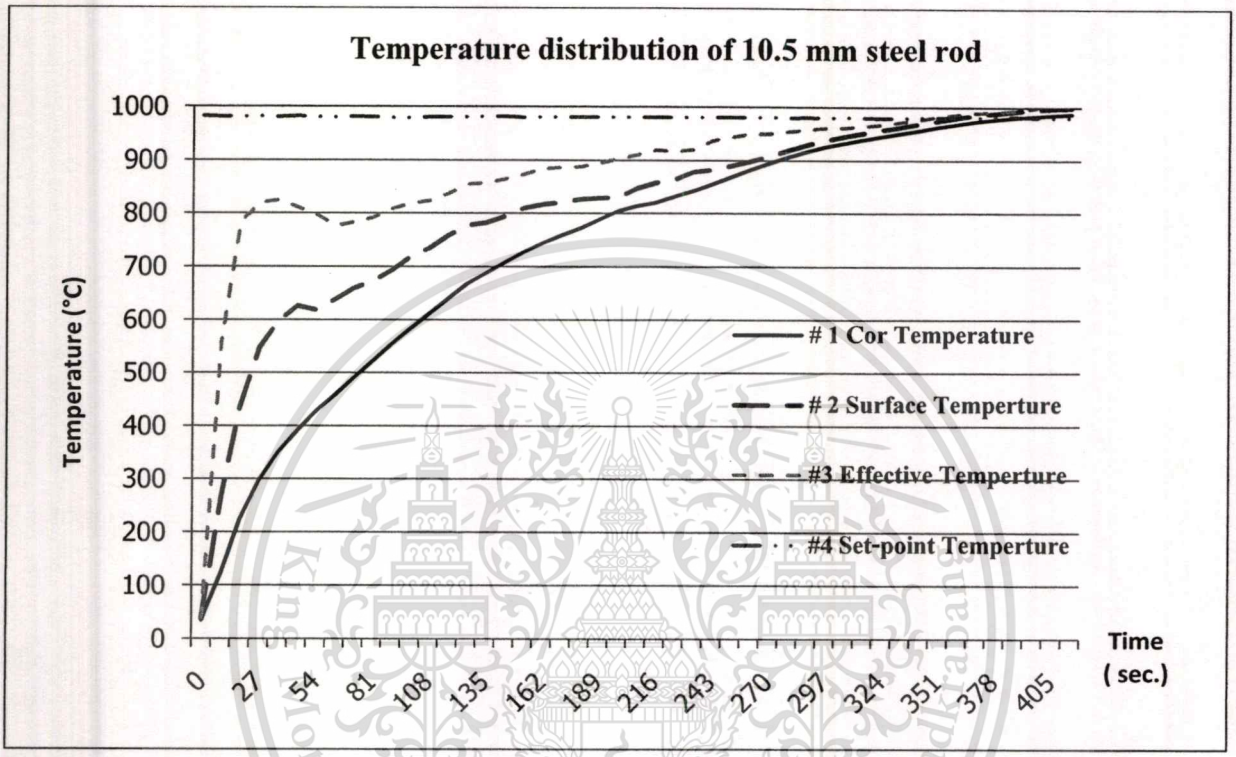

Figure 4.4 Temperature distribution of 10.5 mm round bar at 980 °C set-point and 9 sec feeding time

In case of 13.5 mm. round bar, 980 °C set-point and 9 second feeding time per each of round bar, the heat transfer of ambient vicinity, surface and core can also be described similar to the previous case. For steel quality of the 13.5 mm round bar, the experimental results shows that the core temperature can be reached around 940 °C before it exits the furnace as shown in Figure 4.5. Consequently, it implies that the set-point temperature is quite appropriate for this round bar size.

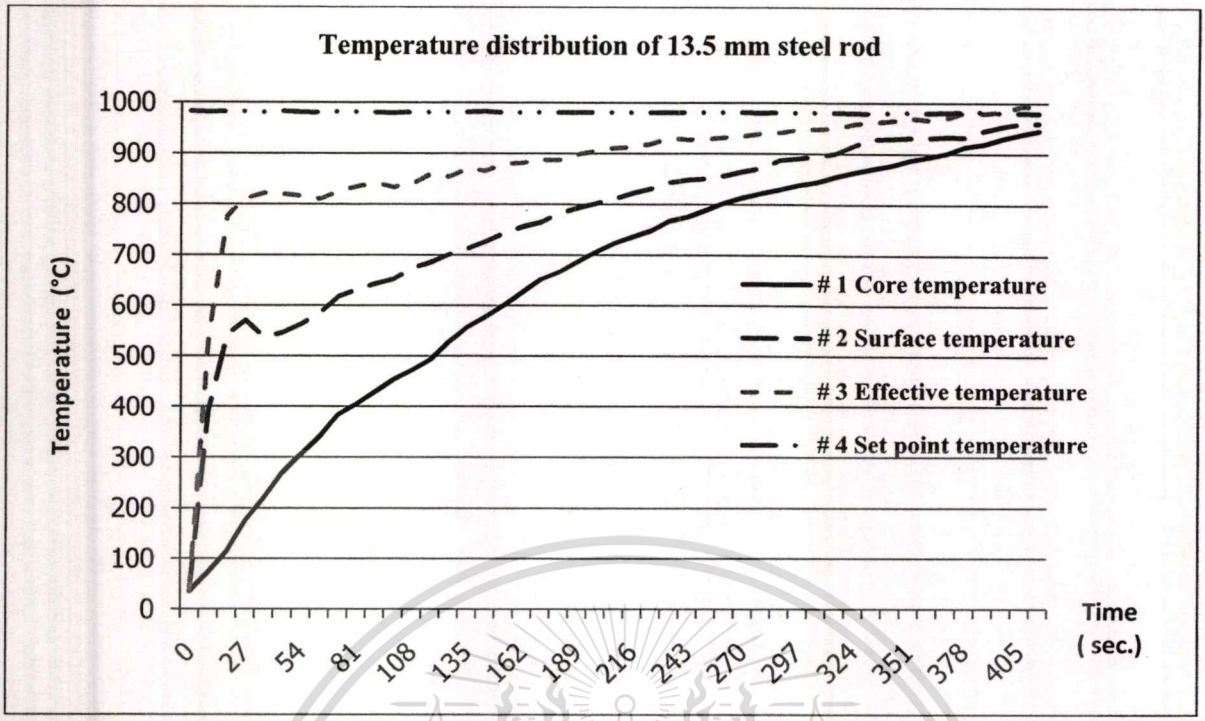

Figure 4.5 Temperature distribution of 13.5 mm round bar at 980 ˚C set-point and 9 sec feeding time

In case of 17.5 millimeter round bar, 980 ˚C set-point and 9 second feeding time per each of round bar, the heat transfer of ambient vicinity, surface and core can also be described similar to the previous two cases. For steel quality of the 17.5 mm round bar, the experimental results shows that the core temperature cannot be raised to 940 ˚C as shown in Figure 4.6, so there are possible two solutions that are either higher set-point temperature setting or increasing the feed time in order to achieve the desired core temperature. But due to limitations of furnace temperature not exceeding 980 ˚C, so the increasing feed time is only way for solving this problem.

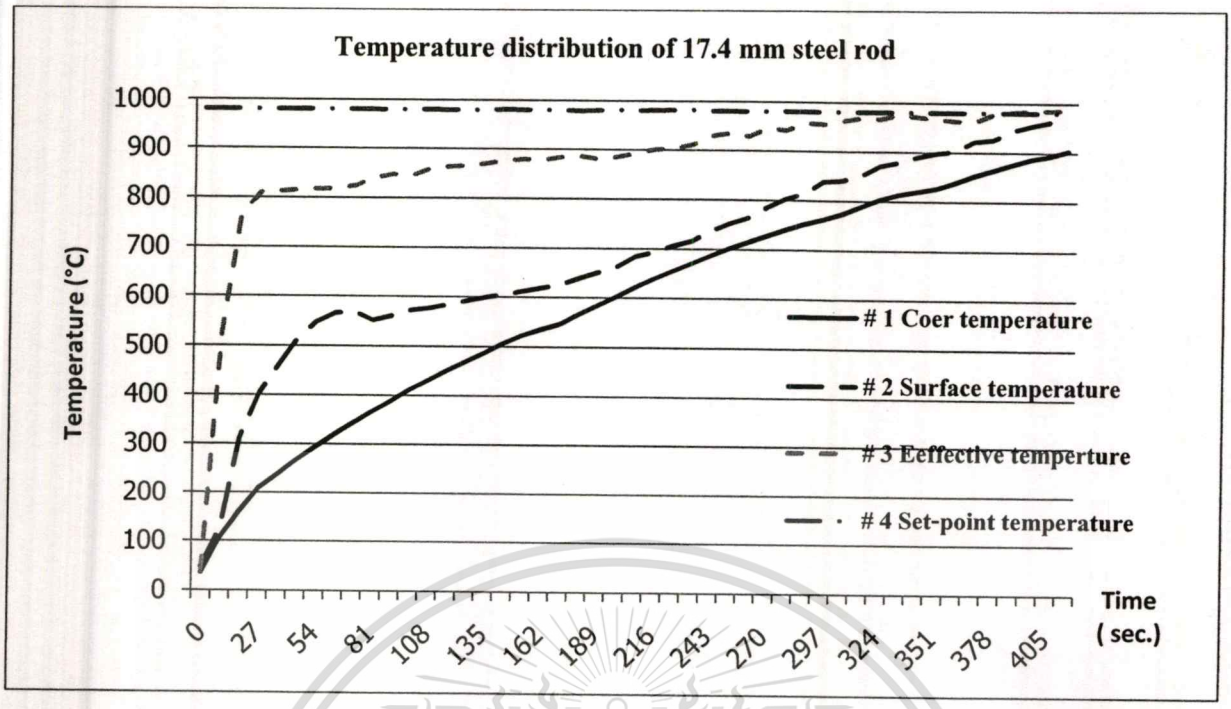

Figure 4.6 Temperature distribution of 17.5 mm round bar at 980 °C set-point and 9 sec feeding time

Additionally, when the ambient vicinity temperature is considered during the steer round bar traveling along furnace, the experimental result illustrates that temperature is relatively high around inlet location and gradually reduced around outlet location due to characteristics of high temperature gas flow within furnace described in section 4.1. In order to remove the complicated convection of hot gas and the round bar within furnace, the ambient vicinity temperature is simply used as the effective temperature source where the heat is radiated to the round bar during heating process instead. When describing the radiation characteristics of effective temperature, it is equivalent to the concept of a blackbody which absorbs all the radiation that falls on it, converts it into internal energy (heat), and then re-radiates this energy into the surroundings. And also, the effective temperature or blackbody temperature is the surface temperature that radiates the same amount of energy per unit area and total energy corresponding to the Stefan-Boltzmann law, which states that the total energy radiated by a blackbody varies as the fourth power of its absolute temperature.

4.3 Simulation and Indirect Measurement of Core Temperature of Heated Steel Round Bar

The objective of this experiment is to build the thermal model of heating process to predict the final core temperature when exiting the furnace based on experimental data of 10.5 mm-diameter steel round bar at 980 °C set-point and 9 second feeding time. Then, the model is applied for core temperature prediction of the13.5, 17.5 mm steel round bar and compared to theirs experimental results.

Referring to the section 4.1.2, it is obvious that the actual heating process is complicated with convection of high temperature gas flow within furnace. In order to predict the core temperature with reduction of this complexity, if the core temperature prediction is simplified based on the sense of lump capacitance and biot number principles which approximate the uniform temperature distribution of steel round bar depending on only time not the locations, but the experimental result of section 4.1.2 shows the large temperature difference between surface and core location as the time continues. Consequently, this simplified thermal model is inappropriate for core temperature prediction. The thermal modeling of furnace system, which is introduced in last of section 4.1.2, can be reasonably formulated by transient 1-dimensional thermal model as illustrated Figure 4.7. The vicinity of space around the steel round bar is modeled as the ideal black body heat source that surrounds and symmetrically radiates the heat to the surface of steel round bar in any direction while the some heat is also radiated from the surface of steel round bar. Then, the net heat flux of the surface is symmetrically 1-dimentional conducted to the center of steel round bar.

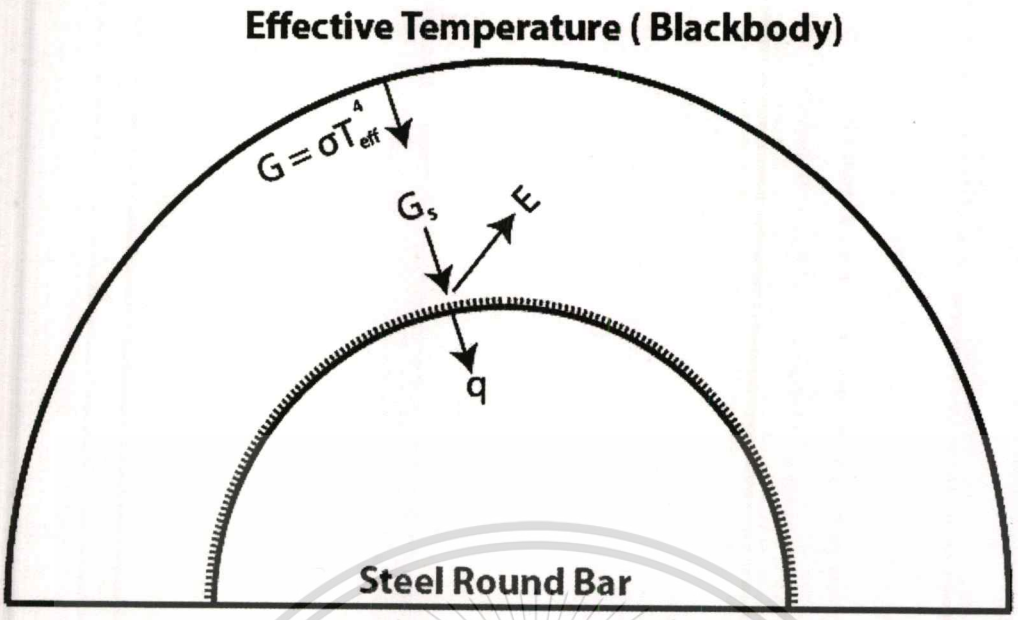

Figure 4.7 Thermal heat absorption and radiation of steel round bar

Firstly, it is to derive net heat flux at surface of steel round bar as shown in Figure 4.7 by energy balance principle. There are only three surface heat fluxes, the net thermal radiation heat flux, $q(W/m^2)$ of steel round bar's surface, the thermal absorbed G_s and thermal radiated heat flux $E(T_s)$ on the surface, that affects to the temperature distribution of steel round bar. So, the net surface heat flux is balanced by equation (1),

$$q = G_s - E(T_s) \qquad (4.1)$$

Where, G_s is the thermal absorbed heat flux that is radiated from effective temperature and $E(T_s)$ is thermal radiated heat flux at steel round bar surface; however the reflected heat flux on surface is not shown because of not affecting to steel round bar temperature.

According to the non-blackbody of steel round bar, the absorbed heat flux G_s is defined as,

$$G_s = \alpha_s \sigma T_{eff}^4(t) \qquad (4.2)$$

Where, $T_{eff}(t)$ is the effective temperature which is depended on time, σ as the Stefan-Boltzmann constant and α_s as the surface absorptance.

For the thermal radiated heat flux of steel round bar's surface $E(T_s)$ which is the non-blackbody , so it can emit the heat less than the black body at the same temperature as,

$$E(T_s) = \varepsilon_s \sigma T_s^4 \qquad (4.3)$$

Where, T_s is the surface temperature of steel round bar. ε_s is the emittance of steel round bar. Note that the l emittance and emissivity are frequently used interchangeably. However, the emissivity is referred to the material property or chemical atomic structure, while emittance is refered to the particular object; surface roughness, contamination, oxide layer. Consequently, the emittance of the same material can be different.

By substituting the equation (2) and (3) into (1), the net thermal radiation heat flux q of steel round bar surface can be arranged as,

$$q = \alpha_s \sigma T_{eff}^4(t) - \varepsilon_s \sigma T_s^4 \qquad (4.4)$$

Normally, the total emittance ε_s of non-black body is,

$$\varepsilon_s = \varepsilon_s(T) = \frac{\int_0^\infty \varepsilon_\lambda(\lambda) E_b(\lambda, T) d\lambda}{\int_0^\infty E_b(\lambda, T) d\lambda} \qquad (4.5)$$

And the total absorptance of non-black body is,

$$\alpha_s = \alpha_s(T) = \frac{\int_0^\infty \alpha_\lambda(\lambda) G_b(\lambda, T) d\lambda}{\int_0^\infty G_b(\lambda, T) d\lambda} \qquad (4.6)$$

From the equation (5) and (6), it is obvious that $\varepsilon_\lambda(\lambda)$, $\alpha_\lambda(\lambda)$ are wavelength dependent function and $\varepsilon_s(T)$, $\alpha_s(T)$ are also dependent on its surface temperature. Consequently, these total emittance and absorptance are rarely investigated for real surface.

The gray surface model is the one way that the emittance wavelength dependence can be simplified under restriction. Its application works well under restriction such no or slight change of emittance over wavelength. However, there is some senses that the gray surface model can be practically approximated even the real surface case [1]. Moreover, the gray surface model is also applied under condition such much change of emittance over wavelength such that the complicated wavelength-

dependent emittance can be separately approximated as linear wise-pieces lines corresponding to each wavelength region [1].

For our furnace heating process, the thermal radiation heat inside the furnace mostly falls over infrared region, so the surface emittance could be approximated as wavelength independence over infrared region. Then the gray surface model can be appropriately applied for the equally total surface emittance and absorptance which are independent of wavelength. Moreover, the our objective is to predict the core temperature of different sizes 10.5 mm, 13.5 mm, 17.4 mm steel round bar when they exit from the furnace. It feasibly helps us for the computation stead of real surface emittance investigation.

$$\varepsilon_s = \alpha_s = \varepsilon_g = \alpha_g \qquad (4.7)$$

Then, the equation (8) is obtained by substituting (7) into (4).

$$q = \sigma\varepsilon_g\left(T_{eff}^4(t) - [T_s]^4\right) \qquad (4.8)$$

Thirdly, it is to model the temperature distribution of steel round bar. As early mentioned that effective temperature, that surrounds the object as shown in Figure 4.7, symmetrically radiates the heat to the steel round bar, the temperature distribution of steel round bar can be reduced to 1-dimensional thermal conduction.

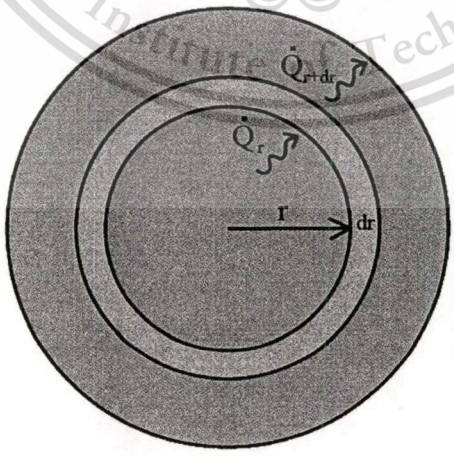

Figure 4.8 1-Dimenional heat conduction of steel roundbar.

To derive this governing equation, let's consider the energy change within infinitesimal volume show in Figure 4.8,

$$\dot{Q}_r - \dot{Q}_{r+dr} = \frac{\Delta E_{element}}{\Delta t}$$

$$= \dot{Q}_r - \dot{Q}_{r+dr} = m_{element} c \cdot \frac{T_{t+\Delta t} - T_t}{\Delta t}$$

$$= \dot{Q}_r - \dot{Q}_{r+dr} = \rho \cdot A \cdot dr \cdot c \cdot \frac{T_{t+\Delta t} - T_t}{\Delta t} \quad (4.9)$$

And from the Fourier law, the thermal conduction heat flux within infinitesimal volume can be expressed as,

$$\dot{Q}_r = -kA\frac{\partial T}{\partial r} \quad (4.10)$$

Where k is thermal conductivity and A is the cylindrical surface area at specified position r.

Then, the $\dot{Q}_{r+dr}$ can be approximated by Taylor series expansion of the equation (10) with neglecting the higher order term as,

$$\dot{Q}_{r+dr} = \dot{Q}_r - k\frac{\partial}{\partial r}\left(A\frac{\partial T}{\partial r}\right)dr \quad \rightarrow \quad \dot{Q}_r - \dot{Q}_{r+dr} = k\frac{\partial}{\partial r}\left(A\frac{\partial T}{\partial r}\right)dr \quad (4.11)$$

After substituting the equation (11) into (9),

$$k\frac{\partial}{\partial r}\left(A\frac{\partial T}{\partial r}\right)dr = \rho \cdot A \cdot dr \cdot c \cdot \frac{T_{t+\Delta t} - T_t}{\Delta t} \quad (4.12)$$

Divide both side of equation (12) with $A \cdot dr$ and substitute A with $2\pi rL$, then

$$\frac{k \cdot 2 \cdot \pi \cdot L}{2 \cdot \pi \cdot r \cdot L}\frac{\partial}{\partial r}\left(r\frac{\partial T}{\partial r}\right)\frac{dr}{dr} = \rho \cdot c \cdot \frac{T_{t+\Delta t} - T_t}{\Delta t} \quad (4.13)$$

From equation (13) with taking $\Delta t \rightarrow 0$ limited to zero, we finally obtain the thermal governor equation (14) that describes the temperature distribution of steel round bar caused by the thermal heat conduction itself.

Governing equation of steel round bar temperature distribution

$$\frac{1}{r}\frac{\partial}{\partial r}\left(r\frac{\partial T}{\partial r}\right) = \frac{\rho c}{k}\frac{\partial T}{\partial t} \tag{4.14}$$

Where ρ is density and c is specific heat capacity.

To solve the partial differential equation of this thermal system, the following boundary and initial conditions is necessarily incorporated.

Boundary and initial conditions

Let's define the temperature distribution of steel round as 2-multivariable function (15)

$$T_{steel} = T(r,t) \tag{4.15}$$

Where $r \in [0, R]$ is the position vector referred to the center of circle and $t \in R^+$ is heating time.

At $r = R$ and any time t, the net thermal radiated heat flux must be equal to the thermal conductive heat flux ***around the surface***.

$$\sigma\varepsilon_g A_R\left(T_{eff}^4(t) - [T_s]^4\right) = -kA_R\frac{\partial T(R,t)}{\partial r}$$

$$\sigma\varepsilon_g A_R\left(T_{eff}^4(t) - [T(R,t)]^4\right) = -kA_R\frac{\partial T(R,t)}{\partial r}$$

$$\sigma\varepsilon_g\left(T_{eff}^4(t) - [T(R,t)]^4\right) = -k\frac{\partial T(R,t)}{\partial r} \tag{4.16}$$

Where A_R is the surface area of the rod

At $r = 0$ and any time t, these is no temperature change is around this location at any specified time because of the symmetrical temperature distribution of any direction around this location.

$$\frac{\partial T(0,t)}{\partial r} = 0 \tag{4.17}$$

The initial temperature of any steel round bar location is the room temperature before entering the furnace.

$$T(r, 0) = \text{Room Temperature} \qquad (4.18)$$

The effective temperature $T_{eff}(t)$ can be expressed as wise-pieces function by the collection of actual ambient vicinity temperature when the steel round bar travels along the furnace.

In our goal of predicting the final core temperature of steel round bar when exiting the furnace, the unknown emittance ε_g is necessary to be firstly found. By varying the ε_g and solving for the temperature distribution of steel round bar in each emittance ε_g, the only ε_s is finally chosen in such the way that error between final actual temperature and prediction yields the minimal over cases. For example of 10.5 mm case, its effective temperature is corresponding to data in second row of table 4.1. The numerical solution is performed by ANSYS-FLUENT by varying the emittance of rod surface in order to obtain the least error of final core temperature and temperature distribution of steel round bar graphically shown in Figure 4.9

Table 4.1 Effective temperature modeling for 10.5 mm, 13.5 mm and 17.4 round bar at 980 °C set-point temperature and 9 second feeding time.

Time (hh:mm:ss)	0:00:00	0:00:18	0:02:51	0:06:54
Temperature (°C),10.5 mm	35.00	782.40	918.80	1001.10
Temperature (°C),13.5 mm	34.4	776.8	886.8	992.6
Temperature (°C),17.4 mm	36.9	768.3	883.9	986.4

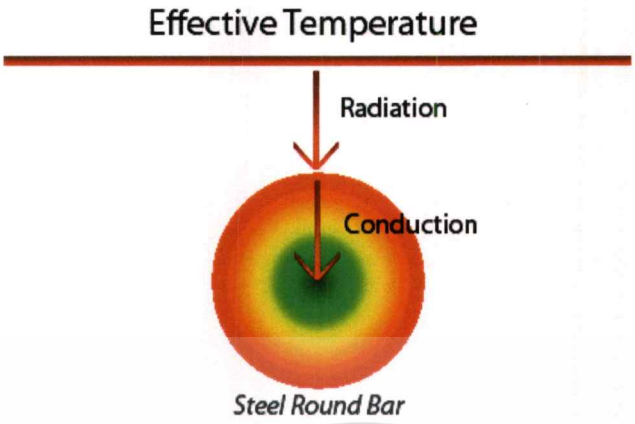

Figure 4.9 (A) Simplied heat transfer model of heating process.

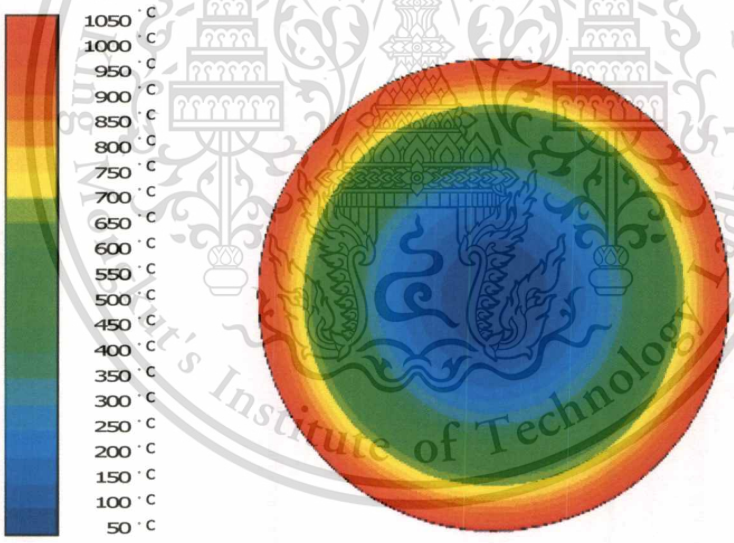

Figure 4.9 (B) Simulation results of round bar temperature distribution

The simulation results shows the predicted core temperature and actual one in Figure 4.10, where the emittance of effective temperature is varied from 0.6 to 1 so that the final core temperature error between simulation and actual is reduced. As illustrated in Figure 4.11, it is obviously seen that the fluctuated error prediction is introduced when the steel round bar early enters the furnace, but it is gradually reduced later when exiting. The reason is that hot gas, which turbulently flows from inlet to exhaust region, causes the high thermal convection. Moreover, the temperature of steel round bar,

which initially starts from the room temperature, highly differs from the hot gas flowing from inlet to exhaust region, so the much temperature difference encourages the effect of thermal convection than the radiation in early. But, the temperature difference is reduced and also leaving from turbulent flowing region, so the thermal radiation mainly effect than convection. However, the final core temperature prediction is most considerable than other predictions. Obviously, there is only one case which emittance is 0.8 as shown in the table 4.2; the predicted final core temperature yields the least error than others. Consequently, the model with emittance 0.8 is the most suitable to predict the final core temperature of steel round bar when it exits the furnace.

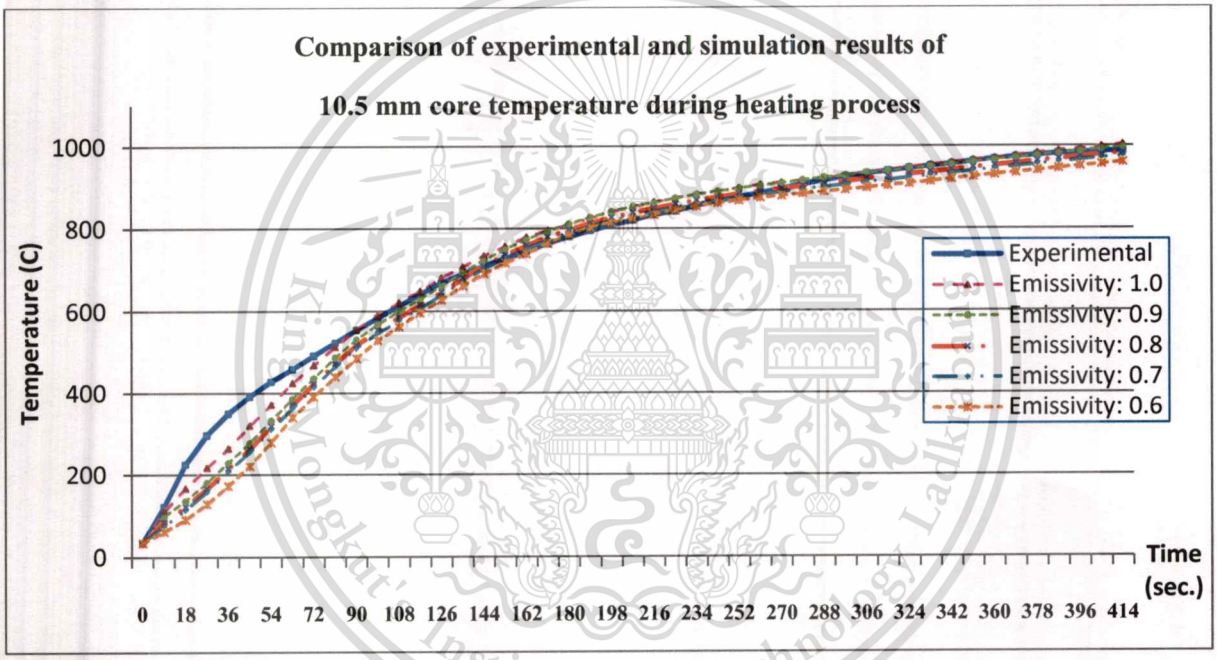

Figure 4.10 The comparison of experimental and simulation result of 10.5 mm round bar temperature during 980 set-point °C and 9 sec feeding time of heating process

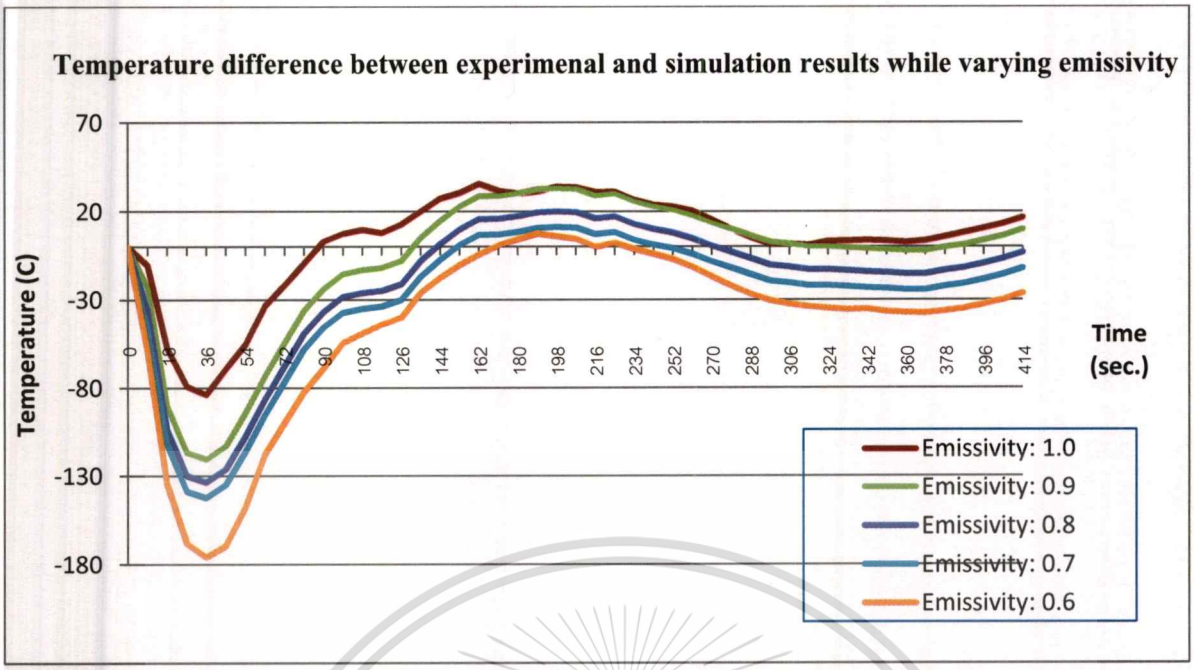

Figure 4.11 The temperature difference between experimental and simulation results while varying emittance during 10.5 round bar, 980 set-point ˚C and 9 sec feeding time of heating process.

Table 4.2 Sum of absolute and final error of 10.5 mm round bar core temperature with various emissivities.

Emittance	1.0	0.9	0.8	0.7	0.6
Sum of absolute error	1001.6	1234.6	1350.8	1539.4	2057
Error at final time	16.7	9.7	-3.3	-12.3	-26.3

At this point, the core temperature prediction model (0.8 emittance) is applied for predicting the other 10.5 mm, 13.5 mm, 17.4 mm round bar with the same 9 second feeding time and 980 ˚C set-point conditions. From the actual ambient vicinity temperature of 10.5 mm, 13.5 mm, 17.4 mm, illustrated in Figure 4.10(A), 4.11(A) and 4.12(B) respectively, the effective temperature can be approximately represented by 3-wisepiece lines which are so convenient application for the thermal simulation.

For the 10.5 mm steel bound bar, the effective temperature is modeled as 3-wisepiece lines corresponding to table 4.1 and also shown in Figure 4.10 (A). The predicted core temperature

illustrated in Figure 4.10(B) shows that the early error is quite large due to un-modeled convection of hot gas flowing within furnace, but it is reduced later when exiting the furnace. The final difference temperature between prediction and actual is -3.3 °C . For remaining 13.5 mm, and 17.4 mm round bar, the results, illustrated in Figure 4.11 and 4.12 respectively, are similar to the previous one with large error in earliest state, but the final difference temperatures are 3.8 and 8 °C respectively. Finally, it is obvious that the application of final core temperature prediction with 0.8 emittance and multi linear effective temperature model are reasonably confirmed by the accurate prediction result of 10.5 mm, 13.5 mm, and 17.4 mm. From those results, the final temperature prediction based on irradiative model is quite appropriate to predict the other different conFigureuration of thermal furnace system.

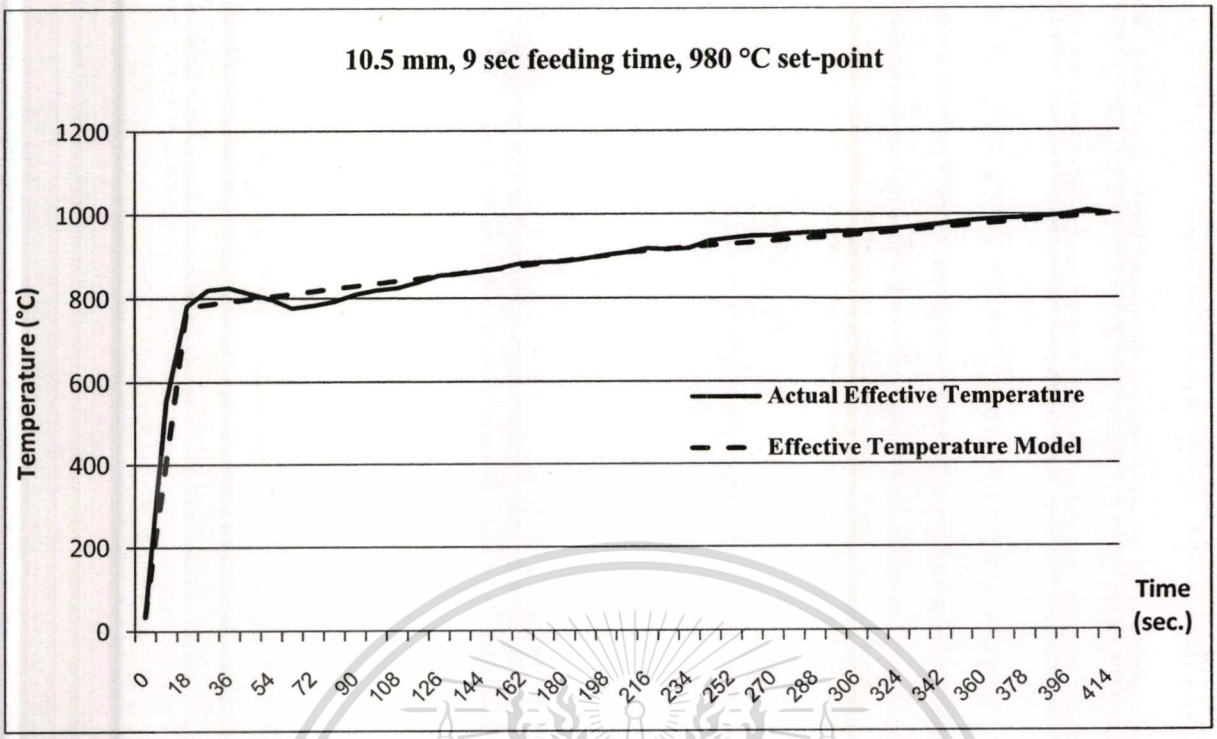

Figure 4.12 (A) The multi-linear model of effective temperature of 10.5 mm round bar, 9 second feeding time and 980 °C set-point.

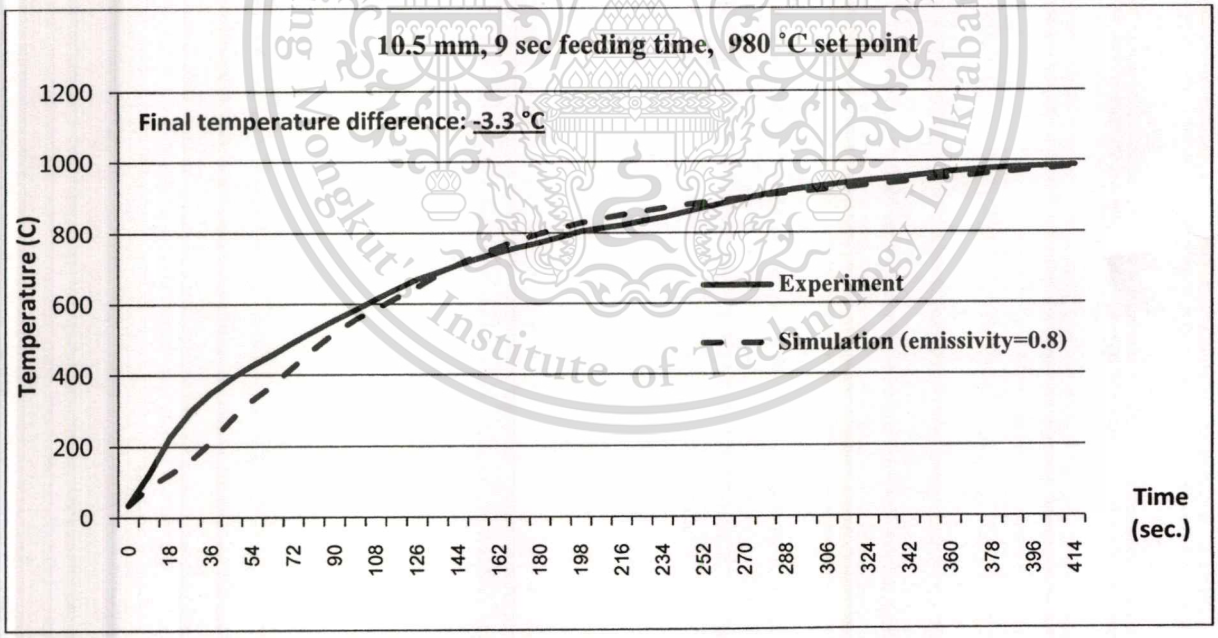

Figure 4.12 (B) The core temperature prediction and actual corresponding to this condition.

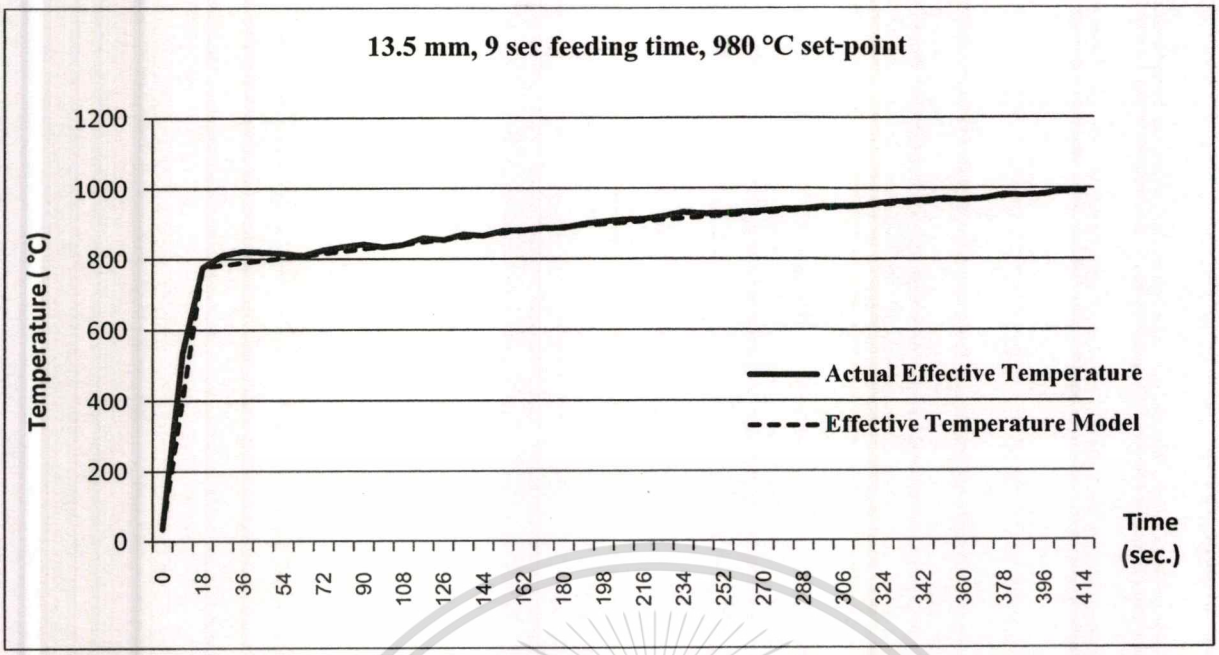

Figure 4.13 (A) The multi-linear model of effective temperature of 13.5 mm round bar, 9 second feeding time and 980 ˚C set-point.

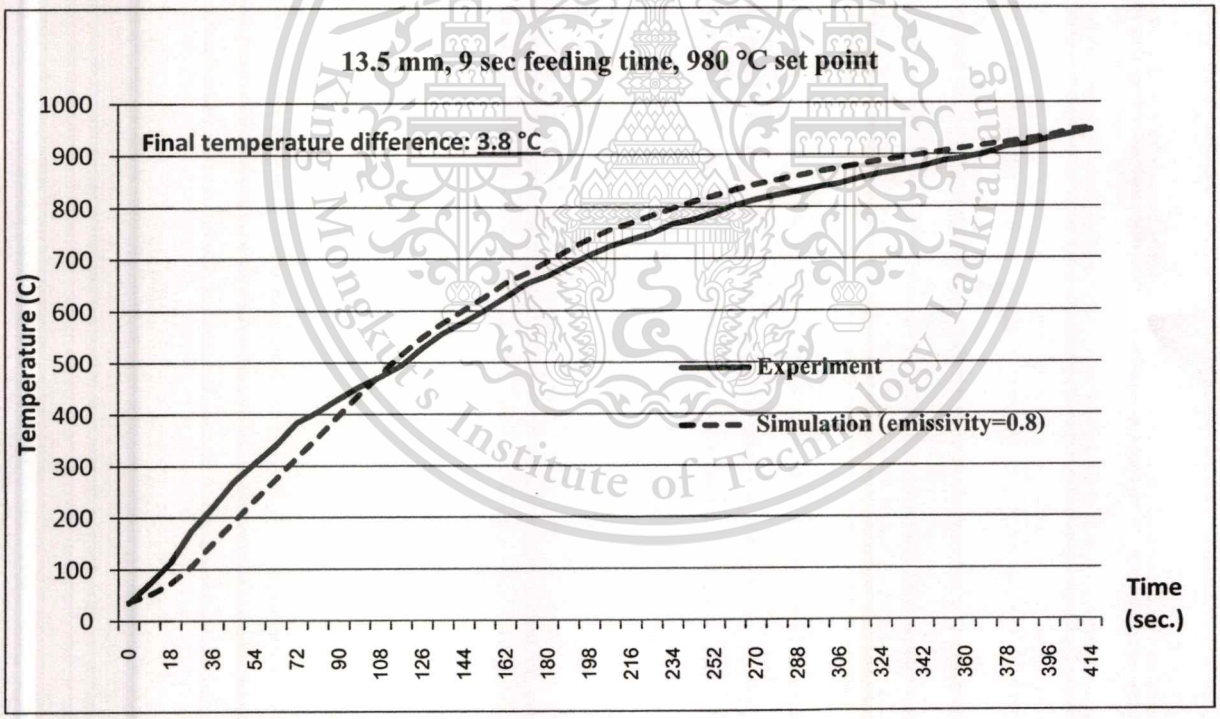

Figure 4.13 (B) The core temperature prediction and actual corresponding to this condition.

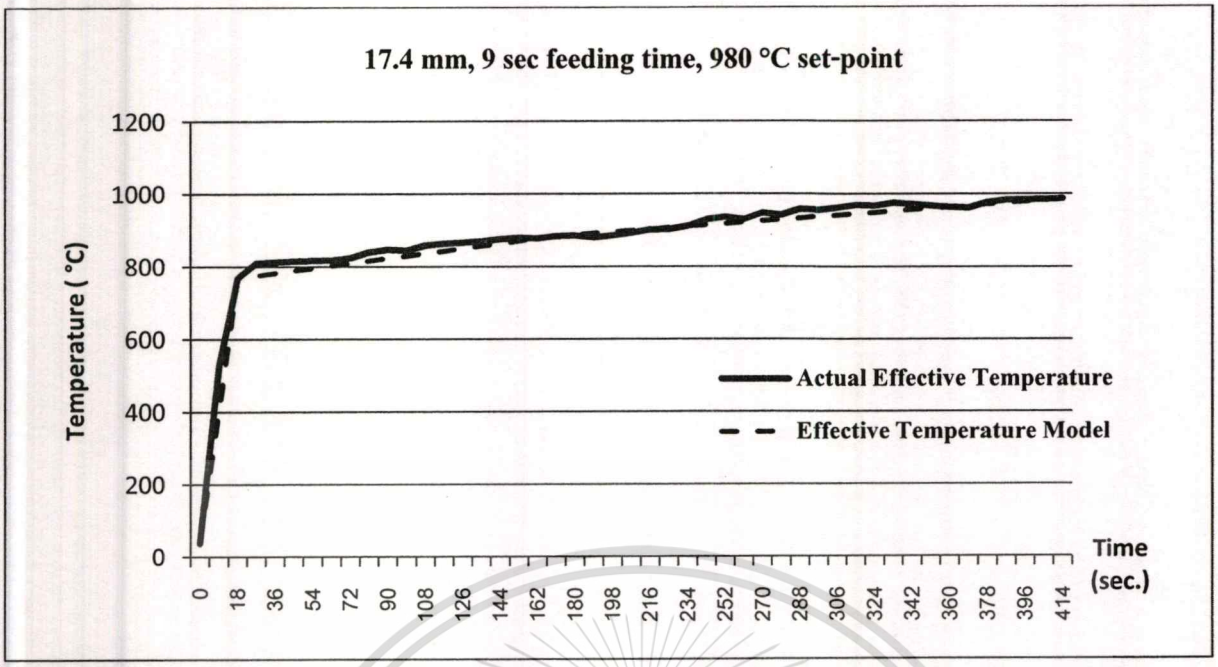

Figure 4.14 (A) The multi-linear model of effective temperature of 17.4 mm round bar, 9 second feeding time and 980 ˚C set-point.

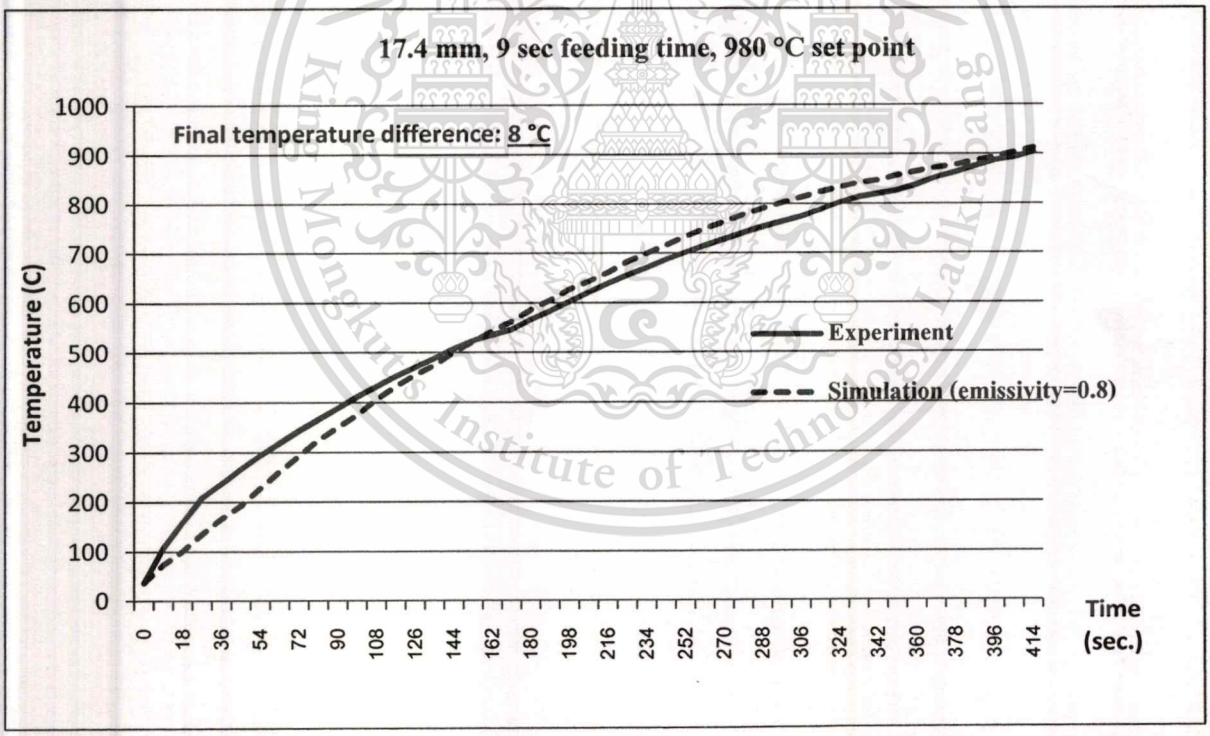

Figure 4.14 (B) The core temperature prediction and actual corresponding to this condition.

4.4 Prediction of Temperature Distribution of Heated Round bar in the Direction of Furnace

The objective of this experiment is to predict the final core temperature of 10.5, 13.5 and 17.4 mm round bar based on effective temperature modeling along the furnace direction. The effective temperature radiates the heat energy to the round bars when they travel along the furnace. Then, it is required to determine the minimum set-point temperature and feeding time that cause the final core temperature to desired heating process temperature around 940 °C which guarantees the standard of steel quality to be further processed in procedure of coil spring manufacturing. Referring to the section 4.2, the final core temperature of only 13.5 mm under 9 second feeding time and 980 °C set-point condition has been obtained at the desired temperature of heating process, so there are two remaining investigation for 10.5 and 17.4 mm round bars.

For 10.5 mm round bar, the feeding time is fixed variable as 9 second so as to give high productivity. The independent variable is the set-point temperatures which are varied from 940, 960 and 980 °C . In order to model the effective temperature along furnace direction in each set-point temperature change, the steady states of ambient vicinity temperature are collected at initial(0), inlet(1), middle(23) and outlet(45) location for 3-wisepiece linear representation of the effective temperature along furnace. The overview temperature distribution of furnace is changed corresponding to the desired set-point temperature as shown in time regions R1, R2 and R3 of Figure 4.13. The steady state of initial, inlet, middle and outlet ambient vicinity temperature of 940,960 and 980 °C set-point temperatures are individually shown in Figure 4.14, 4.15 and 4.16 respectively and approximately used for effective temperature as 3-wisepice linear corresponding to each cases shown in Figure 4.17. It is apparent that the increase of set-point temperature directly affects to the raise of effective temperature along furnace direction, because heat energy carried by hot gas is more absorbed by effective temperature. The table 4.3 also shows the ambient vicinity temperature which is used as 3-wisepiece linear model of effective temperature in each set-point temperature cases shown in Figure 4.17.

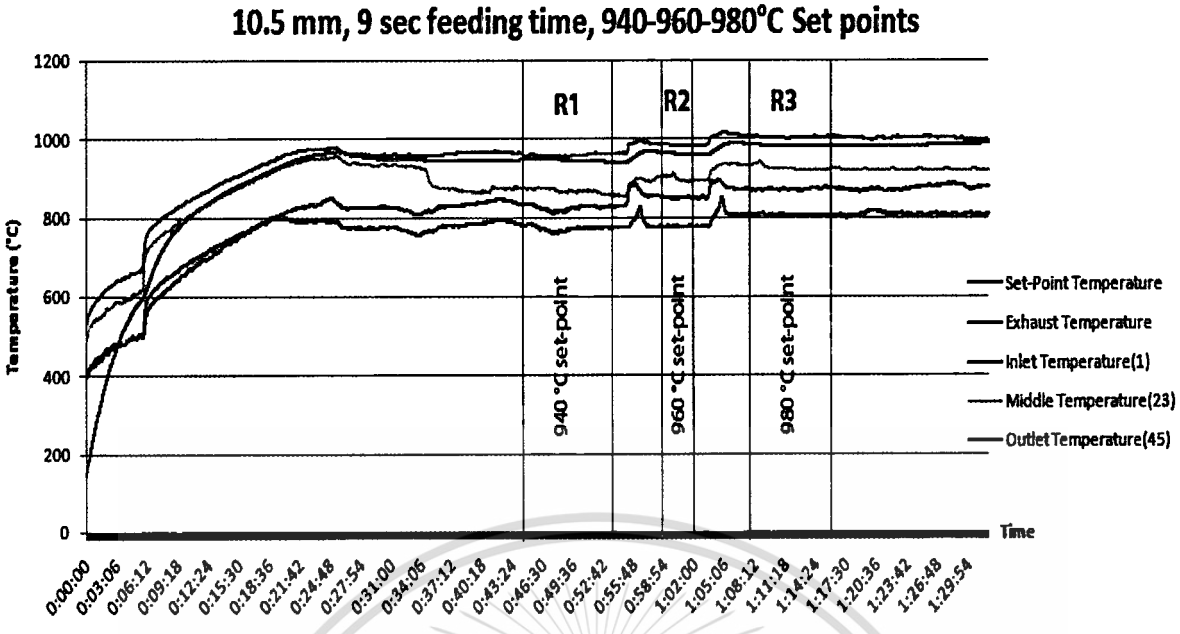

Figure 4.15 Temperature distributions in furnace with three desired set-point temperatures 940, 960, 980 °C while 10.5 mm round bars are traveling with 9 second feeding time.

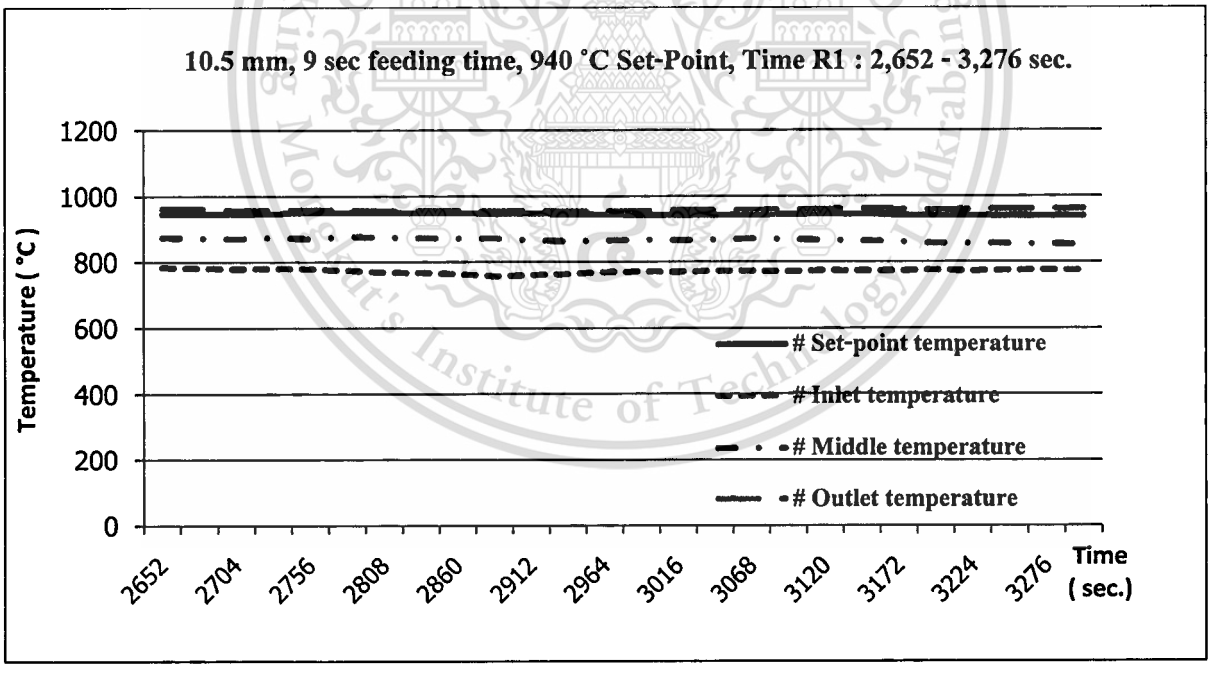

Figure 4.16 Steady state of five locations along furnace at 940 °C set-point temperature while 10.5 mm round bars are traveling with 9 second feeding time.

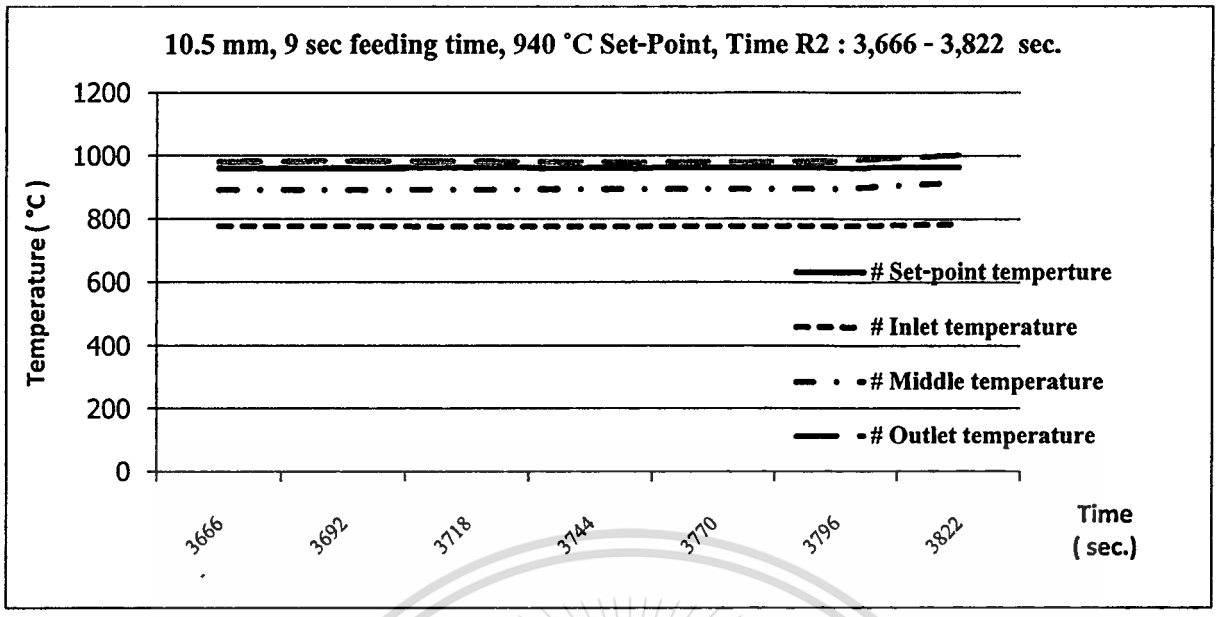

Figure 4.17 Steady state of five locations along furnace at 960 °C set-point temperature while 10.5 mm round bars are traveling with 9 second feeding time.

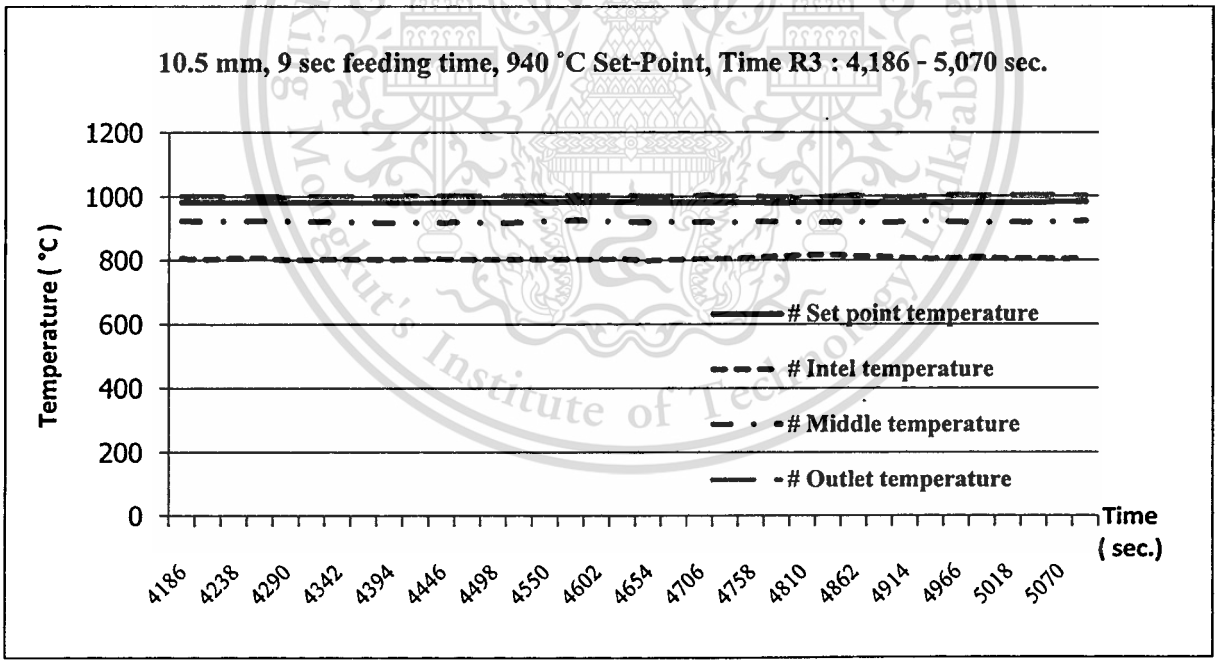

Figure 4.18 Steady state of five locations along furnace at 980 °C set-point temperature while 10.5 mm round bars are traveling with 9 second feeding time.

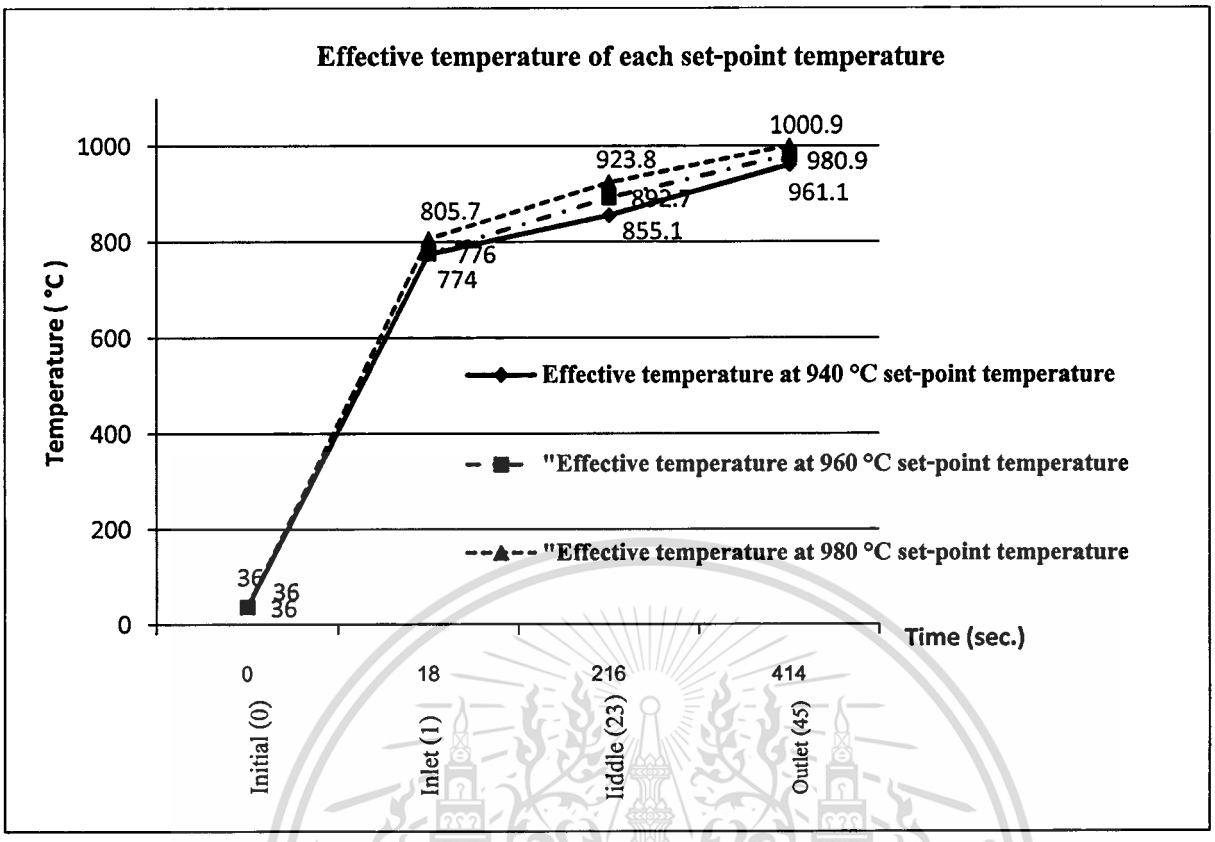

Figure 4.19 Effective temperature modeling along furnace at 940, 960 and 980 °C set-point temperature while 10.5 mm round bars are traveling with 9 second feeding time.

Table 4.3 Effective temperature of 940, 960, 980 °C set-point temperature.

Location	Initial (0) (°C)	Inlet (1) (°C)	Middle (23) (°C)	Outlet (45) (°C)
Effective temperature at 940 °C set-point (0:54:00)	36.0	774.0	855.1	961.1
Effective temperature at 960 °C set-point (1:02:00)	36.0	776.0	892.7	980.9
Effective temperature at 980 °C set-point (1:10:00)	36.0	805.7	923.8	1000.9

As a result of final core temperature predictions of each set-point temperature illustrated in Figure 4.18, it obviously shows that 940 °C set-point temperature predicts the final core temperature of 10.5 mm round bar at 948 °C which is approximately closest to desired heating process temperature

than others. Consequently, the furnace operation of 10.5 mm round bar is 940 °C set-point and 9 second feeding time.

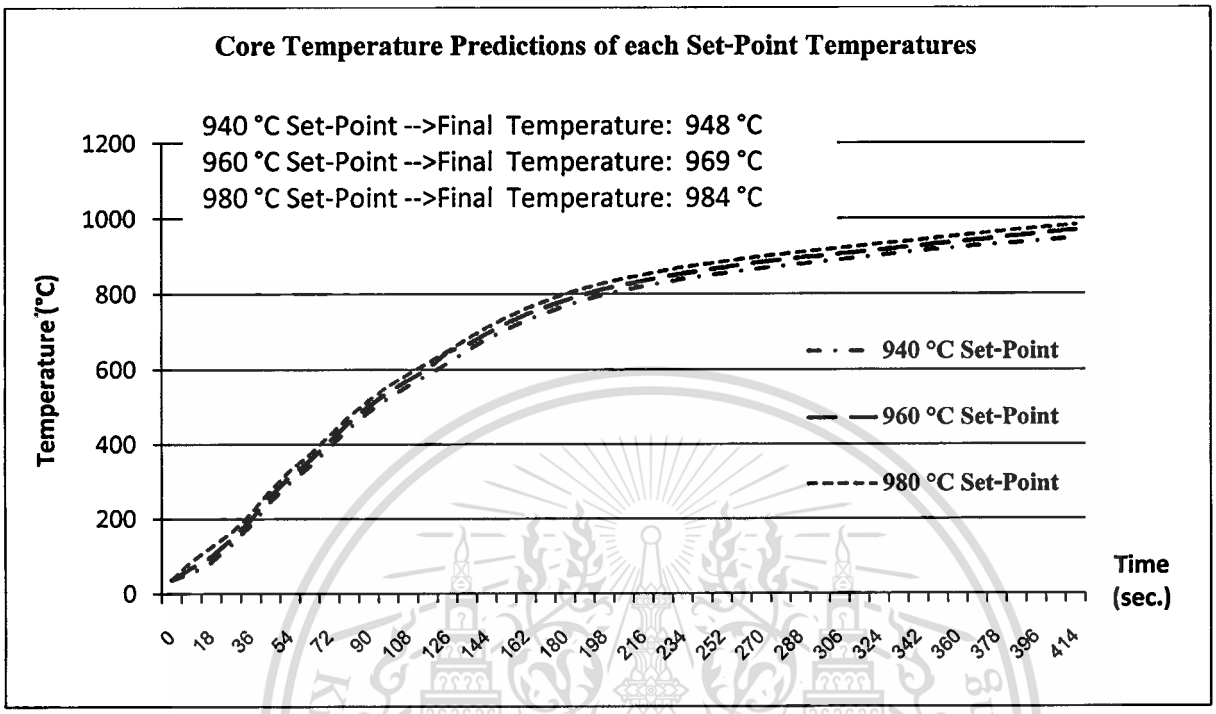

Figure 4.20 the core temperature prediction of 940, 960, 980 °C set-point temperature by using effective temperature model in table 3 and emittance 0.8.

For 17.4 mm round bar, the results of section 4.1.2 shows that the heating processing temperature 940 °C can be achieved if only the feeding time is more than 9 second. The set-point is temperature is fixed variable at the maximum 980 °C due to the furnace limitation. The independent variable is feeding times which are varied from 9, 10, 11, 12 second for round bar completely absorbing the heat to reach the heating process temperature. In order to model the effective temperature along furnace direction in each set-point temperature change, the steady states of ambient vicinity temperature are collected at initial(0), inlet(1), middle(23) and outlet(45) location for 3-wisepiece linear representation of the effective temperature along furnace as previously done for 10.5 mm core temperature prediction. The overview temperature distribution of furnace is changed corresponding to the feeding time as shown in time regions F1, F2, F3 and F4 of Figure 4.19. The steady state of initial, inlet, middle and outlet temperature of 9, 10, 11 and 12 feeding times are individually shown in Figure 4.20, 4.21, 4.22 and 4.23 respectively and approximately used for

effective temperature as 3-wisepice linear corresponding to each cases shown in Figure 4.24. It is apparent that the increase of feeding time inversely affects to the effective temperature along furnace direction because of the round bars longer staying in furnace and absorbing the heat so much that the effective temperature decreases. The table 4.4 also shows the ambient vicinity temperature which is used as 3-wisepiece linear model of effective temperature in each feeding time cases

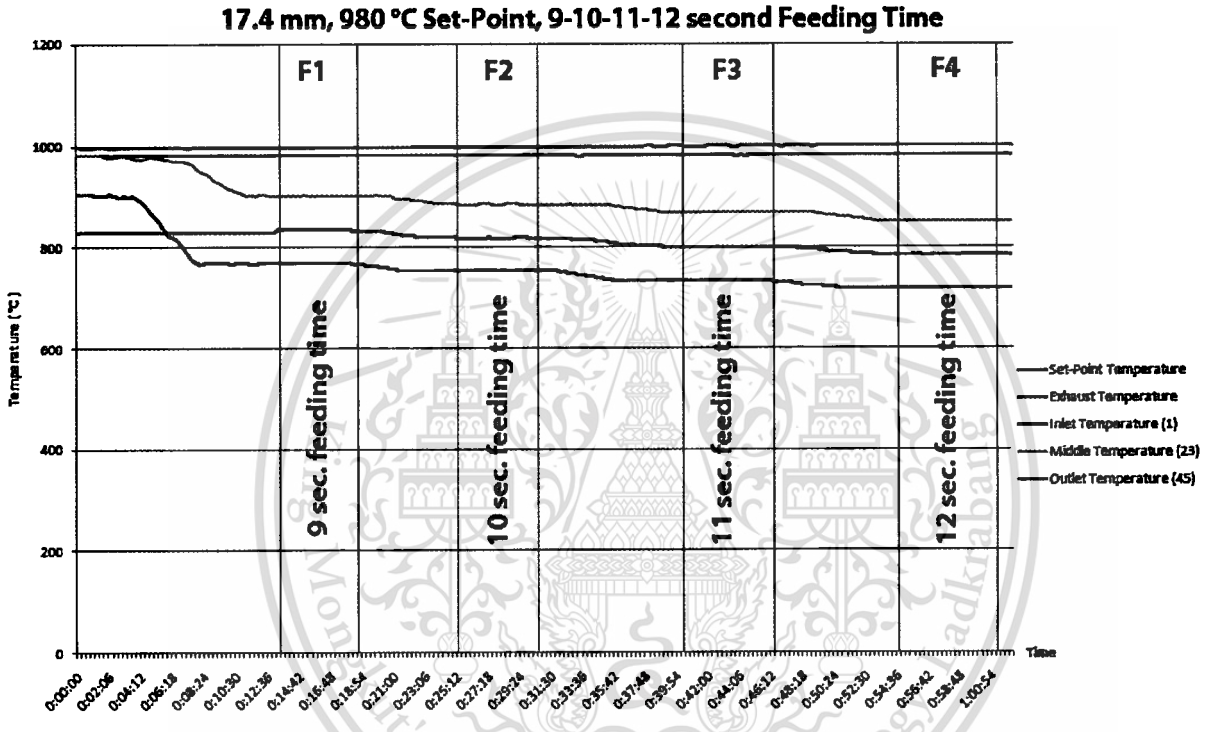

Figure 4.21 Temperature distribution in furnace with four feeding time, 9-10-11-12 second at 980 °C set-point

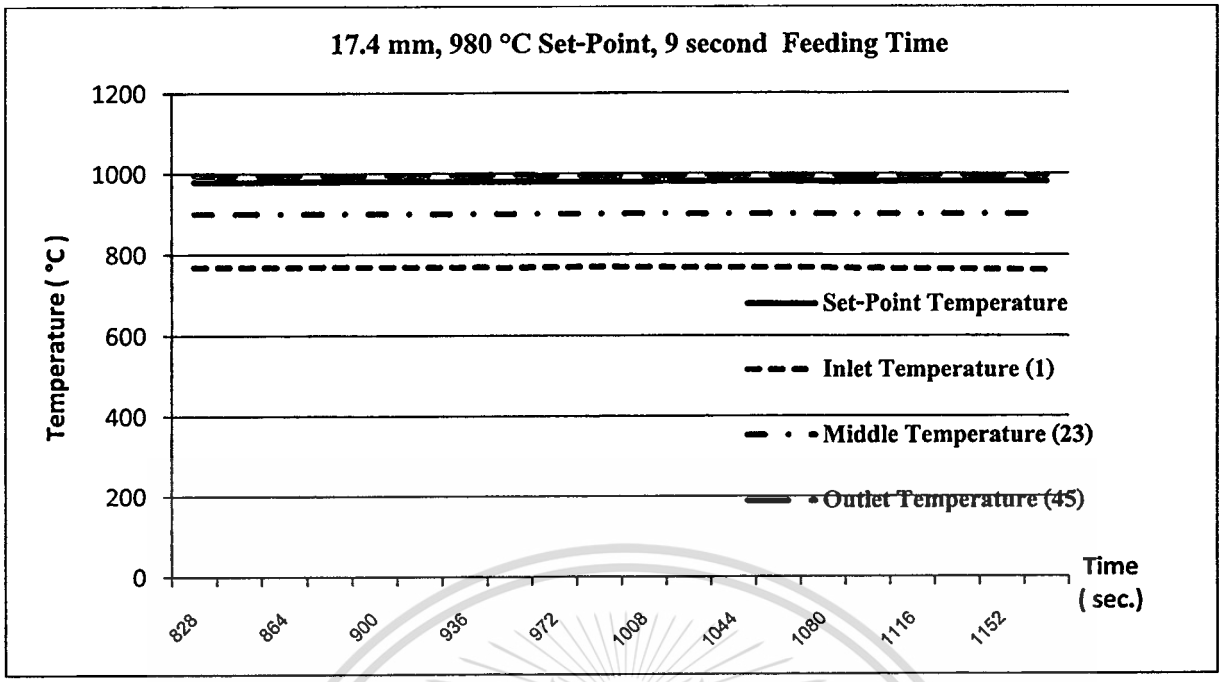

Figure 4.22 Steady state of five locations along furnace at 9 second feeding time, 980 °C set-point temperature.

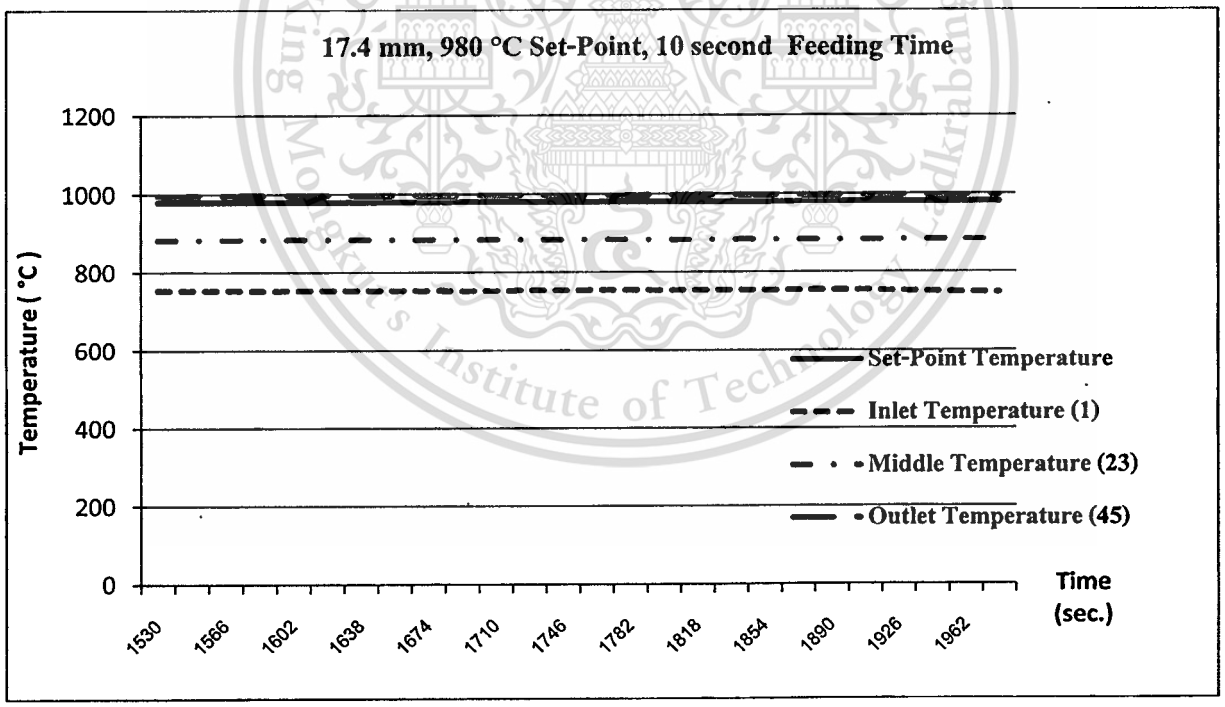

Figure 4.23 Steady state of five locations along furnace at 10 second feeding time, 940 °C set-point temperature.

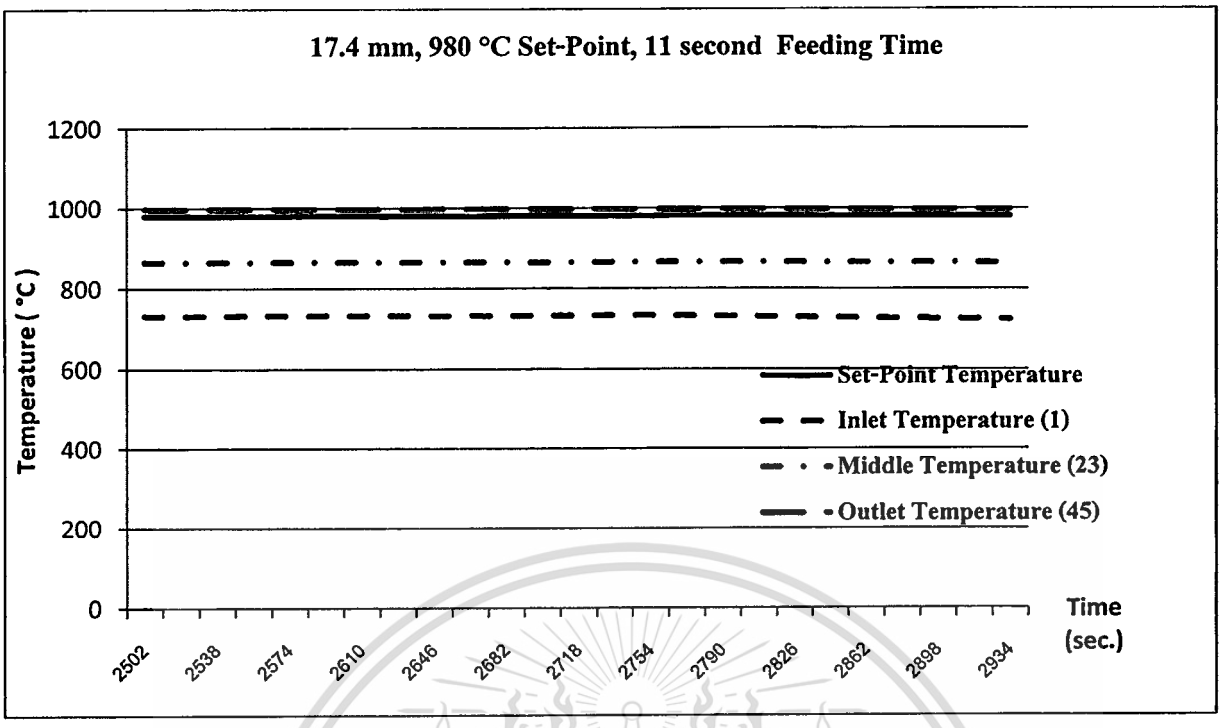

Figure 4.24 Steady state of five locations along furnace at 11 second feeding time, 940 °C set-point temperature.

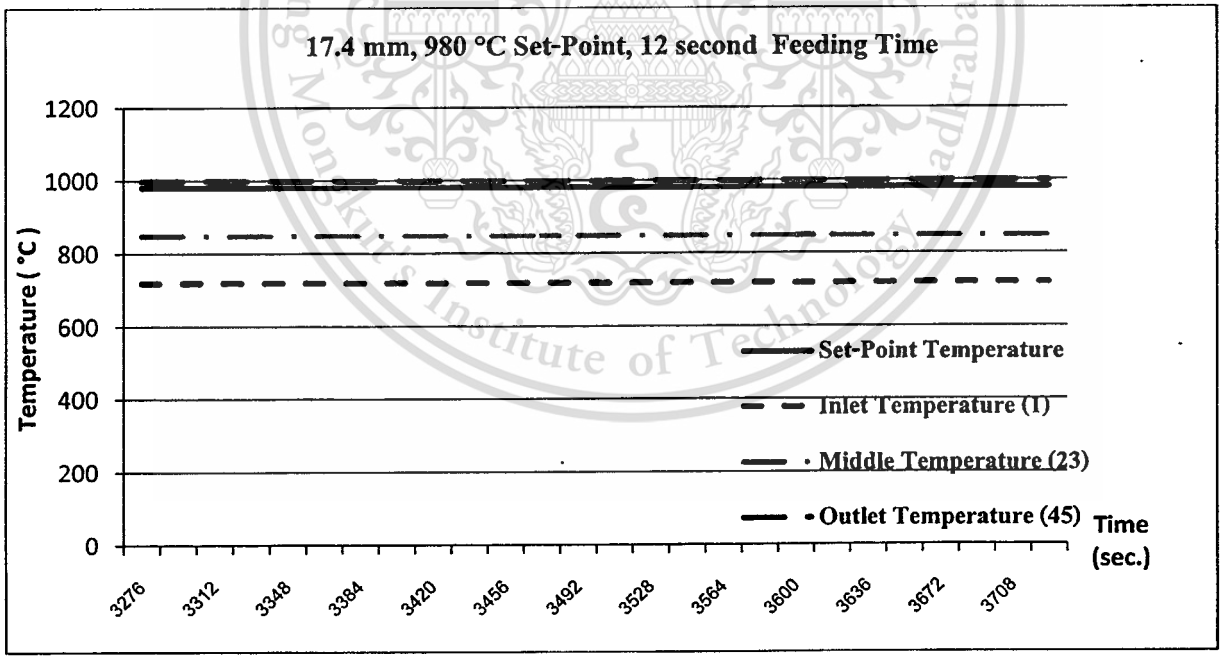

Figure 4.25 Steady state of five locations along furnace at 12 second feeding time, 940 °C set-point temperature.

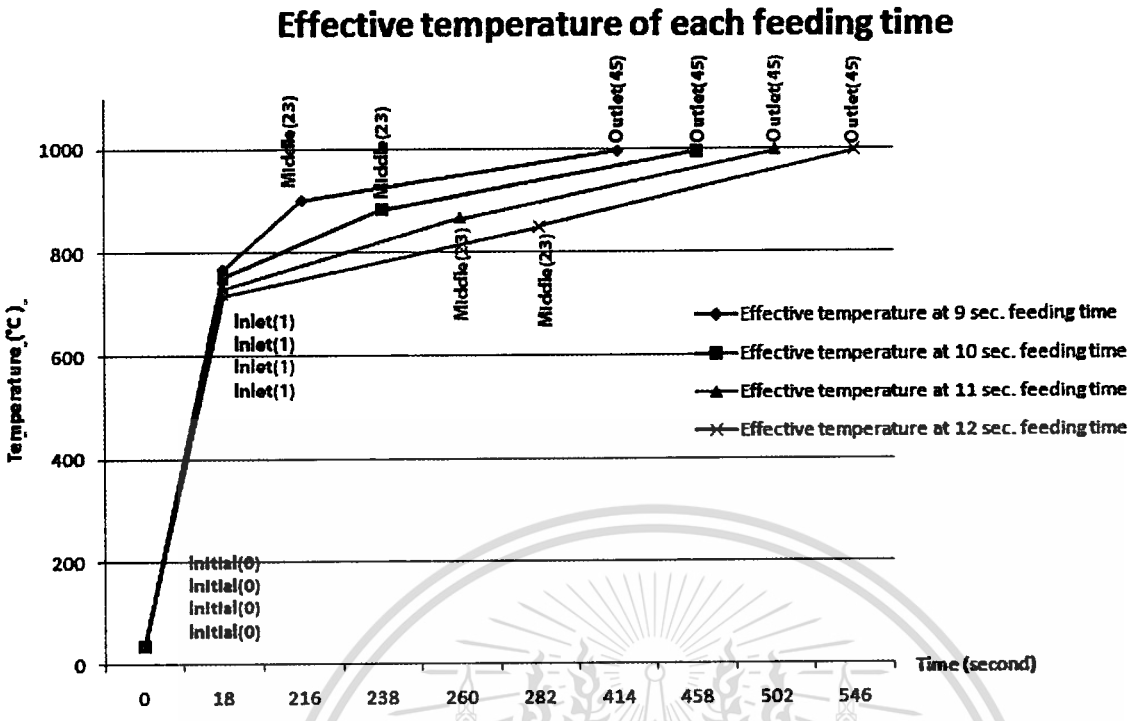

Figure 4.26 Effective temperature modeling along furnace at feeding time 9, 10, 11 and 12 second while 17.4 mm round bars are under 980 °C set-point temperature.

Table 4.4 Effective temperature of 9, 10, 11 and 12 second feeding at fiexed 980 °C set-point temperature.

Location	Initial (0) (°C)	Inlet (1) (°C)	Middle (23) (°C)	Outlet (45) (°C)
9 second feeding time (0:15:54)	36.0	768.3	901.0	996.1
10 second feeding time (0:28:12)	36.0	752.7	883.1	996.7
11 second feeding time (0:44:06)	36.0	732.2	865.8	997.3
12 second feeding time (0:56:06)	36.0	719.1	848.1	998.2

As a result of final core temperature predictions of each feeding time illustrated in Figure 4.25, it obviously shows that 11 second feeding time operation predicts the final core temperature of 17.4 mm round bar at 946 °C which is approximately closest to the heating process temperature than others. Consequently, the furnace operation of 17.4 mm round bar is 980 °C set-point and 11 second feeding time.

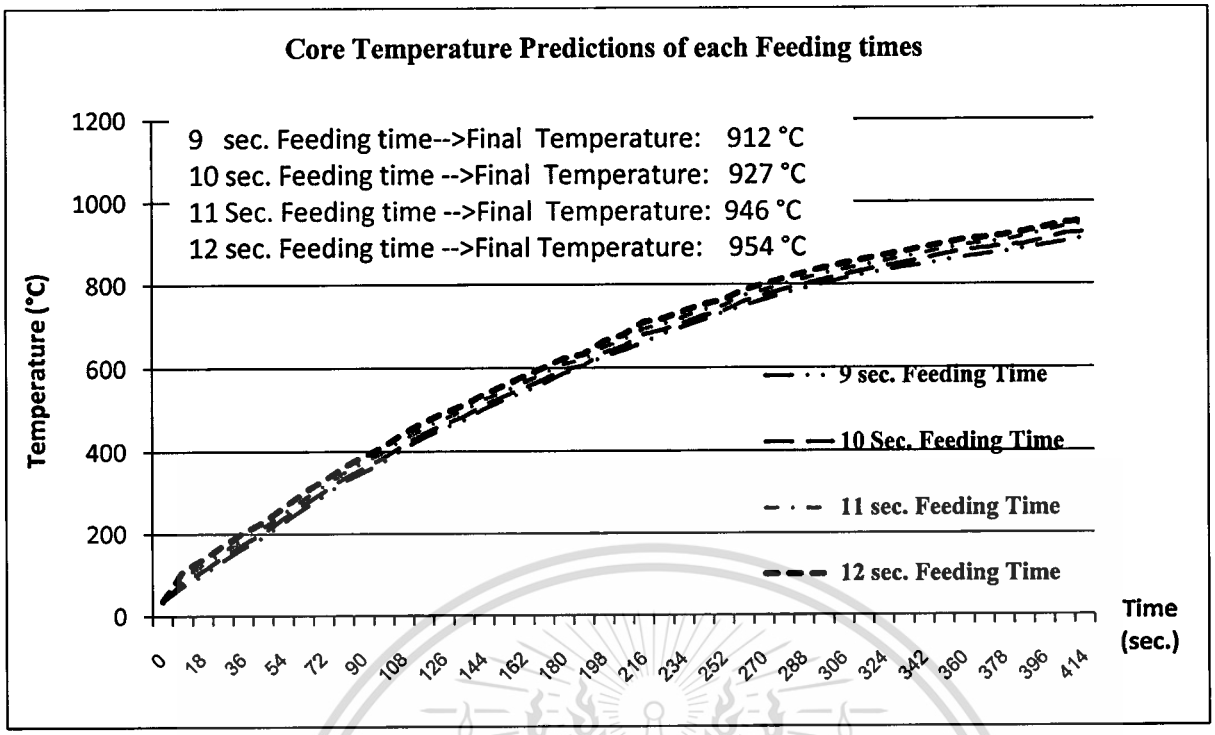

Figure 4.27 The core temperature prediction of 9, 10, 11 and 12 second feeding time with fixed 980 °C set-point temperature by using effective temperature model in table 4.4 and emittance 0.8

4.5 Determination of Optimum Furnace Operating Parameters for the Heating of Round bars of Various Sizes

The objective of this experiment is to determine the furnace optimal operation of heating process which is applied for 10.5, 13.5 and 17.4 mm round bar. There are two important parameters that deal with the heating process; set-point temperature and feeding time. These parameters are optimally conFigure.d so that the core temperature of round bars, that exit from the furnace, are guaranteed to reach around 940 °C for standard steel quality which guarantees the standard of steel quality to be further processed in the procedure of coil spring manufacturing and also feeding time as low as possible to yield the high productivity under the maximum 980 °C set-point temperature constraint of furnace.

The optimal heating operation of 10.5, 13.5 and 17.4 mm round bar can be summarized by experimental and simulation results in section 4.1.2 - 4.1.4 and shown in table 4.5. Under these

optimal conditions, the core temperature of each product can be heated to the desired level with minimal energy. Equivalently, round bars instantly obtain the desired core temperature level when they have just come out the furnace. Note that the more set-point temperature than the optimal value consumes more energy and the steel quality is deviated from standard.

Table 4.5 Optimal heating process operations for 10.5, 13.5 and 17.4 mm round bar.

Product Type	Set-Point Temperature(°C)	Feeding time(second)
10.5 mm round bar	940 °C	9
13.5 mm round bar	980 °C	9
17.4 mm round bar	980 °C	11

CHAPTER 5

CONCLUSION

In this chapter, the experimental results, conducted in chapter 4, are totally summarized and applied for answering the following thesis objectives.

5.1 To investigate the operation of a walking-beam furnace used for reheating steel bars in a coil-spring manufacturing process

- The walking-beam furnace is applied for heating the various sizes of the round bars, which travel along the furnace, to properly reach around 940 °C core temperature that guarantees for stand steel quality which guarantees the standard of steel quality to be further processed in the procedure of coil spring manufacturing. The temperature distribution of furnace is controlled by set-point temperature location which measures the temperature of hot gas flowing inside the furnace as described in section 4.1 and 4.2 In principle of heating process, the hot gas turbulently flows through the heating (middle, outlet) and preheating zones (inlet) where the heat is convected and then conducted to the core of steel round bars that travel along the furnace. However, this complicated thermal system of actual furnace can be appropriately reduced to the transient 1-dimensional thermal system of irradiative and conductive heat transfer instead of convection as described in section 4.3 and 4.4 For obtaining the standard of steel quality, it is required for synchronized control between set-point temperature and feeding time. However, the set-point might be confide at the too temperature, but the feeding time can be resolved so that the round bars stay no longer in furnace to absorb appropriate amount of heat energy before exiting.

5.2 To be capable of specifying optimized operating conditions of the walking-beam furnace's heating operation for the production of different sizes of coil springs

- To improve the performance of walking-bear furnace with optimality, it is necessarily operated for obtaining the standard of steel quality that is guaranteed around 940 °C of round bar core temperature and also high productivity corresponding to their sizes. There are two conFigure urable parameters, which are set-point temperature of furnace and feeding time of each round bar to achieve these optimal conditions. However, the optimal furnace operation of a size of round bar is successfully found by experiment that is conducted in section 4.2, but the simulation results of core temperature prediction can efficiently determine the optimal operation for the others sizes as described in section 4.4 The following table is summarized about the optimal furnace operation for each size of round bar. Note that maximum set-point temperature of furnace is limited at 980 °C.

Table 5.1 Optimal walking-beam furnace operations for 10.5, 13.5 and 17.4 mm round bar.

Product Type	Set-Point Temperature(°C)	Feeding time(second)
10.5 mm round bar	940 °C	9
13.5 mm round bar	980 °C	9
17.4 mm round bar	980 °C	11

- Generally, the walking-beam furnace of coil spring manufacturing is designed for size in the range 8-20 mm, although the current coil spring manufacturing is only in the range 10.5-17.4 mm. It is probably to manufacture the other size for furnace specification, so the method of determining the optimal furnace operation for others size is helpful for initiating the furnace in early. The method is based on linear approximation of experimental result of 10.5, 13.5 and 17.4 mm that is summarized in section 4.1.5. For the larger than 17.4 mm. round bar size, the estimation is done along the blue line, otherwise the red is applied. If it is supposed to estimate the optimal furnace operation of maximum and minimum round bar size

corresponding to this furnace specification, the estimation of 20 mm. maximum size round bar is extrapolated from the blue line of Figure 5.1 as following,

$$\frac{11\ sec. - 9\ sec.}{17.4\ mm. - 13.5\ mm.} = \frac{X\ sec. - 9\ sec.}{18.0\ mm. - 13.5\ mm.}$$

$$X = 11.31\ second$$

Consequently, the optimal operation of furnace, that guarantees the 940 °C core temperature and high productivity, should be likely around 980 °C set-point temperature and 12.33 second of feeding time for 20 mm. round bar. Another is for minimum size 8 mm. round bar; the optimal of furnace operation should be likely around 910 °C and 9 second feeding time for this case by extrapolating from the red line shown in Figure 5.1.

$$\frac{980\ °C - 940\ °C}{13.5\ mm. - 10.5\ mm.} = \frac{T\ °C. - 940\ °C}{8.0\ mm. - 10.5\ mm.}$$

$$T = 906.67\ °C$$

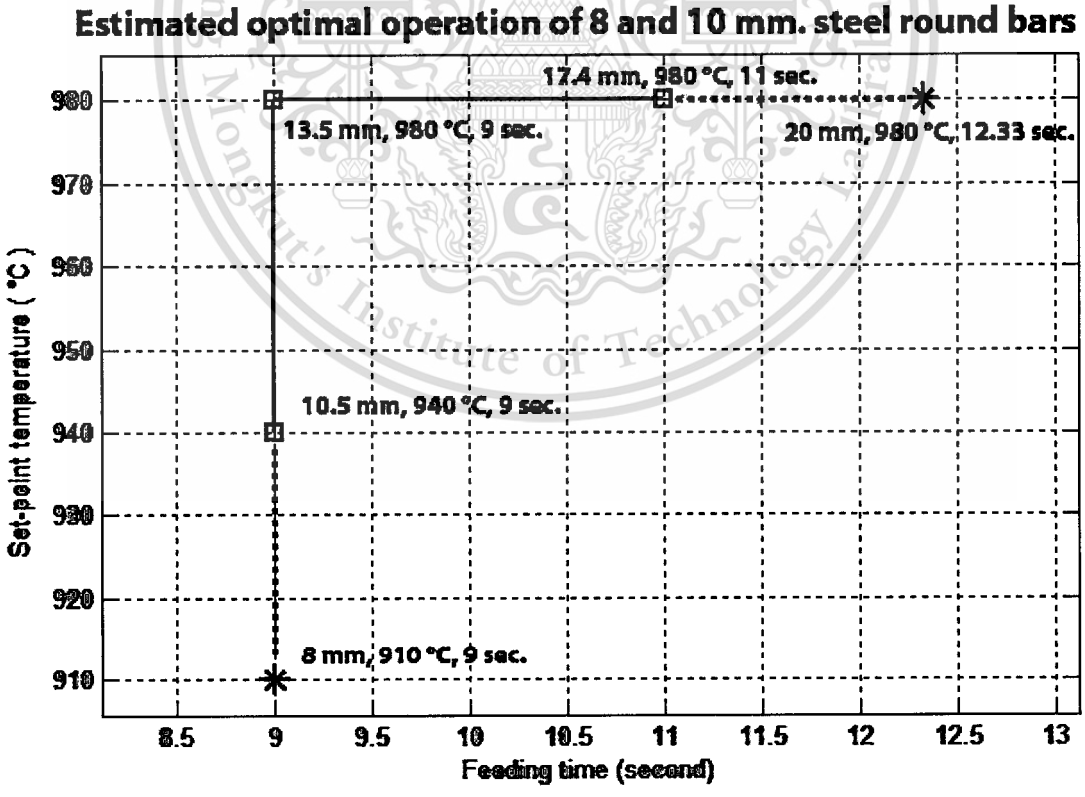

Figure 5.1 Linear approximation of optimal furnace operation for 8 and 20 mm. based on 10.5, 13.5 and 17.4 mm. optimal operation data.

5.3 To summarize about the advantages of all experimental results over the walking-beam furnace of coil spring manufacturing.

- Reduction of the setup time of furnace operation when there is new size of round bar to be processed by the walking-beam furnace.
- Energy saving due to furnace optimal operation corresponding to round bar size.
- Standard steel quality which is the important criteria for coil spring manufacturing.
- Furnace efficiency inspected by collection of operation history.

REFERENCE

[1] Key to Metals AG. 2011. Classification of Carbon and Low-Alloy Steels. [Online]. Available : http://www.keytometals.com/articles/art62.htm.

[2] Knowles, P.R. Design of Structural Steelwork. 2nd ED. London : Taylor and Francis. 1987.

[3] Pollack, H.W. Material Science and Metallurgy. 4th ED. Eaglewood Cliffs, NJ : Prentice-Hall. 1988.

[4] Meyrick, G. 2001. Steel: Physical Metallurgy of Steel. [Online]. Available: http://www.tech.plymouth.ac.uk/sme/Interactive_Resources/tutorials/Failure Analysis/Undercarriage_Leg/.

[5] Wettlaufer, M. and Kaspar, R. "Effect of Phosphorus on the Ductility of High Strngth Spring Stels.", Steel Research, vol.71, no.9, 2000. pp. 357-361.

[6] Bergqvist, L. 2009. "Induction Heating of Steel Bars for Hot Coiled Spring Production." West Yorkshire, Great Britain : Lesjofors Technical Report 2/2009.

[7] Barani, A.A. and Ponge, D. "Optimized Thermo mechanical Treatment for Strong Ductile Martens tic Steels.", Mat. Sci. Forum, vol.539-543, March 2007. pp. 4526-4531.

[8] Li, F., Barani, A.A., Ponge, D., Raabe, D. "Austenite Grain Coarsening Behavior in a Medium Carbon Si-Cr spring steel with and without Vanadium.", Steel Research, vol. 77, no. 8, 2006. pp. 590-594.

[9] Trinks, W., Mawhinney, M.H., Shannon, R.A., Reed, R.J. and Garvey, J.R. Industrial Furnaces. 6th ED. New Jersey : John Wiley & Sons, Inc. 2004.

[10] Sitkovskii, S., Emmanuel, G.A. and Zelenskii, D.V. "Operation of a Walking- Beam Furnace.", Metallurgist, vol.11, no.10, Oct. 1967. pp. 585-587.

REFERENCES (CONT.)

[11] Martensson, A. "Energy Efficient Improvement by Measurement and Control: A Case Study of Reheating Furnaces in the Steel Industry." Proc. 14th NIETC, Texas, USA, April, 1992. pp. 236-243.

[12] Karl-Heinrich Grote, Erik K. Antonsson, Editors. Springer Handbook of Mechanical Engineering. New York : Springer. 2009.

[13] Krishnamurthy, N., Vallinayagam, P. and Madhavan, D. Engineering Chemistry. 2nd ED. New Delhi : PHI Learning Private Limited. 2008.

[14] Maina, N.S. "Development of Petrochemicals From Natural Gas (Methane).", ChemClass J., vol.2, 2005. pp. 25-31.

[15] Gas Authority of India Limited. 2011. Natural Gas: City Gas Distribution. [Online]. Available : http://www.gailonline.com/gailnewsite/businesses/citygasdistribution advantage.html.

[16] United Nations Environment Programme. 2006. Fuels and Combustion. [Online]. Availble : http://www.energyefficiencyasia.org/energyequipment/ee_ts_fuel.html.

[17] Wikipedia. 2011. Combustion. [Online]. Available : http://en.wikipedia.org/wiki/Combustion.

[18] TSI Incorporated. 2004. Combustion Analysis Basics: An Overview of Measurements, Methods and Calculations Used in Combustion Analysis. [Online]. Available : http://www.tsi.com/uploadedFiles/Product_Information/Literature/Handbooks/CA-basic-2980175.pdf.

[19] Lienhard, J.H. IV and Lienhard, J.H. V. A Heat Transfer Textbook. 4th ED. Massachusetts : Phlogyston Press. 2011.

[20] Cengel, Y.A. Heat Transfer: A Practical Approach. 2nd ED. McGraw Hill Professional. 2003.

REFERENCES (CONT.)

[21] National Institute of Standards and Technology. 2011. NIST Standard Reference Database Number 69. [Online]. Available : http://webbook.nist.gov.

[22] Bureau of Energy Efficiency. 2011. Furnaces. [Online]. Available: http://www.bee-india.nic.in/.

[23] Herrmann, E. 2010. "Computational Fluid Dynamics Simulations in Aerosol and Nucleation Studies." Ph.D. dissertation, University of Helsinki. [24] ANSYS, Inc. 2009. ANSYS 12.0 Release ANSYS® FLUENT®. [Online]. Available: http://www.enginsoft.it/software/ansys/cfd/fluent/fluent-brochure- 12.0.pdf.

[25] Agarwal, P. 2009. "Simulation of Heat Transfer Phenomenon in Furnace Using FLUENT-GAMBIT." Bachelor dissertation, National Institute of Technology Rourkela.

[26] Datapaq Ltd. 2004. Furnace Tracker System for Billet Reheat Furnaces. [Online]. Available : http://www.datapaq.com/literature/pdfs/billet-e.pdf.

[27] Jinwu kang, Yiming Rong , Modeling and simulation of load heating in treatment furnace. Journal of Materials Processing technology 174 (2006) 109 – 114 Available: www.sciencedirect.com

[28] Sang Heon Hun, Seung Wook Beak, Sang Hun Kang, Chang Young Kim, Numerical analysis of heating characteristics of a slab in bench scale reheating furnace. [online] Available: www.sciencedirect.com

[29] Man Young Kim, A heat transfer model for the analysis of transient heating of the slab in a direct-fired walking beam type reheating furnace. International Journal of Heat and Mass Transfer 50 (2007) 3740 – 3748, [online] Available: www.sciencedirect.com

[30] Sang Heon Han, Seung Wook Beak, Man Young Kim transient rediative heating characteristics of slabs in a walking beam type reheating furnace. International journal of Heat and Mass Transfer 52 (2009) 1005-1011 [online] Available: www.sciencedirect.com

REFERENCES (CONT.)

[31] Sang Heon Han, Daejun Chang, Chang Young Kim, A numerical analysis of slab heating characteristics in a walking beam type reheating furnace. International journal of heat and mass Transfer 53 (2010) 3855 – 3861 [online] Available: www.sciencedirect.com

[32] Principles of Heat Transfer 7th, 2011, F. Kreith, Raj M. Manglik, Mark S. Bohn.

APPENDIX A

WALKING-BEAM FURNACE:

A.1 Detailed Design

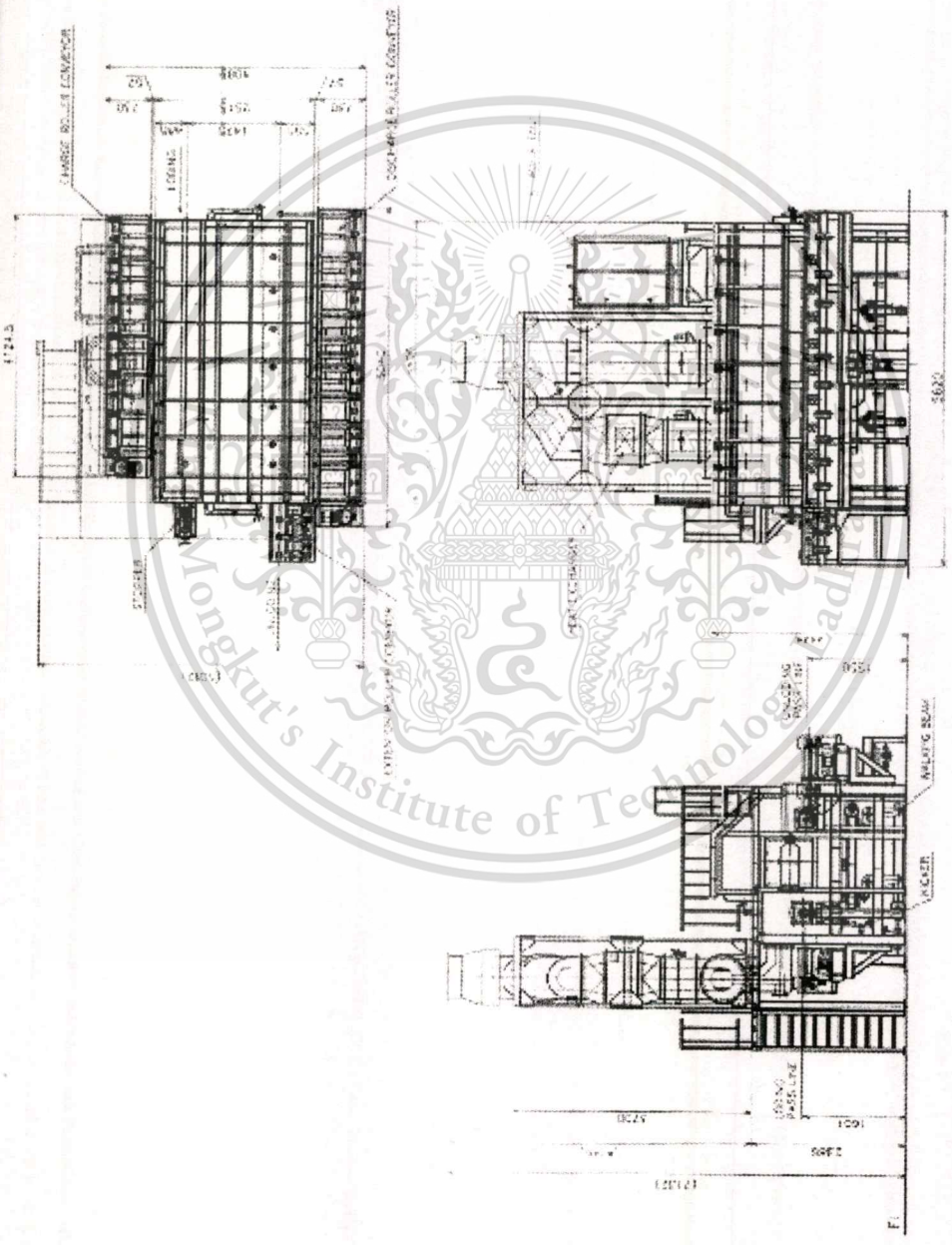

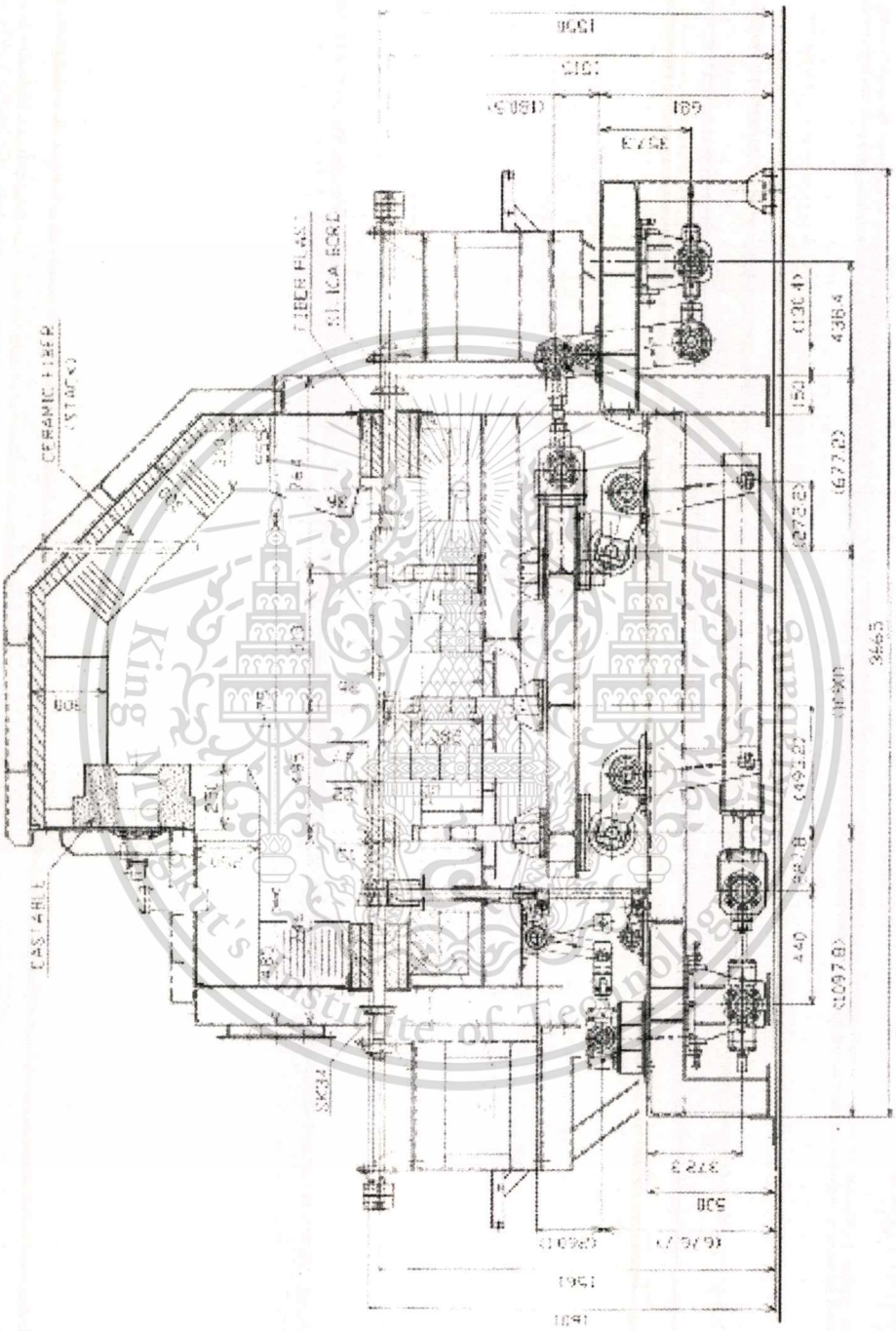

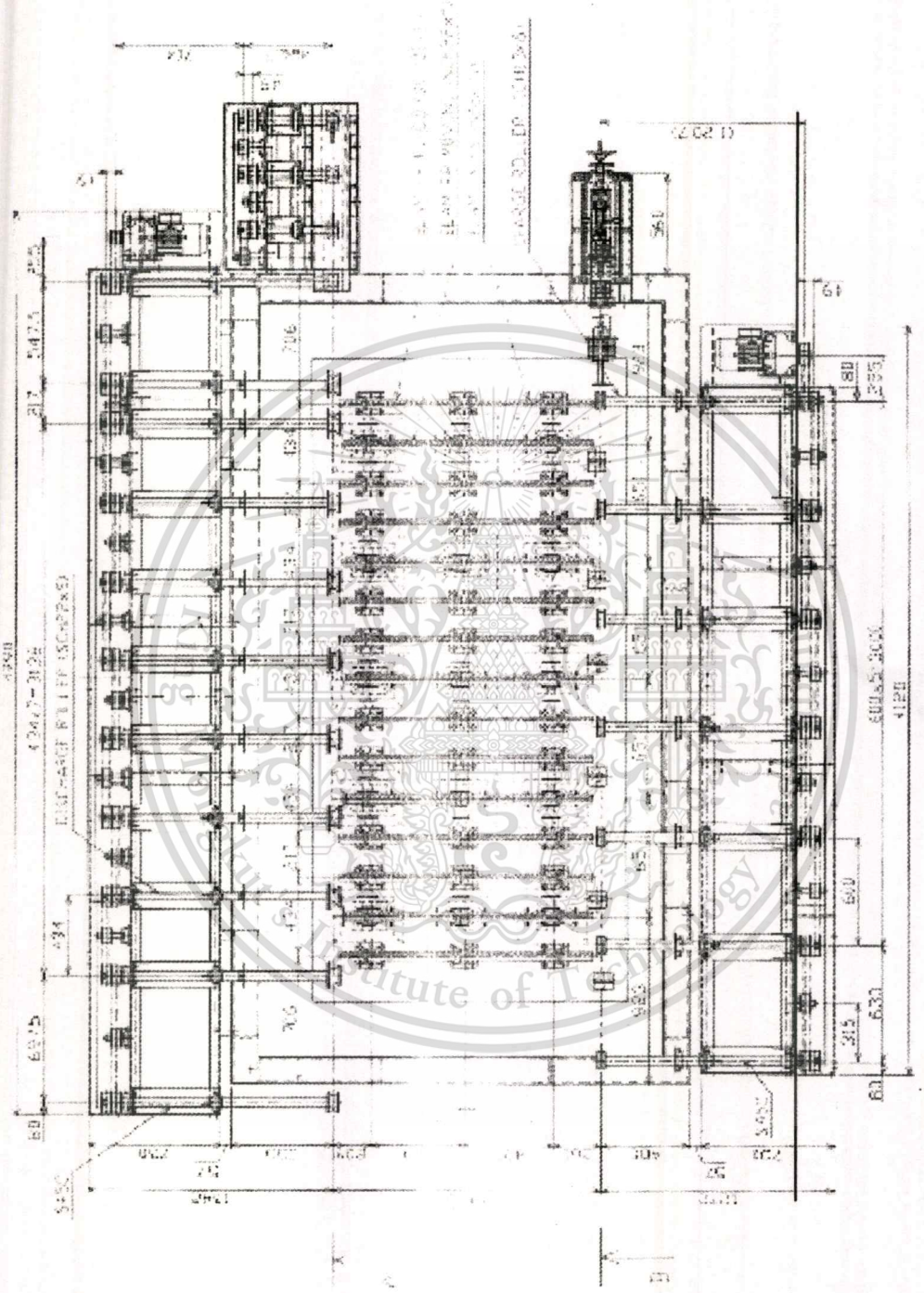

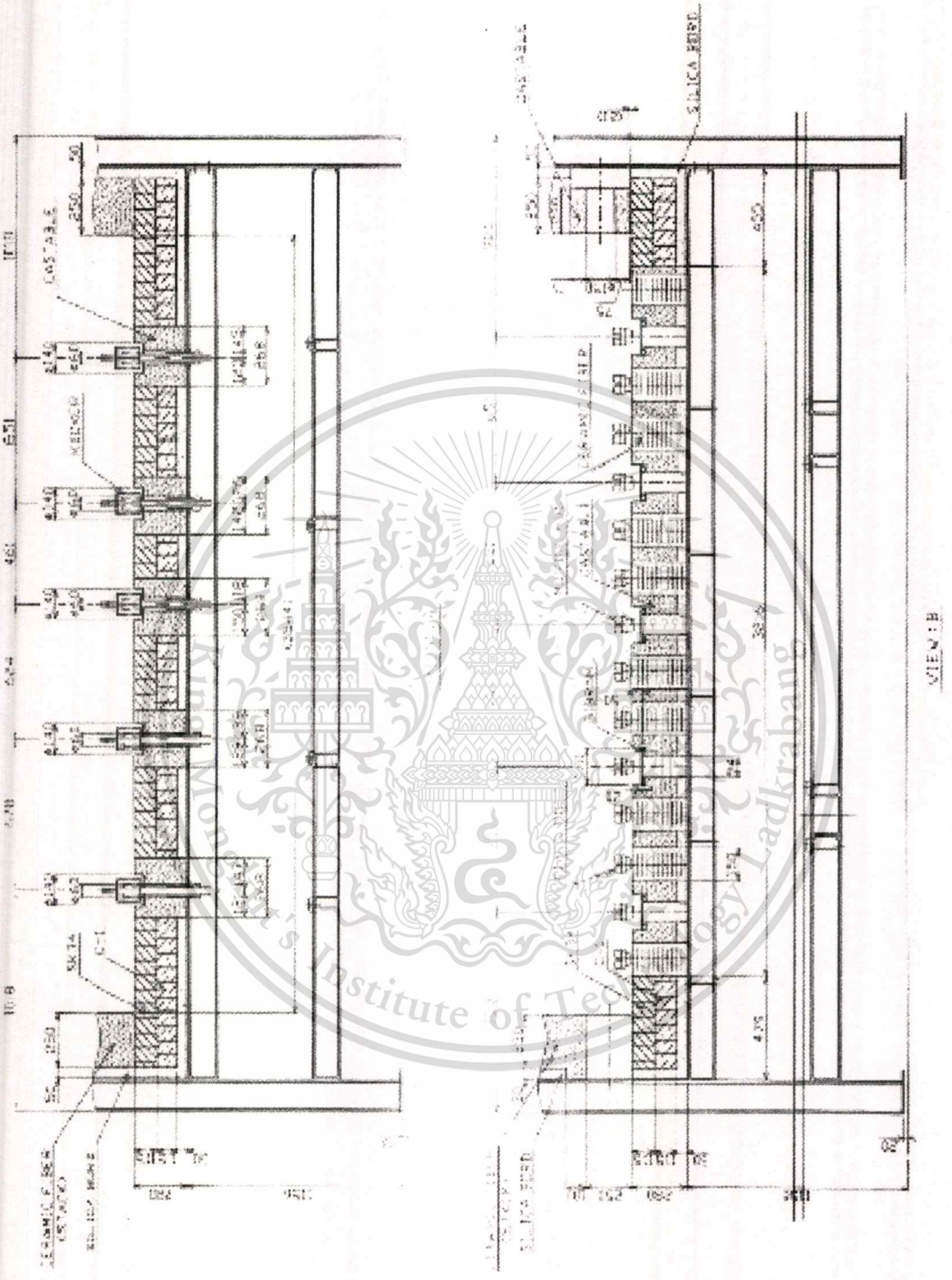

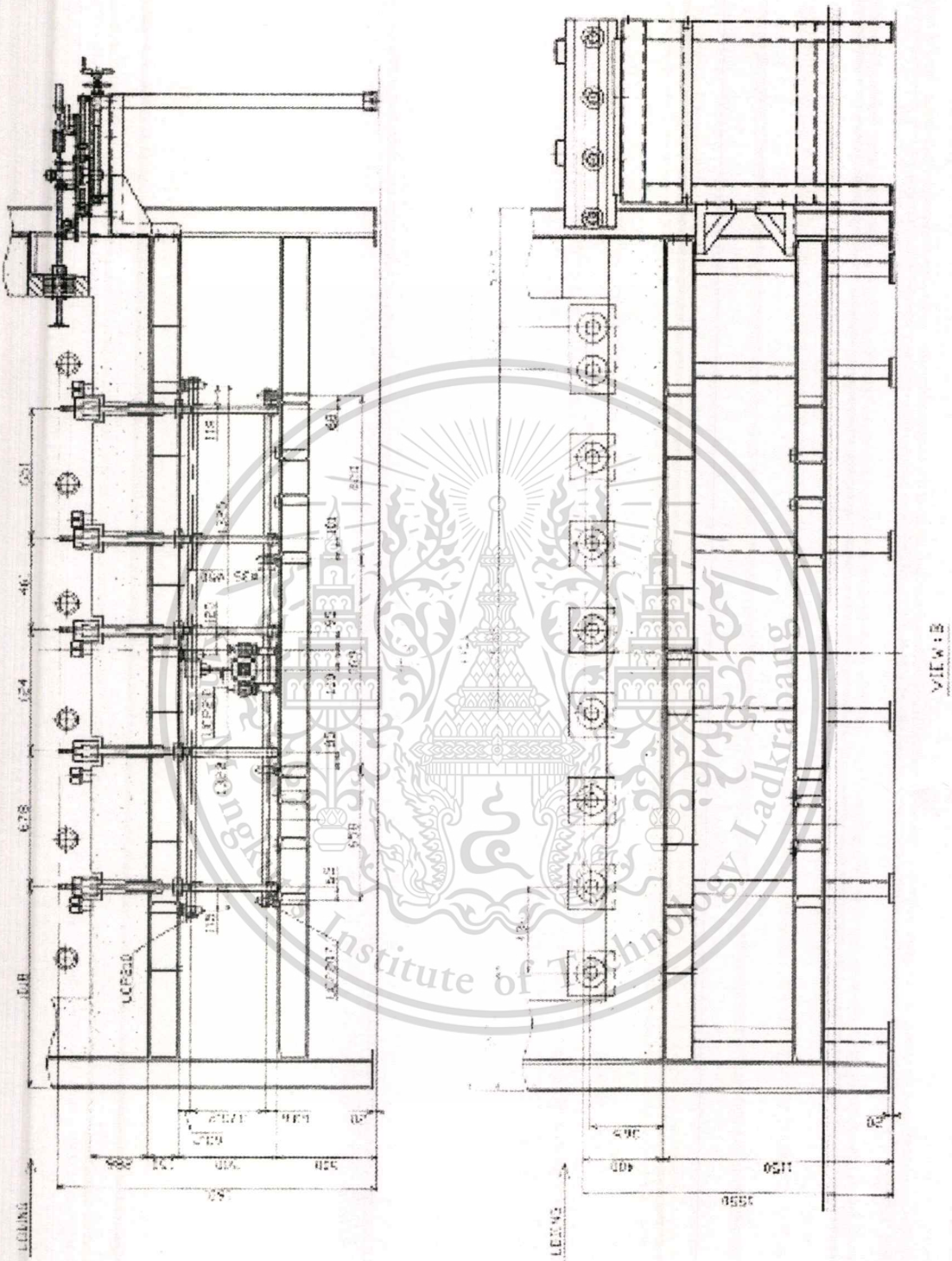

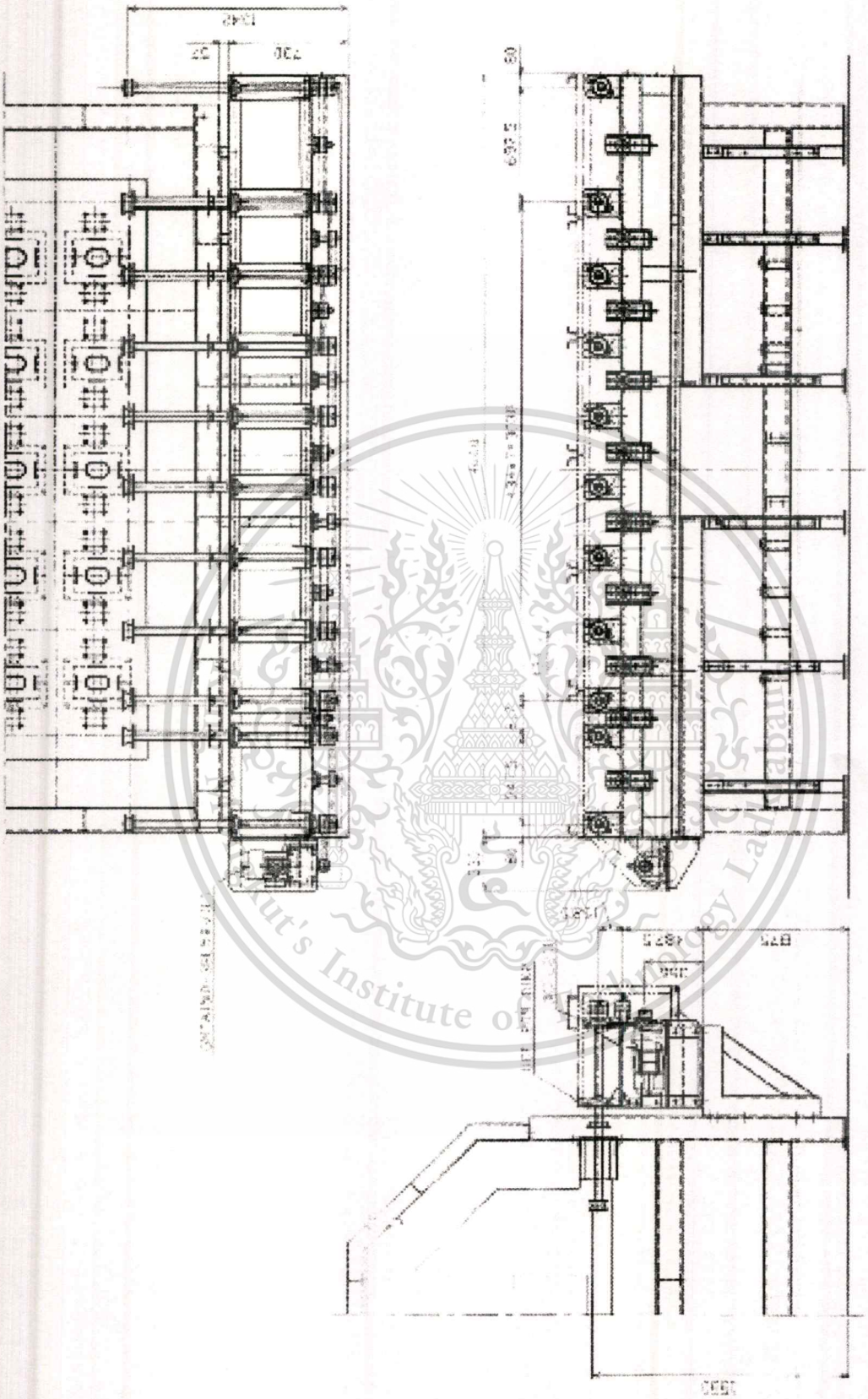

A.2 Specifications

Furnace outline	1. Furnace body 2. Combustion equipment 3. Transport equipment 4. Material-supply device 5. Temperature-control equipment	
Workpiece	Coil Spring	
	Material	Spring steel
	Diameter (mm)	9-20
	Length (mm)	1,730 - 3,250
	Wight (kg)	0.9 - 6.11
Standard workpiece	D 12.8 mm x L 2,750 mm x 2.78 kg.	
Capacity (Standard work)	1,112 kg/hr (400 piece/hr)	
Transfer system	Walking-beam driving	
	Tact time (s/tact)	9 (Standard work)
	Tact time is changeable by timer	
	Machine tact speed (s/tact)	5
	Sending pitch (mm)	30
	Up-down stroke (mm)	47 (22+25)
	Built-in middle stop function	
	Number of beam	15 (5 transfer + 10 fix)
Usable dimension	3,250 w (mm)	
Heating temperature	900 ° C - 1,000 ° C (Atmosphere max. temperature 1,000 °C)	
Temperature precision range	20 ° C (± 10 ° C)	
Temperatrue control	PID ; 3-point measurements	
Heat source	Natural gas (8,800 kcal/Nm^3; 10 kPa)	
Combustion control	Equalizing valve control (Automatic ignition by PL '/B Push button)	

Power source	Supply power	3 phase; 380 V; 50 Hz
	Usage	Motive: 3 phase; 380 V Control & etc.: 1 Phase; 200 V
Furnace frame (1 unit)	1. Steel plate and shape steel welding constructor 2 inspection holes and 4 peepholes are on side-wall 2. Temperature precision measurement tongue for the furnace side 24 places in total (12 places of charge side + extraction side) 3. Measurement tongue for radiation themometers for the furnace top surface 8 places in total Ceiling and side-wall — Ceramic fiber	
	Hearth	Castable + Insulation brick + Silica board
	Circumference of moving post	Gibram
Waste gas duct (1 unit)	Control damper (2 units)	SUS 310s
	Control motor	300 rph/l
	Preheat-Zone exhaust duct	Cermic fiber lining
	Main exhaust duct	SS 400, FL + 6 m
Combustion equiment (1 unit)		
Main burner and pilot burner	Main-gas burner	SGL-1 (110,000 kcal/hr) 6 units
	Pilot-gas burner	PBX-2 (2,900 kcal/hr) 6 units
	Ignition transformer, ignition plug, high-voltage cord, solenoid valve, air-gas cock	
	Equalizing valve	A 25Z-2 (3 units)
	Main-gas solenoid valve	VEN 4020B1200 (6)
	Air control damper	CD 50 M, CM 101 tph/L (3 units)

	Combustion	KFL-7P/5 13.5 m^3/min, 960 mm^2 3 phases; 380 V; 5.5 kW (1 unit)
	Pressure switch	C 6097A0310 (1piece)
	Other (limiting valve, metaling orifice, butterfly	
	valvae, pressure gauge, etc.) (1 unit)	
Fuel supply equipment (1 unit)	Pilot-gas reducing	ABN-1 (1 unit)
	Gas-cutoff valve	SKP10.11112/VGG10. 404P (1 unit)
	Gas-cutoff meter	Turbine type TBX 100 (1 unit)
	Pressure switch	C 6097A0310 (1piece) C 6097A0210 (1piece)
Piping facility (1 unit)		
Transport equipment (1 unnit)		
Waliking-time Transport equinment (1 unit)	Driving form	By oil-pressure driving walking beam transport (arm-lever system)
	Beam number	15 (5 Transfer + 10 Fixed)
	Beam post material	SCH 22
	Send stroke (mm)	30
	Life stroke (mm)	47 (22+25)
	With middle-stop function	
	Fixing beam	SCH 22 (1 unit)
	Moving beam	SCH 22 (1 unit)
	Fixing beam	SCH 22 (1 unit)
	Moving beam	SCH 22 (1 unit)
	Seal plate	SCH 13 (1 unit)
	Driving device	

	Hydraulic pump unit	3 phases, 380 V, 3.7 kW (1 unit)
	Oil-tank hydraulic pump, cooler (water cooling) solenoid valve, etc. (1 unit)	
	Front and rear hydraulic cylinder (1 unit)	
	Elevator hydraulic cylinder (1 unit)	
	Others (hydraulic flexible horse, bearing, shaft, roller, etc.) (1 unit)	
	Front and rear hydraulic cylinder (1 unit)	
Input driving equipment (1 unit)		
Driving form	Roller conveyer	
Roller material	Head, SCH 13	
Number of rollers	Inside	6
	Outside	1
Geard motor for roller spinning	GMTA 150-38L5V1PSE1 3 phase, 380 V, 1.5 kW (1 unit)	
Driving parts	Shaft, bearing, belt-pulley, etc. (1 unit)	
Work transversing equipment (1 unit)	Air cylinder, E2M30S035SD-C (1 unit)	
	Shock absorber, 10S-1DSD40N40 (1 unit)	
	shaft, bearing, heat-resistant metal stopper (1 unit)	
	Others (pressure control valve, strainer, speed controller, solenoid valve and compressed air piping facility) (1 unit)	
Extract driving equipment (1 unit) The materials are brought to the right side of conveyer direction by the rotation of rollers, while the rejected (as NG) material can be brought to the left side by switching on the control panel the rotation of the rollers		
Driving form	Roller conveyer	
Roller material	Head, SCH 22	
Number of rollers	Inside : 9	Outside : 1
Geard motor for roller driving	GMTA 150-38L5V1PSE1 3 phase, 380 V, 1.5 kW (1 unit)	
Driving parts	Shaft, bearing, belt-pulley, etc. (1 unit)	

Greasecenterized oiling equipment (1 unit)	
Oiling type	Grease supply to grease nipple with grease gun
Oiling spot	Bearing of walking beam bearing of charging and extracting roller
Grease nipple	Install on centerized panel (1 unit)
Piping facility	Copper pipe (1 unit)
Work supply equipment (1 unit)	
Roller driving geard motor	GMTA 075-28L5V1P2 3 phase, 380 V, 1.5 kW (1 unit)
Roller	Plain steel made (1 unit)
Roller driving parts	Shaft, bearing, belt-pulley, etc. (1 unit)
Work arranging geard motor	GMTA 075-28L5V1P2 3 phase, 380 V, 1.5 kW (1 unit)
Work arranging disk and shaft	2 units
Work arranging driving parts	Bearing, sprocket, roller, chain, shaft, etc. (1 unit)
Control equipment (1 unit)	
Control panel (1 unit) (Steel plate and shape steel welding construction independence type)	
Sequencer	Q02CPU, Q61P, Q38B, QX41, QY10, QY41, Q68B (1 unit)
Touch panel	GT 1527-VNBA (1 unit)
Integration wattmeter	M2LHM-V 3P3W (1 unit)
Cooler for console	ENC-AR620 (1 unit)
Inverter	FR E740-1.5 K (2 units)
Paets, wiring, etc.	1 unit
Control device parts	
Automatic temperature controller	On-off servo, PID type DB1120-000 (3 unit)
Automatic temperature Controller (for warm water generator)	LT 35030000-00A (1 unit)

Positioner	MEX-M1-A1-K (2 units)
Temperature recorder	Anglog type, 12-points chart width 180 mm EH 100-12 K 0-1,200° C (1 unit)
Thermocouple	K Φ 3.2 Protector SUS 310S (3 units)
Thermocouple	SK 3.2 Φ SUS 304 (1 unit)
Compensating lead wire	K (1 unit)
Flame relay	FRS 100C200 (6 units)
Ultra vision	C 7035A1064J (6 units)
Contactless switch (for walking transport)	EV-118U, EV-130U (1 unit)
Warm water genertor (1 unit)	
Heat exchanger	HR 600-100L 1-30, 30,000 kcal/hr (1 unit)
Storage tank	1 unit
Pump	33 LPD5.75, 3 phases, 380 V, 0.75 kW (1 unit)
Solenoid valve (for supply water)	KW-06-27-AC200V (1 unit)
Floatless switch	61F GPN (1 set)
Piping facility	1 set
Gas detecting warning device (1 unit)	
Gas detecting warning penel	NV-400-2-2-B (1 unit)
Gas detector	KD-5B-N-F1 (2 unit)
Carry-in errection, assembling work (1 unit)	
Test run, adjustment (1 unit)	
Utility	
Fuel	Natural gas, 77 Nm^3/hr, 10 kPa
Power supply	3 phases, 380 V, 15 kW
Supply water	0.2 MPa
Compressed air	0.5 MPa

APPENDIX B

PROPERTIES OF COMPOUNDS

Compound	Compound	Molar mass (g/mol)	Gross heating value (KJ/kg) [12]
Carbon Dioxide	CO_2	44.01	2,411
Butane	C_4H_{10}	58.12	11,820
Ethane	C_2H_6	30.07	12,400
Hexane	C_6H_{14}	86.18	11,600
Hydrogen	H	1.01	141,890
Methane	CH_4	16.04	13,284
Nitrogen	N	14.01	0
Oxygen	O	15.99	-
Pentane	C_5H_{12}	72.15	11,600
Propane	C_3H_5	44.1	12,030
Sulfur	S	32.07	-

APPENDIX C

SPECIFICATIONS OF SPRING STEEL

Material specifications given here are based on Japanese Industrial Standards G 4801 (JIS G 4801), published in 2004, with some modifications of the technical contents.

SUP 12 Steel

Designation of grade	SUP 12								
Remarks	Silicon chromium steel; mainly used for coiled spring								
	C	Si	Mn	P	S	Cr	Mo	V	B
Chemical composition (wt. %)	0.51	1.20	0.60	0.030 max.	0.030 max.	0.60 - 0.90	n.a.	n.a.	n.a.
Diameter (mm)	10 - 16 mm					16 - 21 mm			
Tolerance (mm)	± 0.25					0.25 or under			
Devistion (mm)	± 0.30					0.30 or under			
Ultimate strengh (Mpa/mm^2)	1,000 - 1,200								

APPENDIX D

Table 1. Temperature distribution under no load and load conditions

Time (hh:mm:ss)	Set-point temperature (°C)	Chamber ceiling temperature (°C)	Exhaust temperature (°C)	Inlet temperature (°C)	Middle temperature (°C)	Outlet temperature (°C)
0:00:00	34.7	36.2	34.7	34.9	34.6	34.6
0:00:18	34.7	52	34.7	35	36.6	38.6
0:00:36	34.7	90.2	34.9	35.1	46.3	57.3
0:00:54	35.4	159.8	39.9	57.6	75.3	123.4
0:01:12	41.9	249.1	64.1	123.3	144.6	244.3
0:01:30	54.6	347.8	133.2	219.7	248.8	398.5
0:01:48	96.1	435.5	236.2	330.7	366.8	523.4
0:02:06	149.6	503.4	290.2	356.8	455.7	593.8
0:02:24	204.1	549.3	324.2	374.4	510.7	621.3
0:02:42	256.6	581.6	349.1	390.5	540.8	634.4
0:03:00	306.2	605.9	366.5	398.2	562.7	646.2
0:03:18	352.5	623.9	383.3	413	581	656.5
0:03:36	395	636.1	397.7	412.1	595.9	665.3
0:03:54	432.8	645.7	409.2	422.7	608	673.9
0:04:12	467.6	655	422.3	438.2	617.2	680.9
0:04:30	498.1	667.4	432.9	454.3	631.7	694.7
0:04:48	524.1	683.5	438.7	447.7	654.6	716
0:05:06	553.9	703.4	461.4	492.8	683.6	743.9
0:05:24	586.3	721	495.7	491.9	702.5	763.7
0:05:42	614.7	735.6	512.6	515.7	713.4	775.3
0:06:00	638.4	745.8	524.8	515.1	719.2	781
0:06:18	659	753.5	532.5	533.6	729.9	788.5
0:06:36	677	757.8	539.7	538.2	739.8	795.8
0:06:54	692.2	760.7	549.8	561.1	748.1	801.3
0:07:12	705.5	765.8	557.4	559.1	752.1	804.3
0:07:30	717.8	772.7	569.8	572.8	754.9	806.5
0:07:48	728.6	780.2	580.7	588.9	759.4	810
0:08:06	737.8	784.2	588.5	592.3	766.1	815
0:08:24	746.4	787.8	593.9	604.6	773.8	821.3
0:08:42	754.4	790.1	600.8	615.6	778.8	826.3
0:09:00	761.4	794.1	609.5	619.7	782.9	830.6
0:09:18	767.8	797.4	613.5	622.2	786.8	834.4
0:09:36	774.1	802	623.5	633.9	792.6	838.8
0:09:54	779.9	806.7	626.9	638.6	797.2	842.7

0:10:12	785.3	811.2	634.4	653.6	802.1	846.2
0:10:30	790.1	814.7	639.7	653.3	805.7	849
0:10:48	794.9	817.2	644.3	663.6	809.8	852
0:11:06	799.1	820.5	649.4	670.7	813.1	854.7
0:11:24	803.3	823.7	653.5	671.6	816	857
0:11:42	807.5	826.8	659	680.8	818.8	859.4
0:12:00	811.1	829.3	662.3	688.5	821.9	861.5
0:12:18	815.2	831.9	665.5	695.8	825.2	863.8
0:12:36	818.8	835.8	669.8	698.6	828.8	865.8
0:12:54	822.2	839.3	672	704.9	831.9	868.3
0:13:12	825.3	843.7	675.9	704	835.5	871
0:13:30	828.2	846.9	677.6	703.3	838.7	873.9
0:13:48	830.7	850.8	682	709.6	842.4	876.9
0:14:06	833.8	853.6	681.7	714.2	845.7	879.4
0:14:24	836.9	856.3	685.2	719.2	849.1	882.1
0:14:42	839.9	858.2	688.8	724.2	852.5	885.2
0:15:00	843.4	860.3	690.3	724.1	856.3	888.7
0:15:18	847.2	862.9	694.9	731.3	860	892.1
0:15:36	850.5	866.4	699.8	737.1	863.5	895
0:15:54	854.1	870.4	702.6	740.4	866.5	898
0:16:12	857.7	873.8	706.2	742.2	869	900.9
0:16:30	861.1	876.8	709.7	747.8	871.7	904
0:16:48	864.3	879.9	713.4	754.9	874.5	906.8
0:17:06	867	883.4	716.3	755.8	877.8	909.6
0:17:24	870.3	887.4	719.5	761.7	880.7	912
0:17:42	873.2	890.7	721.6	765.2	883.9	914.7
0:18:00	876.2	894.1	726	768.9	887	917.6
0:18:18	879.7	896.5	729.7	773.8	890.4	921
0:18:36	883	899.4	732.2	777.6	893.4	924.1
0:18:54	886.4	902	734.9	782.4	896.1	926.9
0:19:12	889.4	905.8	738.3	787.3	898.7	929.4
0:19:30	892.2	910.3	741.3	787.4	901.4	931.9
0:19:48	895	915.1	746.8	794.7	904.1	934.4
0:20:06	898.3	918.2	748.9	797.6	907.1	937.4
0:20:24	901.2	920.1	751	801.7	910.2	940.7
0:20:42	904.2	921.8	755.6	808.6	913.3	944
0:21:00	907.3	924.1	758.2	814.3	916	946.7
0:21:18	910.2	927.5	760.9	814.5	918.9	949.4
0:21:36	913.6	931.4	765.1	819.6	921.7	952
0:21:54	916.5	936.6	767.6	824.7	924.6	954.3
0:22:12	919.6	940.6	771	822.6	927	956.4
0:22:30	922.1	944	773.8	830.4	929.7	958.9
0:22:48	924.7	945.3	776.3	831.2	932.7	962
0:23:06	927.6	946.6	779	838.8	936	965.3
0:23:24	930.9	948	782	840.6	939.4	968.4

0:23:42	933.9	950.3	787.9	844.2	942.2	970.9
0:24:00	936.8	953.5	791.8	852.5	944.7	973.1
0:24:18	939.2	956.4	794.6	850.7	946.4	974.9
0:24:36	941.5	959.2	797.5	854.7	948.2	976.4
0:24:54	943.7	961.6	799.1	855.6	949.9	977.7
0:25:12	945.8	964.8	802.3	860.4	951.5	979.1
0:25:30	947.5	967.6	804.6	862.1	953.1	980.6
0:25:48	948.8	969.7	806.2	867.9	954.6	982
0:26:06	950.7	970.7	808.1	868.1	956.1	983
0:26:24	952.1	971.2	810.1	870.1	956.8	983.2
0:26:42	953.3	971.9	811.6	872.8	957.4	982.9
0:27:00	954.3	972.8	813.1	873.4	957.4	982.1
0:27:18	954.9	974	813.6	874.3	957.6	981.3
0:27:36	955.3	974.6	814.4	875.9	957.4	980.3
0:27:54	955.5	974.1	813.8	879.4	957.5	979
0:28:12	955.5	973.1	812.4	878.7	957.2	977.4
0:28:30	955.6	972.5	813.6	880.9	956.9	974.8
0:28:48	955	973.8	813.8	881.5	956.2	972.5
0:29:06	954.2	974.8	815.5	885	955.6	970
0:29:24	953.4	975.3	817.4	888.2	955.8	968.3
0:29:42	952.9	973.9	820.1	887.5	956.3	967
0:30:00	952.9	972.6	819.1	891.3	956.6	965.2
0:30:18	953.7	971	819.7	886.1	955	962.9
0:30:36	953	968.8	813.8	875.7	952.1	959.1
0:30:54	950.5	965.5	809.1	869.3	947.7	956.6
0:31:12	948	961.4	806.3	863.9	943.9	956.2
0:31:30	945.2	957.6	797.5	854.9	940.8	958.1
0:31:48	944.3	953.9	799.2	855.7	938.9	959.8
0:32:06	944.4	950.6	799.7	853	936.7	959.6
0:32:24	943.5	947.4	798.4	849.4	934.7	958.2
0:32:42	941.8	946.7	796.9	848.9	934.1	957.5
0:33:00	941.2	947.7	796.4	851.4	935.2	958.4
0:33:18	941.1	949.8	798	851.2	936.6	959.1
0:33:36	941.3	950.3	797	851	936.6	958.9
0:33:54	941.6	950.4	796.2	850.6	935.4	957.6
0:34:12	940.7	950.1	794.9	847.8	934.6	957.2
0:34:30	940	951.2	796.1	850.2	934.8	957.3
0:34:48	939.9	951.4	796.4	850.5	935	957.4
0:35:06	940.1	951.6	797.2	850.9	935.2	957.2
0:35:24	943.5	947.4	798.4	849.4	934.7	958.2
0:35:42	941.8	946.7	796.9	848.9	934.1	957.5
0:36:00	941.2	947.7	796.4	851.4	935.2	958.4
0:36:18	941.1	949.8	798	851.2	936.6	959.1
0:36:36	941.3	950.3	797	851	936.6	958.9
0:36:54	941.6	950.4	796.2	850.6	935.4	957.6

0:37:12	940.7	950.1	794.9	847.8	934.6	957.2
0:37:30	940	951.2	796.1	850.2	934.8	957.3
0:37:48	939.9	951.4	796.4	850.5	935	957.4
0:38:06	940.1	951.6	797.2	850.9	935.2	957.2
0:38:24	941.3	950.3	797	851	936.6	958.9
0:38:42	941.6	950.4	796.2	850.6	935.4	957.6
0:39:00	940.7	950.1	794.9	847.8	934.6	957.2
0:39:18	940	951.2	796.1	850.2	934.8	957.3
0:39:36	939.9	951.4	796.4	850.5	935	957.4
0:39:54	940.1	951.6	797.2	850.9	935.2	957.2
0:40:12	940.2	950.7	795.5	848.8	935	957.1
0:40:30	940.4	950.5	796.4	850.5	935.5	957.6
0:40:48	940.6	950.2	795.6	849.5	935.7	958.5
0:41:06	940.7	953.1	796.8	849	940	963.1
0:41:24	940.1	960.4	795.7	850.3	947.6	971.4
0:41:42	947.5	972.4	823.1	882.3	958.6	982.1
0:42:00	955.8	983	826.5	891.4	965.1	988
0:42:18	960.5	989.7	829.2	888.8	968	988.5
0:42:36	963.9	991.6	828.9	888.1	967	984.8
0:42:54	966.2	991.2	825.7	882.3	965.4	980.6
0:43:12	965.6	989.6	822	881.1	963.5	978.6
0:43:30	964.9	986.4	821.3	877.5	961.5	978.8
0:43:48	965.3	982.9	820.8	879.4	960.5	980.4
0:44:06	965.2	979.1	819	875.4	959	980.9
0:44:24	964.3	976.9	820.2	873.6	958	980.6
0:44:42	963.9	975.6	819.1	874.1	956.7	980.2
0:45:00	963.2	975.6	817.6	873.7	957.5	981.6
0:45:18	965.2	979.1	819	875.4	959	980.9
0:45:36	964.3	976.9	820.2	873.6	958	980.6
0:45:54	963.9	975.6	819.1	874.1	956.7	980.2
0:46:12	963.2	975.6	817.6	873.7	957.5	981.6
0:46:30	964.3	976.9	820.2	873.6	958	980.6
0:46:48	965.2	979.1	819	875.4	959	980.9
0:47:06	964.3	976.9	820.2	873.6	958	980.6
0:47:24	963.9	975.6	819.1	874.1	956.7	980.2
0:47:42	963.2	975.6	817.6	873.7	957.5	981.6
0:48:00	965.2	979.1	819	875.4	959	980.9
0:48:18	964.3	976.9	820.2	873.6	958	980.6
0:48:36	963.9	975.6	819.1	874.1	956.7	980.2
0:48:54	963.2	975.6	817.6	873.7	957.5	981.6
0:49:12	966.2	991.2	825.7	882.3	965.4	980.6
0:49:30	965.6	989.6	822	881.1	963.5	978.6
0:49:48	964.9	986.4	821.3	877.5	961.5	978.8
0:50:06	965.3	982.9	820.8	879.4	960.5	980.4
0:50:24	965.2	979.1	819	875.4	959	980.9

0:50:42	964.3	976.9	820.2	873.6	958	980.6
0:51:00	965.2	979.1	819	875.4	959	980.9
0:51:18	964.3	976.9	820.2	873.6	958	980.6
0:51:36	963.9	975.6	819.1	874.1	956.7	980.2
0:51:54	963.2	975.6	817.6	873.7	957.5	981.6
0:52:12	962.9	978.2	818.4	874.8	962.3	986.5
0:52:30	963.1	984.5	819.5	878.4	970.1	994.4
0:52:48	971.3	994	841.8	905.5	978.7	1002.6
0:53:06	977.4	1002.2	845.2	908.8	983.3	1006.4
0:53:24	980.4	1007.9	849.6	912.3	985.7	1007
0:53:42	982.8	1010.8	854.8	915.2	986.7	1005.7
0:54:00	985.4	1012.1	850.9	912.6	987.9	1004.3
0:54:18	987.3	1011.4	847.3	906.9	987.6	1002.6
0:54:36	987.3	1009	843.8	904.5	986	1000.8
0:54:54	986.7	1005.9	843.7	904	983.7	1000.2
0:55:12	986.5	1003.2	843.6	903.2	981.5	1000
0:55:30	985.8	1000.8	840.4	900.2	979.8	1000.3
0:55:48	985	998.9	839.7	899.6	979.3	1000.6
0:56:06	984.2	997.3	839.6	897.6	979	1000.8
0:56:24	983.7	996.6	840.7	901.4	978.6	1000.4
0:56:42	983.2	995.7	840	897.5	977.6	999.5
0:57:00	983	994.7	840.6	899.1	976.3	998.6
0:57:18	982.8	993.8	840.2	897.4	975.5	998.2
0:57:36	982.2	993.6	840.9	898.5	975.5	998.5
0:57:54	981.8	994.3	840.3	897.8	976.4	999.2
0:58:12	981.9	994.5	841.9	901.9	977.3	999.9
0:58:30	982.3	993.6	841	898.7	977.4	999.9
0:58:48	981.8	994.3	840.3	897.8	976.4	999.2
0:59:06	981.9	994.5	841.9	901.9	977.3	999.9
0:59:24	982.3	993.6	841	898.7	977.4	999.9
0:59:42	983.2	995.7	840	897.5	977.6	999.5
1:00:00	982.3	993.6	841	898.7	977.4	999.9
1:00:18	982.8	993.8	840.2	897.4	975.5	998.2
1:00:36	982.2	993.6	840.9	898.5	975.5	998.5
1:00:54	981.8	994.3	840.3	897.8	976.4	999.2
1:01:12	981.9	994.5	841.9	901.9	977.3	999.9
1:01:30	982.3	993.6	841	898.7	977.4	999.9
1:01:48	981.8	994.3	840.3	897.8	976.4	999.2
1:02:06	981.9	994.5	841.9	901.9	977.3	999.9
1:02:24	982.3	993.6	841	898.7	977.4	999.9
1:02:42	983.2	995.7	840	897.5	977.6	999.5
1:03:00	983	994.7	840.6	899.1	976.3	998.6
1:03:18	982.8	993.8	840.2	897.4	975.5	998.2
1:03:36	982.2	986	842.5	900.9	968.1	990.7
1:03:54	981.7	971.5	842	897.4	952.8	975.8

1:04:12	969.8	955.3	804.4	837.3	937.5	960.9
1:04:30	951.2	950	796.2	848.3	939.4	963.2
1:04:48	954.4	958.4	827	885.9	950	972.3
1:05:06	963.2	968.6	835.5	893	958.3	977.9
1:05:24	964.5	972.1	827.4	877.9	957	973.4
1:05:42	959.6	968.5	823.6	870.5	954	970.1
1:06:00	958.4	966.7	827.6	876.9	954.8	972.6
1:06:18	960.1	968	832.6	882.1	956.4	976.7
1:06:36	961.5	970.8	827.8	879.6	955.8	977.1
1:06:54	961.4	972	826.9	878.1	953.7	975.2
1:07:12	960.3	972.2	825.2	875.6	952.3	974.1
1:07:30	960.1	971.6	826.6	877.4	952.5	974.7
1:07:48	960.1	971	825.8	875.8	953.2	975.8
1:08:06	960.6	970.4	825.6	877.2	953.9	976.4
1:08:24	960.5	970.3	825	876.2	954	976.4
1:08:42	960.7	970.6	826.8	875.4	953.8	976.1
1:09:00	960.7	970.7	825.8	877.2	953.4	975.8
1:09:18	961.5	970.8	827.8	879.6	955.8	977.1
1:09:36	961.4	972	826.9	878.1	953.7	975.2
1:09:54	960.3	972.2	825.2	875.6	952.3	974.1
1:10:12	960.1	971.6	826.6	877.4	952.5	974.7
1:10:30	960.1	971	825.8	875.8	953.2	975.8
1:10:48	960.6	970.4	825.6	877.2	953.9	976.4
1:11:06	960.5	970.3	825	876.2	954	976.4
1:11:24	960.7	970.6	826.8	875.4	953.8	976.1
1:11:42	960.7	970.7	825.8	877.2	953.4	975.8
1:12:00	960.1	971.6	826.6	877.4	952.5	974.7
1:12:18	960.1	971	825.8	875.8	953.2	975.8
1:12:36	960.6	970.4	825.6	877.2	953.9	976.4
1:12:54	960.5	970.3	825	876.2	954	976.4
1:13:12	960.7	970.6	826.8	875.4	953.8	976.1
1:13:30	960.7	970.7	825.8	877.2	953.4	975.8
1:13:48	961.5	970.8	827.8	879.6	955.8	977.1
1:14:06	961.4	972	826.9	878.1	953.7	975.2
1:14:24	960.3	972.2	825.2	875.6	952.3	974.1
1:14:42	960.1	971.6	826.6	877.4	952.5	974.7
1:15:00	960.6	970.4	825.6	877.2	953.9	976.4
1:15:18	960.8	967.1	826.1	876.6	946.8	969.1
1:15:36	960.6	955.5	827.1	875.3	932.1	954.2
1:15:54	954.6	939.9	799.9	831.2	915.6	937.7
1:16:12	935.6	930.8	778.4	820.3	911.6	934.2
1:16:30	931.4	935.9	802.9	855.3	922	943.6
1:16:48	939.3	947.4	819.9	875.5	932.4	951.6
1:17:06	942.9	953.5	815.5	865.1	934.5	950
1:17:24	939	951.9	804.8	854.5	930.9	946

1:17:42	936.5	948.5	804.7	854.8	930.1	947.4
1:18:00	938.1	948.4	810.6	859	931.4	951.9
1:18:18	939.7	950.1	809.6	856.5	931.8	953.6
1:18:36	939.7	951.5	809.7	857.3	930.9	953
1:18:54	939.2	952.1	811	857.7	930.2	952
1:19:12	939.2	951.9	812.2	856.2	930.4	952.2
1:19:30	939.2	951.9	809.7	856.6	930.9	952.9
1:19:48	939.6	951.6	809.5	856.8	931.5	953.9
1:20:06	940.1	951.2	810.4	857.5	931.5	954.2
1:20:24	940.2	950.3	808.5	855.1	931.1	954.2
1:20:42	939.7	950.5	808.7	855.1	930.7	954.2
1:21:00	939.7	950.1	809.6	856.5	931.8	953.6
1:21:18	939.7	951.5	809.7	857.3	930.9	953
1:21:36	939.2	952.1	811	857.7	930.2	952
1:21:54	939.2	951.9	812.2	856.2	930.4	952.2
1:22:12	939.2	951.9	809.7	856.6	930.9	952.9
1:22:30	939.6	951.6	809.5	856.8	931.5	953.9
1:22:48	940.1	951.2	810.4	857.5	931.5	954.2
1:23:06	940.2	950.3	808.5	855.1	931.1	954.2
1:23:24	939.7	950.5	808.7	855.1	930.7	954.2
1:23:42	939.2	951.9	809.7	856.6	930.9	952.9
1:24:00	939.6	951.6	809.5	856.8	931.5	953.9
1:24:18	940.1	951.2	810.4	857.5	931.5	954.2
1:24:36	940.2	950.3	808.5	855.1	931.1	954.2
1:24:54	939.7	950.5	808.7	855.1	930.7	954.2
1:25:12	939.7	950.1	809.6	856.5	931.8	953.6
1:25:30	939.7	951.5	809.7	857.3	930.9	953
1:25:48	939.2	952.1	811	857.7	930.2	952
1:26:06	939.2	951.9	812.2	856.2	930.4	952.2
1:26:24	940.2	950.3	808.5	855.1	931.1	954.2
1:26:42	939.7	950.5	808.7	855.1	930.7	954.2
1:27:00	939.5	952.7	809	857	933.5	957.3
1:27:18	940.6	960.8	810.4	857.8	943.2	963.8
1:27:36	942.5	974.4	817.1	868.2	959	974
1:27:54	956.4	991.7	848.6	904.6	975.4	982.4
1:28:12	969.8	1004.7	854.2	915.3	984.8	988.8
1:28:30	977.4	1012.4	855	918.9	988.5	991.2
1:28:48	981.9	1015.2	858.9	922.5	989.7	993.7
1:29:06	985.3	1017.5	865	921.5	992.3	994.9
1:29:24	988.7	1019	866.6	21:36:00	12:00:00	995.7
1:29:42	991.5	1019.1	865.6	14:24:00	16:48:00	995
1:30:00	992.4	1017.5	861.2	918.6	992.1	994.3
1:30:18	991.2	1014.3	859.3	914.8	988.6	994.6
1:30:36	990	1010.6	856.2	909.7	984.9	995.9
1:30:54	989.3	1007	855	906.9	982.6	997.6

1:31:12	988.5	1004.2	855.9	907.2	980.7	998.4
1:31:30	987.7	1001.9	855.3	907.3	979.6	998.4
1:31:48	986.5	1000.2	853.8	903.4	978.1	997.8
1:32:06	985.5	998.7	853.4	903.4	977.2	997.1
1:32:24	984.8	997.3	853	903.9	976.4	996.5
1:32:42	984	996	853	904.6	976.4	996.4
1:33:00	983.3	994.9	852.6	903.3	976	996.5
1:33:18	982.7	994.6	851.8	902.1	976	996.6
1:33:36	982.6	994.7	851.6	901.8	975.5	996.2
1:33:54	982.6	995.4	853.7	906	975.8	996.3
1:34:12	981.9	995.7	852.3	903.5	975.6	996.3
1:34:30	981.3	996	852.8	904	975.8	996.8
1:34:48	981.5	995.8	853.7	904.4	975.4	996.4
1:35:06	981.5	995.4	852	903.6	974.9	995.8
1:35:24	981.8	994.7	852.8	902.5	974.1	995
1:35:42	981.1	994.1	852.8	895.5	973.5	995.1
1:36:00	980.5	993.7	849.2	888.4	972.9	995.7
1:36:18	980.2	993.6	846.7	873.8	972.4	996.4
1:36:36	980.5	993.7	843.1	855.3	971.4	996.2
1:36:54	980	993.9	841	841.8	970.6	996.1
1:37:12	979.6	993.9	836.7	826.3	969.6	995.6
1:37:30	979.3	993.5	831.3	815.7	968.4	995.7
1:37:48	980.1	993	826.8	801.4	966.5	995.5
1:38:06	980.4	992.6	818.8	783.8	964.6	995.7
1:38:24	980.3	992.2	809.7	770.3	962	995.2
1:38:42	981.7	991.8	801	761.8	957.5	994.4
1:39:00	981.9	991.3	791.3	756.7	946.5	992.7
1:39:18	981.5	990.9	790.4	757.1	929.8	991.6
1:39:36	982.2	990.6	788.3	758.1	910.4	991.1
1:39:54	982.5	990.4	789.6	757	896.8	992.1
1:40:12	981.3	990.4	790.8	753.9	890	992.9
1:40:30	981.6	990.5	790.5	755.4	888.3	993.6
1:40:48	982.2	990.5	794.1	756.7	887.3	993.3
1:41:06	981.4	990.6	792.4	754.7	886.3	993.3
1:41:24	981.2	990.6	790.5	758.2	885.6	993.4
1:41:42	981.5	990.8	789.2	754.9	885.6	993.8
1:42:00	980.7	991.1	790.7	752.2	885.8	993.8
1:42:18	980.5	991.3	791.3	751.9	885.7	993.8
1:42:36	980.8	991.4	793.1	758.8	884.9	993.4
1:42:54	981.8	991.3	793.6	754.3	883.9	993
1:43:12	980.5	991.4	792.1	759.9	883.5	993.5
1:43:30	980.9	991.4	790.1	756	883.5	995.1
1:43:48	980.8	991.3	792.8	757.9	883.6	997.2
1:44:06	981.2	990.9	795.6	758.9	883	998.2
1:44:24	981.3	990.3	795	759.4	882.2	997.6

1:44:42	981.4	989.9	793.4	762.6	881.7	995.7
1:45:00	981.8	989.6	790.6	760.4	881.6	993.2
1:45:18	981.3	989.7	790	760.9	881.7	991.7
1:45:36	981.5	989.8	791.9	761.2	881.6	991.2
1:45:54	981.7	990	794.1	759.8	881.2	992.2
1:46:12	981.9	990.2	795.8	758.7	880.7	993
1:46:30	981.4	990.5	795.3	756.5	880.1	993.7
1:46:48	981.1	990.6	791.5	758.6	880	993.4
1:47:06	980.8	990.8	790.5	757.5	880.3	992.6
1:47:24	980.6	990.9	790.7	757.6	880.9	991.8
1:47:42	980.5	990.8	794	761.6	880.8	991.1
1:48:00	980.4	990.5	797.5	761.2	880	991.5
1:48:18	980.4	990.2	795.5	761.4	878.8	992.3
1:48:36	980.6	990.1	793.4	759.7	878.2	993
1:48:54	980.7	990.3	793.2	759.2	878.1	992.8
1:49:12	980.5	990.6	792.2	759.4	878.1	992.1
1:49:30	980.6	991	795.1	757.4	877.7	991
1:49:48	980.5	991.2	798.1	755.7	877.3	990.2
1:50:06	980.4	991.2	794.8	758.5	877	989.5
1:50:24	980	991	792.8	760.1	877.3	989.3
1:50:42	980.2	990.7	791.3	761.2	877.8	990.1
1:51:00	980.7	990.4	793.4	761.9	878	991.9
1:51:18	980.8	990.1	798.6	761.4	877.5	994.3
1:51:36	980.2	990	801.2	759.4	876.5	996.5
1:51:54	980.5	990.2	797.8	759.2	875.7	997.4
1:52:12	980.1	990.4	796.4	760.4	875.7	997.2
1:52:30	980.4	990.5	793.7	761.6	876.2	996.5
1:52:48	980.8	989.4	794.2	761.4	876.4	996
1:53:06	980.9	988.2	798.3	761.7	875.8	995
1:53:24	980.2	987.1	800.6	761.1	875	992.9
1:53:42	980.3	988.2	798.8	761.8	874.8	991.2
1:54:00	980	989	797.9	762.8	875.6	990.8
1:54:18	980.1	989.8	797.2	762.8	876.7	992.1
1:54:36	980.4	989.7	796.8	762.7	877.2	993.9
1:54:54	980.6	989.9	799.4	763.5	876.5	995.8
1:55:12	980.6	990.2	800.8	762.6	875.4	997.9
1:55:30	980.6	990.3	798.6	761.1	874.7	999.6
1:55:48	980.7	990.3	797.1	759.9	875.1	1000.5
1:56:06	979.9	990.4	795.8	759.3	876.2	1000.6
1:56:24	979.6	990.5	797.5	759.1	877	1000.4
1:56:42	980.1	990.5	800.2	760.7	876.8	1000.4
1:57:00	980.6	990.6	802.1	760.2	875.9	999.7
1:57:18	980.2	990.5	801.4	760.4	875.3	998.3
1:57:36	980.4	990.4	797.3	759.2	875.6	995.5
1:57:54	980.5	990.3	799.3	758.8	876.4	993

1:58:12	980.7	990.4	800.1	759.4	876.9	991.8
1:58:30	980.3	990.5	801.7	759.2	876.7	992.8
1:58:48	980.1	990.9	802.5	760.4	876.2	993.8
1:59:06	980.8	991.1	798.5	760.6	876.2	993.1
1:59:24	980.9	991.3	798.2	761.1	877.1	991.7
1:59:42	981.2	991.2	798.1	761.3	878.2	992
2:00:00	981.4	991.1	798.2	761.4	878.9	994.1

APPENDIX E

Table 2. Temperature distribution of 10.5 mm steel round bar at 980 °C set-point and 9 sec feeding time

Time (hh:mm:ss)	Core Temperature(°C)	Surface Temperature (°C)	Set-point temperature (°C)	Furnace ambient temperature (Effective) (°C)	Exhaust gas temperature (°C)
0:00:00	34.3	37.8	982.5	35	848.4
0:00:09	121.3	264.5	981.3	556	845
0:00:18	225.3	436.7	981.6	782.4	850.5
0:00:27	297	546.8	981.8	819.9	850.8
0:00:36	349.7	597.2	980.8	825.1	855.8
0:00:45	391.3	626.8	982.4	811.2	849
0:00:54	427.4	618.7	980.7	797.4	850.6
0:01:03	458.6	638.6	980.2	776.8	851.5
0:01:12	490.7	659.7	981.6	783.3	848.2
0:01:21	522.3	672.8	980.9	791.9	840.4
0:01:30	554.1	693.5	979.8	808.4	839.9
0:01:39	583.5	718.5	979.3	819	844.7
0:01:48	612.2	734.2	980.8	824.1	847.5
0:01:57	641	758.6	980.7	837.9	847
0:02:06	668.2	777.3	980.8	854.6	851.9
0:02:15	688	782.5	981.4	858.5	851.3
0:02:24	708.4	793.8	982.3	864.3	848.2
0:02:33	727.2	809.4	980.1	873.4	850.3
0:02:42	744.3	816.8	980.8	884.4	849.5
0:02:51	759.3	820.3	980.8	886.8	848.6
0:03:00	772.4	826.5	980.7	888.2	846.8
0:03:09	788.3	829.2	980.8	894.9	848.8
0:03:18	804.2	830.5	980.8	903.4	848.9
0:03:27	814	847.8	980.8	910	843.6
0:03:36	820.5	858.4	980.8	918.8	846.4
0:03:45	832.3	864.2	980.8	916.8	844
0:03:54	843	878.6	980.8	919.4	839.3
0:04:03	856	882.6	980.8	936.8	842.7
0:04:12	869.6	890	980.8	943.3	842.6
0:04:21	882.9	899	980.8	948.7	839.8
0:04:30	895.5	907.5	980.7	949.1	836.4
0:04:39	907	919	980.2	953.8	839.2
0:04:48	916.8	928.8	980.8	957.1	836.9

0:04:57	925.4	937.4	980.1	960.1	839.2
0:05:06	932.5	944.5	980.8	960.9	839.9
0:05:15	939	951	980.4	964.1	834.4
0:05:24	944.9	956.9	979.8	967.1	835.8
0:05:33	950.6	962.6	979.3	971.9	835.1
0:05:42	956.2	968.2	980.6	976.8	836.6
0:05:51	962.7	974.7	980.9	982.5	836.3
0:06:00	968.3	980.3	980.8	986.7	835
0:06:09	973.4	985.4	980.9	990	837.3
0:06:18	977.3	989.3	981.8	991.4	836.2
0:06:27	980.9	992.9	982.8	994.2	840
0:06:36	983.5	995.5	980.8	999	838.1
0:06:45	985.8	997.8	980.5	1008.7	841.5
0:06:54	987.3	999.3	980.2	1001.1	843.5

APPENDIX F

Table 3. Temperature distribution of 13.5 mm steel round bar at 980 °C set-point and 9 sec feeding time

Time (hh:mm:ss)	Core Temperature(°C)	Surface Temperature (°C)	Set-point temperature (°C)	Furnace ambient temperature (Effective) (°C)	Exhaust gas temperature (°C)
0:00:00	34.4	34.4	982.5	34.4	829.7
0:00:09	73.1	392.5	981.3	535.4	818.9
0:00:18	113.8	542.8	981.6	776.8	811.9
0:00:27	175.3	570.3	981.8	811.2	809
0:00:36	219.8	536.8	980.8	821.1	810.2
0:00:45	269.5	546.1	982.4	819.1	806.2
0:00:54	306.1	563.4	980.7	815.2	810.4
0:01:03	340.6	584.7	980.2	809.9	805
0:01:12	383.9	617.1	981.6	825.2	795.9
0:01:21	404.8	630.8	980.9	834.6	789.8
0:01:30	429.7	642.5	979.8	841.6	784.8
0:01:39	452.8	652.4	979.3	833.4	783.9
0:01:48	472.2	673.6	980.8	839.9	778
0:01:57	493.4	685.2	980.7	859.4	778.4
0:02:06	528.2	700.7	980.8	853.8	772.1
0:02:15	556.8	712.6	981.4	869.8	769.2
0:02:24	577.1	726.3	982.3	865.4	768
0:02:33	600.5	743.6	980.1	879.2	763.4
0:02:42	625.7	755.7	980.8	881.2	763.3
0:02:51	651.8	764.1	980.8	886.8	762.3
0:03:00	666.3	781.5	980.7	887.3	771.3
0:03:09	686.5	792.3	980.8	898.6	778.5
0:03:18	706.2	801.5	980.8	905.3	779.3
0:03:27	723.4	810.2	980.8	910.8	784.4
0:03:36	736.5	822.1	980.8	912.8	786
0:03:45	748.7	830.5	980.8	919.8	788.2
0:03:54	767.2	842.8	980.8	930.6	788.8
0:04:03	774.9	848.3	980.8	927.6	783.1
0:04:12	788.3	850.6	980.8	928.6	783.7
0:04:21	802.8	856.2	980.8	932.1	781.2
0:04:30	813.6	864.8	980.7	934.4	781.4
0:04:39	821.9	871.2	980.2	939.8	787.2
0:04:48	829.4	887.3	980.8	941.2	789.8

0:04:57	837.5	890.6	980.1	947.5	792.8
0:05:06	844.2	895.2	980.8	948.5	796.6
0:05:15	855.3	900.8	980.4	950.5	797.8
0:05:24	863.7	916.3	979.8	958.5	794.7
0:05:33	870.2	929.1	979.3	962.1	790.9
0:05:42	876.8	930.2	980.6	965.4	791.3
0:05:51	887.2	931.8	980.9	970.3	793.1
0:06:00	893.2	932.2	980.8	966.9	794.2
0:06:09	901.2	933.7	980.9	970.7	795.6
0:06:18	914.7	933.2	981.8	981.8	795
0:06:27	919.5	946.3	982.8	979.7	801.9
0:06:36	930.6	954.5	980.8	982.6	804.1
0:06:45	938.7	960.6	980.5	993.6	809.6
0:06:54	946.2	960.7	980.2	992.6	812.8

APPENDIX G

Table 4.Temperature distribution of 17.5 mm steel round bar at 980 °C set-point and 9 sec feeding time

Time (hh:mm:ss)	Core Temperature(°C)	Surface Temperature (°C)	Set-point temperature (°C)	Furnace ambient temperature (Effective) (°C)	Exhaust gas temperature (°C)
0:00:00	36.3	48.3	980.8	36.9	787.9
0:00:09	107	125.6	980.8	526.5	760.4
0:00:18	159.6	312.3	980.8	768.3	762
0:00:27	208.3	402.9	980.8	809.4	782.9
0:00:36	236.9	460.2	980.8	812.1	792.2
0:00:45	266.4	512.7	980.8	815.1	798.2
0:00:54	293.7	548.4	980.8	816.7	800.3
0:01:03	318.7	565.9	980.7	817.9	800.2
0:01:12	343.5	568.9	980.2	823.6	793.3
0:01:21	366.6	552.1	980.8	839.7	795.3
0:01:30	388.5	560.7	980.1	847.3	790.7
0:01:39	412	572.3	980.8	844.1	810.4
0:01:48	432	576.4	980.4	858.8	817.5
0:01:57	452.2	583.8	979.8	863.2	814
0:02:06	470.4	592.1	979.3	865.7	791.2
0:02:15	488.3	598.9	980.6	869.9	787
0:02:24	507.7	605.3	980.9	876	779.1
0:02:33	523.6	612.4	980.8	879.1	780.6
0:02:42	535.5	618.8	980.4	877.7	791.9
0:02:51	546.4	625.3	979.8	883.9	783.5
0:03:00	566.3	638.8	979.3	885.9	786.6
0:03:09	583.7	650.4	980.6	879.8	788.1
0:03:18	602.6	662.3	980.9	885.3	789.4
0:03:27	621.5	684.2	980.8	892.9	806.9
0:03:36	638.7	693.1	980.9	901.5	803.4
0:03:45	655.5	705.9	981.8	902.9	790.3
0:03:54	670.9	716.2	982.8	911.8	797.3
0:04:03	686.9	736.9	980.8	929.7	797.5
0:04:12	701.3	752.1	980.5	935.3	789.3
0:04:21	715	764.6	980.1	929.3	790.5
0:04:30	728.1	785.6	980.8	946.9	785.8
0:04:39	740.6	802.8	980.8	942.1	780.8
0:04:48	752.6	813.6	980.7	957.7	782.6

0:04:57	762.6	838.4	980.8	955.4	780.9
0:05:06	773.4	841.2	980.8	961.8	780.9
0:05:15	787.9	850.8	980.8	968.7	774
0:05:24	802.7	870.7	980.8	966.9	767.5
0:05:33	813.5	878.5	980.8	975.3	769.9
0:05:42	819.9	889.9	980.8	971.5	774.8
0:05:51	826.6	897.6	980.8	967	779.3
0:06:00	838.2	902.2	980.8	963.4	779.2
0:06:09	852.5	922.5	980.8	961.7	787.4
0:06:18	863.3	926.3	980.7	977	793.3
0:06:27	875.4	944.4	980.2	982.7	794.1
0:06:36	886.8	953.8	980.8	984.3	793.9
0:06:45	893	962	980.8	984.9	795.1
0:06:54	904	968	980.8	986.4	801.8

APPENDIX H

Table 5. Experimental and simulation result of 10.5 mm steel round bar temperature during 980 set-point °C and 9 sec feeding time of heating process.

Time (hh:mm:ss)	Experimental temperature (°C)	Predicted temperature emissivity 1.0 (°C)	Predicted temperature emissivity 0.9 (°C)	Predicted temperature emissivity 0.8 (°C)	Predicted temperature emissivity 0.7 (°C)	Predicted temperature emissivity 0.6 (°C)
0:00:00	34.3	34.3	34.3	34.3	34.3	34.3
0:00:09	121.3	111	98	85	74	62
0:00:18	225.3	168	138	122	109	91
0:00:27	297	212	189	160	141	119
0:00:36	349.7	261	234	213	195	168
0:00:45	391.3	312	291	276	253	222
0:00:54	427.4	361	340	329	319	280
0:01:03	458.6	415	388	372	359	341
0:01:12	490.7	459	437	423	414	391
0:01:21	522.3	513	489	473	459	443
0:01:30	554.1	557	534	517	503	485
0:01:39	583.5	591	568	555	542	531
0:01:48	612.2	622	599	586	574	563
0:01:57	641	649	628	616	609	597
0:02:06	668.2	681	660	647	635	624
0:02:15	688	708	689	680	671	662
0:02:24	708.4	721	712	710	701	691
0:02:33	727.2	737	731	737	726	717
0:02:42	744.3	758	743	760	753	748
0:02:51	759.3	776	774	780	782	779
0:03:00	772.4	791	794	798	801	799
0:03:09	788.3	802	809	814	822	825
0:03:18	804.2	814	822	828	836	842
0:03:27	814	824	834	840	848	854
0:03:36	820.5	834	845	850	857	865
0:03:45	832.3	843	856	860	867	874
0:03:54	843	852	865	869	876	883
0:04:03	856	861	863	877	884	892
0:04:12	869.6	869	880	884	891	899
0:04:21	882.9	875	887	891	899	907
0:04:30	895.5	880	894	898	906	912
0:04:39	907	885	900	904	911	917
0:04:48	916.8	889	906	910	917	922

0:04:57	925.4	895	911	915	923	927
0:05:06	932.5	900	916	921	930	934
0:05:15	939	905	920	926	937	940
0:05:24	944.9	910	924	932	943	948
0:05:33	950.6	915	928	937	948	954
0:05:42	956.2	921	933	942	952	960
0:05:51	962.7	926	938	948	957	966
0:06:00	968.3	931	943	953	962	971
0:06:09	973.4	936	948	958	967	977
0:06:18	977.3	941	953	964	972	983
0:06:27	980.9	946	958	969	978	989
0:06:36	983.5	951	963	974	986	994
0:06:45	985.8	956	968	979	991	999
0:06:54	987.3	961	973	984	996	1005

APPENDIX I

Table 6. The core temperature prediction of 10.5 mm steel round bar and actual temperature during 980 set-point °C and 9 sec feeding time of heating process (Emissivity 0.8)

Time (hh:mm:ss)	Experiment temperature (°C)	Predicted temperature (°C)
0:00:00	34.3	34.3
0:00:09	121.3	85
0:00:18	225.3	122
0:00:27	297	160
0:00:36	349.7	213
0:00:45	391.3	276
0:00:54	427.4	329
0:01:03	458.6	372
0:01:12	490.7	423
0:01:21	522.3	473
0:01:30	554.1	517
0:01:39	583.5	555
0:01:48	612.2	586
0:01:57	641	616
0:02:06	668.2	647
0:02:15	688	680
0:02:24	708.4	710
0:02:33	727.2	737
0:02:42	744.3	760
0:02:51	759.3	780
0:03:00	772.4	798
0:03:09	788.3	814
0:03:18	804.2	828
0:03:27	814	840
0:03:36	820.5	850
0:03:45	832.3	860
0:03:54	843	869
0:04:03	856	877
0:04:12	869.6	884
0:04:21	882.9	891
0:04:30	895.5	898
0:04:39	907	904
0:04:48	916.8	910

0:04:57	925.4	915
0:05:06	932.5	921
0:05:15	939	926
0:05:24	944.9	932
0:05:33	950.6	937
0:05:42	956.2	942
0:05:51	962.7	948
0:06:00	968.3	953
0:06:09	973.4	958
0:06:18	977.3	964
0:06:27	980.9	969
0:06:36	983.5	974
0:06:45	985.8	979
0:06:54	987.3	984

APPENDIX J

Table 7. The core temperature prediction of 13.5 mm steel round bar and actual temperature during 980 set-point °C and 9 sec feeding time of heating process (Emissivity 0.8)

Time (hh:mm:ss)	Experiment temperature (°C)	Predicted temperature (°C)
0:00:00	34.4	36
0:00:09	73.1	51
0:00:18	113.8	73
0:00:27	175.3	106
0:00:36	219.8	150
0:00:45	269.5	193
0:00:54	306.1	234
0:01:03	340.6	275
0:01:12	383.9	317
0:01:21	404.8	355
0:01:30	429.7	398
0:01:39	452.8	438
0:01:48	472.2	477
0:01:57	493.4	515
0:02:06	528.2	549
0:02:15	556.8	576
0:02:24	577.1	601
0:02:33	600.5	626
0:02:42	625.7	653
0:02:51	651.8	672
0:03:00	666.3	694
0:03:09	686.5	716
0:03:18	706.2	737
0:03:27	723.4	756
0:03:36	736.5	769
0:03:45	748.7	783
0:03:54	767.2	797
0:04:03	774.9	810
0:04:12	788.3	821
0:04:21	802.8	832
0:04:30	813.6	843
0:04:39	821.9	851
0:04:48	829.4	859

0:04:57	837.5	867
0:05:06	844.2	874
0:05:15	855.3	881
0:05:24	863.7	888
0:05:33	870.2	894
0:05:42	876.8	900
0:05:51	887.2	906
0:06:00	893.2	912
0:06:09	901.2	918
0:06:18	914.7	923
0:06:27	919.5	929
0:06:36	930.6	934
0:06:45	938.7	945
0:06:54	946.2	950

APPENDIX K

Table 8. The core temperature prediction of 17.4 mm steel round bar and actual temperature during 980 set-point °C and 9 sec feeding time of heating process (Emissivity 0.8)

Time (hh:mm:ss)	Experiment temperature (°C)	Predicted temperature (°C)
0:00:00	36.3	36.3
0:00:09	107	73
0:00:18	159.6	101
0:00:27	208.3	135
0:00:36	236.9	166
0:00:45	266.4	192
0:00:54	293.7	227
0:01:03	318.7	261
0:01:12	343.5	292
0:01:21	366.6	325
0:01:30	388.5	350
0:01:39	412	375
0:01:48	432	406
0:01:57	452.2	432
0:02:06	470.4	455
0:02:15	488.3	474
0:02:24	507.7	501
0:02:33	523.6	522
0:02:42	535.5	543
0:02:51	546.4	563
0:03:00	566.3	586
0:03:09	583.7	605
0:03:18	602.6	627
0:03:27	621.5	643
0:03:36	638.7	661
0:03:45	655.5	682
0:03:54	670.9	699
0:04:03	686.9	716
0:04:12	701.3	733
0:04:21	715	749
0:04:30	728.1	763
0:04:39	740.6	777
0:04:48	752.6	790

0:04:57	762.6	802
0:05:06	773.4	813
0:05:15	787.9	824
0:05:24	802.7	833
0:05:33	813.5	842
0:05:42	819.9	847
0:05:51	826.6	857
0:06:00	838.2	865
0:06:09	852.5	872
0:06:18	863.3	878
0:06:27	875.4	886
0:06:36	886.8	894
0:06:45	893	903
0:06:54	904	912

APPENDIX L

Table 9.Temperature distribution in furnace with three desired set-point temperatures 940, 960, 980 °C while 10.5 mm steel round bars are traveling with 9 second feeding time

Time (hh:mm:ss)	Set-point temperature (°C)	Exhaust gas temperature (°C)	Inlet temperature (°C)	Middle temperature(°C)	Outlet temperature (°C)
0:00:00	150.4	400.7	399	492.4	537.5
0:00:26	201.3	417.9	417.4	524.8	561
0:00:52	254.9	433.8	427	539	581.4
0:01:18	305.7	444.7	436.4	544	595.7
0:01:44	352.1	454.8	446.5	555.4	609.5
0:02:10	393.9	465.5	460.9	570.6	620.7
0:02:36	430.7	469.9	471.4	575.7	628.2
0:03:02	463.4	480	476.2	586.6	636.9
0:03:28	492	482	477	585.3	642.2
0:03:54	518.3	481.3	482.4	593	649
0:04:20	541	489.3	491.5	593.1	652.3
0:04:46	560.8	492.4	499	605.1	659
0:05:12	578	492.5	496.3	608.5	662.9
0:05:38	593.3	505.2	503.5	615.4	668.1
0:06:04	611.6	570.2	538.1	699.1	741.9
0:06:30	642.6	602	574.9	727.4	769.5
0:06:56	671.8	617.9	589.4	740.6	780.4
0:07:22	697.4	626.3	598.6	750.7	790.1
0:07:48	718.6	636.3	607.2	758.2	798.8
0:08:14	737.4	648.9	619.2	767.4	808
0:08:40	752.9	652.6	629.2	771.5	812.3
0:09:06	766.5	661	637.2	783.8	821.2
0:09:32	778.6	669.6	646.5	790.2	829.9
0:09:58	789.5	678.6	654.9	794.7	833.5
0:10:24	799.4	684.7	665.3	802.9	840.4
0:10:50	807.9	689.3	669	807.4	846.7
0:11:16	816.5	698.1	680.2	815.3	853.5
0:11:42	824.3	705.1	689.5	821.8	858.8
0:12:08	831.5	708.9	692.7	827.2	863.1
0:12:34	837.9	717.6	699.3	833.8	869.5
0:13:00	844.9	723.5	710.1	841.3	875.1
0:13:26	851.9	729.8	712.3	848.3	882.1
0:13:52	858.7	735	725.2	854.1	887.4
0:14:18	864.9	740.1	734.8	860.2	893.9

0:14:44	870.3	746.3	735.6	863.4	896.5
0:15:10	875.7	751.3	743.3	869.3	902.4
0:15:36	880.8	757.5	749.5	874.9	906.1
0:16:02	885.6	761.1	755.2	880.7	910.2
0:16:28	890.9	767.4	763.6	885.8	916.9
0:16:54	895.7	773.1	772.8	891	920.9
0:17:20	901.3	778.6	774.2	896.7	925.8
0:17:46	906.8	785	782.6	901.3	931.7
0:18:12	912	787.3	783.5	906	935.4
0:18:38	917	793.6	796.8	911.5	940.2
0:19:04	921.6	799.1	795.7	916	943
0:19:30	926.6	804.9	798.3	922.1	949.6
0:19:56	931.6	810.1	795	926.5	953.7
0:20:22	936.4	812.7	796.5	929.7	958.9
0:20:48	941.1	817.3	792.4	933.9	961.3
0:21:14	945.1	822	789.8	938.6	964.2
0:21:40	949	826	790.9	939.7	967.2
0:22:06	952.1	828.6	790.4	942.1	968.5
0:22:32	955.1	829.6	789.4	945.3	971.3
0:22:58	957.8	831.8	789.6	947.6	972
0:23:24	959.5	831.7	789.5	946.3	971.7
0:23:50	960.9	835.2	790.8	948.4	973.9
0:24:16	962.5	840.1	793.7	949.7	973.1
0:24:42	964	849.6	789.4	951.2	973.6
0:25:08	966	847.4	789.1	952.7	975.8
0:25:34	967.3	836.7	788.5	953.7	974.3
0:26:00	966.2	827.2	777.3	947.4	966.7
0:26:26	962.6	824	773.8	938.4	961.5
0:26:52	958.8	824.3	772.3	936.1	959.9
0:27:18	957.1	825.8	773.6	938.8	961.1
0:27:44	956	824.9	772.7	937.3	959.9
0:28:10	954.4	824.9	772.7	934.9	958
0:28:36	953	824.6	772.4	934.5	957.3
0:29:02	952	823.9	771.7	932.5	956
0:29:28	950.6	824.1	771.9	933	955.2
0:29:54	949.7	826.8	774.6	932.9	956.7
0:30:20	950	827.8	775.6	934.5	957.8
0:30:46	949.8	825.2	773	932.4	955
0:31:12	949.5	825.4	773.2	934.7	958.2
0:31:38	950.4	826	773.8	930.9	957.7
0:32:04	949.5	820.8	768.6	930.1	954.6
0:32:30	948.5	817.7	765.5	928.8	955.8
0:32:56	948.8	816	763.8	931.2	958
0:33:22	948.4	810.2	758	928.9	956.6
0:33:48	947.4	807.2	755	926.8	954.9

0:34:14	946.4	811.4	759.2	923.9	955.5
0:34:40	945.3	812.7	760.5	914.7	955.2
0:35:06	944	816.4	764.2	887.1	954.8
0:35:32	943.2	819	766.8	877.5	954.7
0:35:58	943.1	827.6	775.4	874	957
0:36:24	942.7	829.1	776.9	871.7	958.1
0:36:50	943.3	830.6	778.4	872.3	959.1
0:37:16	944.5	829.5	777.3	871.8	959.9
0:37:42	944.8	830.4	778.2	871.6	962.1
0:38:08	944.2	830.8	778.6	865.8	964.9
0:38:34	943.5	831.6	779.4	866.7	963.4
0:39:00	943	833.7	781.5	865.2	963.7
0:39:26	942.9	833.7	781.5	864.6	964.2
0:39:52	943.1	835.9	783.7	862.3	964.2
0:40:18	943.8	836.5	784.3	864.1	964.3
0:40:44	943.8	838.4	786.2	863.1	962.9
0:41:10	943.7	841.7	789.5	862.8	963.5
0:41:36	944	842.1	789.9	877.2	965.8
0:42:02	944.8	845	792.8	871.5	966.2
0:42:28	945	843.7	791.5	872.7	962.5
0:42:54	944.9	841.5	789.3	873.7	963.8
0:43:20	945.4	840.9	788.7	870.3	962.6
0:43:46	945.5	836.6	784.4	875	960.8
0:44:12	946.3	834.4	782.2	872.7	961.5
0:44:38	946.7	832.2	780	871.5	955.3
0:45:04	946.9	833.4	781.2	873.5	956.7
0:45:30	948.9	831.9	779.7	871.2	958.6
0:45:56	949.7	827.2	775	876.3	956.4
0:46:22	949.4	820.9	768.7	875.2	954.1
0:46:48	948.7	820.5	768.3	872.9	955
0:47:14	948.2	816.6	764.4	871.7	955
0:47:40	947.6	810.2	758	871.5	954.4
0:48:06	947.1	813.1	760.9	866.6	955.1
0:48:32	946	816.5	764.3	863.1	953.1
0:48:58	944.6	820.5	769.2	864.8	952.9
0:49:24	943.3	822.7	770.9	867.9	954.1
0:49:50	943.2	822.8	770.4	866.5	955.8
0:50:16	943	823.8	773.2	867.9	955.8
0:50:42	943.3	828.3	773.2	870	957
0:51:08	944.1	830.2	771	868.7	957.9
0:51:34	944.9	829.5	773.6	864.6	960.5
0:52:00	944.4	828.2	772.8	863.8	962.2
0:52:26	943.3	825.1	772.9	860.9	959.8
0:52:52	941.9	826.2	774.5	856.4	957.8
0:53:18	941	827.2	771.9	856.5	959.9

0:53:44	940.7	828.9	774.2	855.4	960.8
0:54:10	940.5	829	774.5	854.2	961.4
0:54:36	940.9	829.5	774	853.3	961.7
0:55:02	940.9	831.9	774.4	852.4	959.5
0:55:28	945.7	878	777.4.	884.1	986.1
0:55:54	953.7	881.4	794.5	893.7	987.7
0:56:20	960.9	873	817.7	897	993.7
0:56:46	966.2	859.4	796.9	896.3	991.9
0:57:12	968	853.8	776.6	891.3	987.7
0:57:38	967.8	854.8	776	892.8	986
0:58:04	967.1	854.2	775.8	896.7	985.8
0:58:30	966	852.8	776.7	904.4	983.6
0:58:56	964.8	850.9	776.7	903.1	983.4
0:59:22	964.3	850.4	777.2	904.6	983.1
0:59:48	963.4	848.2	777.3	911.8	981.3
1:00:14	962.3	848.6	776.6	898.3	979.9
1:00:40	960.8	849.8	775.1	891.4	979.3
1:01:06	960.4	850.2	776.3	891.6	981
1:01:32	960.5	851.9	777.1	891.6	982.5
1:01:58	960.7	848.5	775.8	893.3	981.2
1:02:24	960.3	845.8	776.1	894.5	979.3
1:02:50	960.6	852.4	776.7	894.1	979.8
1:03:16	961	846.9	778	895.1	982.9
1:03:42	963.4	889.3	783.6	915.7	1002.7
1:04:08	970.3	891.3	803.8	922.3	1002.7
1:04:34	976.9	895.3	824.6	929.8	1009.7
1:05:00	983.3	882.5	833.4	934	1013
1:05:26	986.9	875.9	806.7	933.4	1010.7
1:05:52	988.7	875.6	805.4	934.2	1009.8
1:06:18	989.5	870.7	804	933.8	1008.7
1:06:44	988.7	870.2	805.6	931.9	1006.9
1:07:10	986.9	873.4	804.2	930.3	1004.9
1:07:36	985.5	871	806.3	931.1	1004.8
1:08:02	984.7	870.1	806.6	933.6	1004.8
1:08:28	983.9	870.8	805.9	936	1004.6
1:08:54	983	868.4	808.8	934.5	1001.8
1:09:20	982.5	869.8	804	927.4	1001
1:09:46	981.7	871.5	804.7	923.6	1000.7
1:10:12	981	869.9	802.7	921.4	1000.7
1:10:38	980.9	870.1	804.7	922.5	1000.1
1:11:04	980.7	872.9	806.2	923.7	1000.4
1:11:30	980.5	870.7	801.3	922.4	998
1:11:56	980.5	871.4	800.7	921.3	1001.2
1:12:22	980.7	870.4	803.1	920	1000.9
1:12:48	980.2	868.3	803.1	919.1	1000.1

1:13:14	979.9	870.7	802.2	917.6	1001
1:13:40	980.2	871.9	802.6	918.5	1001.6
1:14:06	980.8	875.7	804.3	919	1002.9
1:14:32	981.3	875.5	802	920	1002.1
1:14:58	981.2	872.1	802.3	917.8	1001.3
1:15:24	981.6	877.3	803.3	919	1002.9
1:15:50	982.3	874.1	802.5	922.4	1002.7
1:16:16	982.9	876.5	803.1	924.4	1003.2
1:16:42	983	873.1	802.6	923.3	1003.5
1:17:08	982.5	872.7	804.7	920.2	1002.6
1:17:34	982	869.1	797.5	918.1	1001.3
1:18:00	981.3	869.9	801.9	920.2	999.7
1:18:26	981	869.6	803.9	919.3	1001.8
1:18:52	981	865.1	804.2	918	1000.7
1:19:18	980.8	869.5	807.7	921.3	998.9
1:19:44	980.2	868.3	812.1	920.3	997.1
1:20:10	980.4	874.5	815.8	918.5	994.5
1:20:36	981	874.6	817.3	918.7	998.8
1:21:02	982.1	870	812.8	920.1	1002.3
1:21:28	982	867.8	811.9	917.8	998.5
1:21:54	980.8	869.1	807.1	919.5	995
1:22:20	980.6	871	804.4	921.1	1001.2
1:22:46	981.3	870.4	806.9	919.3	1003.3
1:23:12	981	869.3	809.3	917.7	1000.4
1:23:38	980.9	872.7	804.1	920	1001.9
1:24:04	981.1	874.8	805.6	918.6	1002.4
1:24:30	981.7	875.9	802.7	919.1	1002.2
1:24:56	982.1	876.1	806.2	922.1	1000.2
1:25:22	982.4	877.4	804.1	920	1002.5
1:25:48	983.5	880.8	803.4	917.8	1003
1:26:14	984.5	880.6	806.7	919	1002.5
1:26:40	984.7	880	810	919.4	1000.9
1:27:06	984.4	881.7	803.4	917.9	1001.5
1:27:32	984.9	882.2	804.4	920.9	1001.1
1:27:58	984.9	885.9	802.4	923.5	1000.8
1:28:24	985.2	886.4	805.7	918.8	1000.5
1:28:50	985	884.1	803.6	919.4	998.1
1:29:16	985	884.9	804.1	919.9	1000.4
1:29:42	985.8	878	806.1	918.1	991.7
1:30:08	984.8	873.7	809.3	918.8	990.9
1:30:34	986.1	874.4	802.4	921.1	994.7
1:31:00	987.4	877.6	803.1	920	991.2
1:31:26	987.6	878.4	802.1	918.3	991.8
1:31:52	988	879	806.8	920.6	992.2

APPENDIX M

Table 10. Temperature distribution in furnace with four feeding time, 9-10-11-12 second at 980 °C set-point

Time (hh:mm:ss)	Set-point temperature (°C)	Exhaust gas temperature (°C)	Inlet temperature (°C)	Middle temperature(°C)	Outlet temperature (°C)
0:00:00	980.1	830.4	902.6	981.7	995.2
0:00:18	980	829.5	902.9	981.4	994
0:00:36	980.3	828.6	901.5	982.6	994.9
0:00:54	980.2	829	902	981.8	994.4
0:01:12	980	830.7	901.2	982.3	995.9
0:01:30	980.4	830.8	900.2	981.8	995.2
0:01:48	980.3	827.9	899.9	979.4	996.1
0:02:06	980.2	828.7	901.6	977.7	995.1
0:02:24	980.1	830.1	901.4	979.7	994.8
0:02:42	980.1	829.8	897.5	979	996
0:03:00	980.3	830	899.1	979.3	995.9
0:03:18	980.1	830.1	897.4	978.1	996
0:03:36	980.1	830.2	898.5	975.9	995.2
0:03:54	980.2	830.3	893.2	974.9	995.6
0:04:12	980.1	830.4	887.7	974.1	995.5
0:04:30	980.1	830.2	878.9	976.6	995.6
0:04:48	980.4	830.5	866.9	978.3	996.2
0:05:06	980.1	830.1	856.9	978	996
0:05:24	980.1	829.7	848	977.5	995.3
0:05:42	980.2	829.9	835.1	974.6	995.3
0:06:00	980.1	830.1	822.1	972.9	995.9
0:06:18	980	830.3	818.4	971.7	996.1
0:06:36	980.1	830.2	812.5	970.7	996.1
0:06:54	980	830.1	798.8	970.7	995.2
0:07:12	980	830.1	785.7	967.5	995.1
0:07:30	980.1	830.2	773.6	964.3	995.8
0:07:48	980.1	830.1	768.4	954.5	995.2
0:08:06	980.1	829.3	767.1	949	996
0:08:24	980	830	768.5	945.8	995.9
0:08:42	980.1	830	768.4	938.3	996.4
0:09:00	980.1	830.3	767.4	931	995.7
0:09:18	980.1	830.2	768.6	927	996.3
0:09:36	980.3	830.1	770.1	921	995.7
0:09:54	980.1	830.3	768.7	916.3	996
0:10:12	980.1	830.4	766.8	912.1	996

0:10:30	980.4	830.2	768.4	907.8	995.4
0:10:48	980.1	829.8	767.5	905	995.7
0:11:06	980.1	828.7	768.3	901.3	995.8
0:11:24	980	829	766.3	901.8	995.6
0:11:42	980.1	829.5	765.2	901.4	995.4
0:12:00	980.1	830	767.6	902.6	995.3
0:12:18	980.1	830.4	767.9	901.8	995.4
0:12:36	980.1	829.5	768.5	900.4	995.4
0:12:54	980.3	828.6	768	900.3	995.2
0:13:12	980.1	834.6	768.2	901.1	995.7
0:13:30	980.1	834.8	768.2	901.4	996.2
0:13:48	980.2	834.9	768.6	901.3	996.5
0:14:06	980.1	835	768.6	901.4	995.9
0:14:24	980.1	834.8	768.4	901.3	995.9
0:14:42	980.4	835.5	769.5	901.4	995.3
0:15:00	980.5	835.3	769.1	901.5	995.6
0:15:18	980.3	834.8	768.4	901.3	996.2
0:15:36	980.2	834.8	768.5	901.1	996.5
0:15:54	980.1	834.6	768.3	901	996.1
0:16:12	980.1	834.8	768.5	901.1	995.9
0:16:30	980.1	835.2	769.3	901	995.5
0:16:48	980.2	835.1	769.1	901.1	995.8
0:17:06	980.1	834.4	768.3	900.6	995.9
0:17:24	980.2	834.4	767.9	900.9	995.7
0:17:42	980.1	834.7	768.3	901.2	995.5
0:18:00	980.3	834.5	767.7	901.3	995.2
0:18:18	980.1	833.8	766.6	901.1	995.5
0:18:36	980.1	833	765.1	900.9	995.7
0:18:54	980.1	832.9	764.9	900.9	995.4
0:19:12	980	832.3	763.6	901.1	995.9
0:19:30	980	831.5	762.1	901	995.7
0:19:48	980.1	831.5	761.5	901.5	995.6
0:20:06	980	831	760.1	901	995.6
0:20:24	980.1	829.9	759	900.8	995.9
0:20:42	980.1	828.3	758	898.6	995.9
0:21:00	980.2	826.1	756.9	895.3	996
0:21:18	980.3	824.7	755.1	894.4	996.1
0:21:36	980.4	823.9	754.5	893.3	996.5
0:21:54	980.3	823.3	753.7	892.6	996.3
0:22:12	980.1	822.3	753.3	891.3	996.1
0:22:30	980.1	821.4	752.6	890.2	996
0:22:48	980.1	821.2	752.9	889.6	996
0:23:06	980.1	820.6	752.7	888.5	995.7
0:23:24	980	820.4	753	887.8	995.9
0:23:42	980.1	819.6	753.2	886.1	995.9

0:24:00	980.1	819.7	753.7	885.7	996.1
0:24:18	980.1	819.2	754.1	884.3	996
0:24:36	980	819.5	754.5	884	996.9
0:24:54	980	818.7	753.9	883.6	996.2
0:25:12	980	818.3	753.5	883.1	996.6
0:25:30	980	818.1	753.2	883	996.8
0:25:48	980	818	753.1	882.9	996.7
0:26:06	980.1	817.9	752.8	883	996.7
0:26:24	980.1	817.9	752.7	883.1	996.5
0:26:42	980	818.3	753.2	883.3	996.6
0:27:00	980	818.3	753.4	883.2	996.5
0:27:18	980	818.4	753.6	883.2	996.7
0:27:36	980	818.1	753.1	883.1	996.8
0:27:54	980	817.9	752.8	883.1	996.8
0:28:12	980	817.9	752.7	883.1	996.7
0:28:30	980	817.9	752.6	883.2	996.9
0:28:48	980	818.1	753	883.2	996.7
0:29:06	979.9	818.4	753.4	883.3	996.5
0:29:24	979.9	818.4	753.8	883.1	996.1
0:29:42	980	818.4	753.7	883.1	996.4
0:30:00	980	818.2	753.5	883	996.7
0:30:18	979.9	818.2	753.4	883	996.8
0:30:36	980	817.9	752.8	883	996.9
0:30:54	980	817.9	752.9	882.9	996.6
0:31:12	980.1	818	753.2	882.9	996.3
0:31:30	980.1	818.2	753.6	882.9	996.1
0:31:48	980.2	818	753.1	883	996.6
0:32:06	980.1	817.4	751.6	883.1	996.7
0:32:24	980.1	816.7	750.3	883.1	996.8
0:32:42	980.1	816	748.5	883.2	996.7
0:33:00	980	815.1	747.2	883	996.5
0:33:18	979.3	814.5	745.9	883.1	996.1
0:33:36	980	813.5	743.9	883.1	997.1
0:33:54	980	812.8	742.6	883	997.3
0:34:12	980.1	812.2	741.5	882.9	996.7
0:34:30	980.1	811.3	739.8	882.9	996.8
0:34:48	980	810.7	738.5	883	996.6
0:35:06	980	809.2	736.8	881.7	996.1
0:35:24	980.1	808	735.4	880.9	995.9
0:35:42	980.1	806.3	733.5	879.1	996.5
0:36:00	980	805.5	732.8	878.3	996.7
0:36:18	980	804.6	732.4	876.8	996.8
0:36:36	980	804.1	732.4	875.9	996.7
0:36:54	980	803.2	732.3	874	996.7
0:37:12	980	802.8	732.2	873.4	996.8

0:37:30	980.1	802	732.1	872	996.9
0:37:48	980	801.7	732.3	871.1	997.3
0:38:06	980	800.9	732.4	869.5	997.3
0:38:24	980	800.6	732.4	868.9	997.2
0:38:42	980.2	799.8	732.5	867.1	997.1
0:39:00	980.1	799.2	732.6	865.8	997.2
0:39:18	980.1	799.2	732.5	865.8	997.3
0:39:36	980	799.2	732.4	865.9	997.3
0:39:54	980	799.2	732.4	865.9	997.4
0:40:12	980.2	799.2	732.4	866	997.3
0:40:30	980.1	799.1	732.3	865.8	997.2
0:40:48	980.3	799	732.3	865.7	997.2
0:41:06	980.1	798.8	732.1	865.6	997.1
0:41:24	980	798.9	732.2	865.6	997.1
0:41:42	980.1	798.9	732.1	865.7	997.2
0:42:00	980.1	799	732.3	865.8	997.3
0:42:18	980	799	732.3	865.8	997.4
0:42:36	980.2	799.2	732.4	865.9	997.4
0:42:54	980.1	799.1	732.4	865.8	997.3
0:43:12	980.1	799.1	732.6	865.7	997.3
0:43:30	980	799.2	732.7	865.8	997.2
0:43:48	979.7	799.1	732.4	865.8	997.2
0:44:06	979.8	799	732.2	865.8	997.3
0:44:24	978.9	799.1	732.4	865.9	997.4
0:44:42	980	799	732.3	865.8	997.4
0:45:00	980.1	798.9	732.4	865.4	997.5
0:45:18	980.2	799	732.5	865.5	997.4
0:45:36	980	799.1	732.6	865.6	997.3
0:45:54	980	799.1	732.4	865.8	997.5
0:46:12	980	799	732.2	865.8	997.4
0:46:30	980	798.7	731.5	865.9	997.3
0:46:48	980	798.3	730.5	865.8	997.1
0:47:06	980	797.6	729.5	865.8	997.3
0:47:24	980	797.2	728.7	865.8	997.3
0:47:42	980	796.8	727.9	865.7	997.3
0:48:00	980	796.1	726.4	865.8	997.5
0:48:18	980.1	795.5	725.3	865.6	997.6
0:48:36	980.1	795.3	725.1	865.4	997.3
0:48:54	980	794.7	724.2	865.1	997.1
0:49:12	980	793.6	723.3	863.9	997.3
0:49:30	980.1	792.8	722.8	862.8	997.5
0:49:48	980	791.5	721.7	861.3	997.3
0:50:06	980	790.3	720.3	860.3	997.4
0:50:24	980.1	789.7	719.7	859.7	997.7
0:50:42	980.1	788.6	718.9	858.3	997.9

0:51:00	980.3	787.3	718.1	857.2	998
0:51:18	980.2	787.5	718.3	856.7	998.1
0:51:36	980.1	786.7	718.6	854.9	998.2
0:51:54	980	786.2	718.8	853.7	998.3
0:52:12	980.1	785.7	718.9	852.6	998.2
0:52:30	980	784.9	718.9	851	998.1
0:52:48	980.1	784.6	718.8	850.4	998.2
0:53:06	980	783.9	718.7	849.1	998.2
0:53:24	980.1	783.5	718.9	848.1	998.2
0:53:42	980	783.2	718.6	847.9	998.3
0:54:00	980	783.1	718.4	847.9	998.2
0:54:18	980	783.3	718.7	848	998.2
0:54:36	980.1	783.4	718.8	848	998.2
0:54:54	980.1	783.5	718.9	848.1	998.3
0:55:12	980	783.5	719	848.1	998.2
0:55:30	980	783.5	718.9	848.1	998.2
0:55:48	980.1	783.6	719	848.2	998.2
0:56:06	980	783.6	719.1	848.1	998.2
0:56:24	980	783.4	718.9	848.2	998.1
0:56:42	980	783.4	718.7	848.1	998.2
0:57:00	980.1	783.5	718.6	848.1	998.2
0:57:18	980.2	783.6	718.8	848.1	998.3
0:57:36	980.1	783.6	718.9	848.3	998.2
0:57:54	980.2	783.8	719.4	848.2	998.4
0:58:12	980.2	783.7	719.2	848.1	998.2
0:58:30	980.3	782.6	718.6	848.1	998.2
0:58:48	980.3	783.5	718.9	848.1	998.3
0:59:06	980.4	783.4	718.9	848	998.2
0:59:24	980.3	783.4	718.8	848.1	998.2
0:59:42	980.3	783.4	718.8	848	998.1
1:00:00	980.4	783.2	718.4	848.1	998.1
1:00:18	980.2	783.4	718.6	848.2	998.2
1:00:36	980.3	783.4	718.7	848.1	998.2
1:00:54	980.4	783.5	718.8	848.2	998.3
1:01:12	980.3	783.4	718.9	848.2	998.3
1:01:30	980.2	783.4	718.7	848.1	998.2
1:01:48	980.1	783.5	718.9	848.1	998.3
1:02:06	980.1	783.6	719	848.3	998.4

BIOGRAPHY

Name Mr. Chavalit Jaroenrat

Date of Birth July 6, 1975

Place of Birth Bangkok, Thailand

Education

1995-1997	B. Industrial Technology in Mechanical Technology, King Mongkut's Institutes of Technology North Bangkok (KMITNB)
1997-2000	M. Business Administration (MBA), Mahanakorn University of Technology (MUT)
2007-2011	M. Eng. in Automotive Engineering (International program) International College, King Mongkut's Institute of Technology Ladkrabang (KMITL)

Work experience

1997-2005	NHK Spring (THAILAND) Co., Ltd
2005-Present	Bangkok Spring Industrial Co., Ltd

Honour and Scholarship

2007-2009	Full scholarship for study in the master degree from National Science and Technology Development Agency (NSTDA)

Publications

1. J. Chavalit , P. Pongjet and N. Warakom "Transient Thermal Characteristics of automotive leaf Spring in direct-fired walking beam type reheating furnace" , **Proceeding of the 2th International Conference on Green and Sustainable Innovation,** Chiang Rai, Thailand, December 2-4, 2009 pp.569 – 576.